2003

# Effects of Frost Heave on a Soil Nail Wall in Brunswick, Maine

Sandra McRae Duchesne
*University of Maine - Main*

# EFFECTS OF FROST HEAVE ON A SOIL NAIL WALL IN BRUNSWICK, MAINE

By

Sandra McRae Duchesne

B.S. University of Maine, 1993

B.A. Smith College, 1978

A THESIS

Submitted in Partial Fulfillment of the

Requirements for the Degree of

Master of Science

(in Civil Engineering)

The Graduate School

The University of Maine

May, 2003

Advisory Committee:

Thomas C. Sandford, Associate Professor of Civil and Environmental Engineering, Advisor

Dana N. Humphrey, Malcolm G. Long Professor of Civil and Environmental Engineering

Thomas C. Sheahan, Associate Professor of Civil and Environmental Engineering, Northeastern University

# EFFECTS OF FROST HEAVE ON A SOIL NAIL WALL IN BRUNSWICK, MAINE

by Sandra McRae Duchesne

Thesis Advisor: Thomas C. Sandford, Ph.D., P.E.

An Abstract of the Thesis Presented
in Partial Fulfillment of the Requirements for the
Degree of Master of Science
(in Civil Engineering)

May, 2003

Soil nail walls have been used as retaining structures worldwide since the early 1970s. The technology is particularly well suited for constructing walls in areas with limited overhead clearance and maneuvering room for heavy equipment, such as highway bridge underpasses. However, designers have been reluctant to experiment with soil nailing in areas with cold-weather climates and frost-susceptible soils, due to the lack of quantifiable data on the behavior of these walls when subjected to freezing conditions.

The University of Maine collaborated with the Maine Department of Transportation (MDOT) in a research initiative on the first soil nail wall project in Maine, constructed along Route 1 as part of the Brunswick-Topsham Bypass Project. Selected components of the wall were instrumented to determine what effects the freezing winter temperatures would have on the wall and surrounding soil. Instrumentation included strain gages, load cells, a total pressure cell, thermocouples, and survey points. Despite a transient peak tensile stress exceeding the desired factor of safety of three in one of the

nails during the coldest period of the study, analysis of the instrumentation data indicated that the wall was not significantly affected by freezing temperatures during the wall's first post-construction winter season.

The findings from this undertaking directly influenced MDOT's planning process for a larger and more extensively monitored soil nail wall on Route 201 in Moscow, Maine, and contributed to the limited existing compendium of knowledge concerning the behavior of soil nail walls under cold weather conditions.

## ACKNOWLEDGMENTS

I wish to thank my advisor, Professor Thomas C. Sandford, for his help, guidance, and encouragement through all phases of this research project. Working with him has broadened my academic and practical knowledge base immeasurably, and I will always value his professional expertise and his friendship. I thank Professor Dana Humphrey for coaxing me into the master's program, serving on my graduate committee, and providing many hours of assistance with field instrumentation. I thank Professor Thomas Sheahan of Northeastern University, my committee member "from away," who shared his extensive library of soil nailing reference works and provided a useful connection to French academic research on frost and soil nailing. My committee members' critiques and suggestions have greatly improved the overall quality of this publication.

Will Manion created the prototype computer program for remote monitoring of my field instrumentation, and skillfully operated a ditchwitch to excavate a 700-yard channel for electrical hookup. Fellow graduate students Tricia Cosgrove, Leif Dixon, Peter Koch, Brian Lawrence, and Park Ki-Surk assisted with numerous tasks in the laboratory and field, some of them involving strenuous physical labor. I thank them all for their help and their friendship.

My undergraduate assistants were great. Bart Bauer and Brian Keezer logged instrument readings in the field throughout the cold Maine winter, and spreadsheeted data for further analysis. Aaron Smart spent many weeks programming and testing the remote

monitoring system, tweaking it until it worked. Aaron also helped with the labor-intensive installation and connection of wall instrumentation and electrical lines.

I am indebted to the Maine Department of Transportation (MDOT) for sponsoring my research. MDOT Construction Inspector Debbie Coffin provided me with detailed daily construction records, photos, and sketches. I thank the construction crews of H.E. Sargent and Pennsylvania EarthTech for their cameraderie and cheerful assistance with my instrument installation. The Meteorological and Oceanographic Detachment at Brunswick Naval Air Station faxed hourly readings of Brunswick air temperatures and barometric pressures directly to our Orono office at no charge, and I gratefully acknowledge their continuous and reliable support.

I would like to thank my family: my father and mother, Tom and Nancy McRae, who raised all of their children to value education and to follow their individual dreams; my aunt Helen Hollingworth, who thinks I'm just plain wonderful and tells me so regularly; and my incredibly cool brothers, Rick, Jim, and Dave McRae, who along with their families provided gentle inspiration and encouragement even when I most felt like giving up. My family's loving support was a great motivator as I worked to reach my academic goals. I feel truly blessed to have been born into this loving, tightknit clan.

Finally, I thank my husband, Bob Duchesne, for hanging in there with me through some weird and difficult times. It's one of the many reasons I love him. At this point, we're both looking forward to a grand post-thesis future.

## TABLE OF CONTENTS

ACKNOWLEDGMENTS ..... ii

LIST OF TABLES ..... viii

LIST OF FIGURES ..... ix

Chapter

1. INTRODUCTION ..... 1

    1.1. Overview ..... 1

    1.2. Objectives of this research ..... 3

    1.3. Organization of the thesis ..... 3

2. LITERATURE REVIEW ..... 5

    2.1. Introduction ..... 5

    2.2. Soil nail wall design ..... 5

        2.2.1. Mechanisms and construction ..... 5

        2.2.2. Design methods ..... 7

            2.2.2.1. Major methods ..... 7

            2.2.2.2. Alternative methodologies and recent innovations ..... 8

            2.2.2.3. Accommodations for frost in soil nail wall design ..... 9

2.3. Heat transfer in soil nail walls ..... 14
2.3.1. Overview ..... 14
2.3.2. Heat transfer in soil, grout, and nails ..... 15
2.3.3. Conductivity of soil, grout, and nails ..... 16
2.3.4. Frost penetration prediction models ..... 18
2.3.5. Frost penetration modeling for walls ..... 21
2.4. Case histories ..... 32
2.4.1. Seasonal stresses in anchored tieback walls, Canada ..... 35
2.4.2. Seasonal stresses on temporary soil nail walls, French Alps ..... 36
2.4.3. Winter failure of reinforced earth wall with successful soil nail reconstruction, France ..... 38
2.4.4. Seasonal stresses in FHWA demonstration soil nail wall, Cumberland Gap, Kentucky ..... 40
2.4.5. Seasonal stresses on a terraced highway wall, Germany ..... 41
2.4.6. Design to accommodate severe frost heave in soil nail walls, Canada ..... 42
2.4.7. Use of insulation to reduce the effects of frost heave in soil nail walls, Maine ..... 45
2.5. Summary ..... 48
3. PROJECT CONSTRUCTION AND INSTRUMENTATION ..... 51
3.1. Overview ..... 51
3.2. Site characteristics ..... 51

3.3. Soil conditions ..... 55

3.4. Wall design and construction ..... 61

3.5. Instrumentation ..... 62

3.5.1. Strain gages ..... 66

3.5.2. Load cells ..... 76

3.5.3. Concrete strain gages ..... 82

3.5.4. Total pressure cell (TPC) ..... 83

3.5.5. Thermocouples ..... 84

3.5.6. Slope indicators ..... 85

3.5.7. Survey points ..... 86

3.5.8. Data acquisition system ..... 87

3.6. Construction sequence ..... 89

4. INSTRUMENTATION RESULTS ..... 99

4.1. Introduction ..... 99

4.2. Strain gages ..... 100

4.3. Load cells ..... 110

4.4. Concrete strain gages ..... 113

4.5. Total pressure cell ..... 115

4.6. Thermocouples ..... 117

4.7. Survey data ..... 129

5. ANALYSIS ..... 132

5.1. Introduction ..... 132

5.2. Magnitude and rate of freezing penetration ..... 132

5.3. Effect of soil nail walls on freezing penetration ..... 137

5.4. Magnitude of stresses on nails and wall over the course of the freeze-thaw season ..... 139

5.5. Effects of freezing and frost heave on wall performance ..... 150

6. SUMMARY AND CONCLUSIONS ..... 153

6.1. Recommendations for incorporating frost effects into soil nail wall design ..... 156

7. AREAS FOR FUTURE INVESTIGATION ..... 160

REFERENCES ..... 164

BIOGRAPHY OF THE AUTHOR ..... 170

## LIST OF TABLES


Table 4-1. Load cell stress vs. averaged strain gage stress, 7/18/96 ..... 111

Table 4-2. Load cell stress vs. averaged strain gage stress, 2/20/97 ..... 111

Table 4-3. Load cell stress vs. averaged strain gage stress, 4/16/97 ..... 111

Table 5-1. Average monthly temperatures and departures from historical averages, October 1996 – April 1997 (NOAA, 1996-1997) ..... 133

Table 5-2. Schematic representation of frost penetration behind wall ..... 135

Table 5-3. Extreme bending stress in nails at 0.9 m and 1.5 m, February 20, 1997 ..... 147

## LIST OF FIGURES


Figure 2-1. Design air-freezing index values in New England ..... 22

Figure 2-2. Geometry of the retaining wall/Mesh created using FEM ..... 24

Figure 2-3. Isotherms after 60 days/Deformed FEM mesh ..... 25

Figure 2-4. Isotherms after 120 days/Deformed FEM mesh ..... 26

Figure 2-5. FEM mesh used for GEL 2D modeling of soil nail wall at La Plagne, France, subjected to frost during the winter of 1988-1989 ..... 27

Figure 2-6. Hydraulic gradient field: GEL 2D simulations on wall at La Plagne ..... 28

Figure 2-7. GEL 2D simulations for wall at La Plagne: isotherms and thermal flux ..... 29

Figure 2-8. GEL 2D simulation of wall deformations at La Plagne ..... 30

Figure 2-9. Results of finite element modeling of frost penetration in a Maine soil nail wall under varying thermal regimes ..... 33

Figure 2-10. Schematic representation of slope facing reconstruction using geosynthetics ..... 47

Figure 3-1. View (facing northeast) of existing railroad bridge during initial clearing operations for soil-nail wall, showing abutments and three center piers ..... 53

Figure 3-2. View of abutment and pier adjacent to eastbound lane of Route 1. Existing 2:1 slope (shown) was replaced with a soil-nail wall to create a new exit lane ..... 53

Figure 3-3. Grain size distribution curve from embankment, 0.9-1.8 m (3-6 ft) depth ..... 58

Figure 3-4. Grain size distribution from embankment, 0.8-4.0 m (2.6-13 ft) depth ..... 59

Figure 3-5. Grain size distribution from embankment, 4.6-7.6 m (15-25 ft) depth ..... 60

Figure 3-6. Profile of instrumented north-facing soil nail wall, Brunswick-Topsham Bypass ..... 63

Figure 3-7. Section view A-B through north-facing abutment ..... 64

Figure 3-8. Plan view of north-facing bridge abutment, batter piles, and nail placement ..... 65

Figure 3-9. Typical layout of strain gages along soil nail ..... 67

Figure 3-10. Typical layout of thermocouples along soil nail ..... 68

Figure 3-11. Typical layout of thermocouples along wooden rod ..... 69

Figure 3-12. Instrumented nails in wooden carrying cradles ..... 74

Figure 3-13. Detail showing stabilizer applied to HDPE sheathing ..... 74

Figure 3-14. Installation of nail through drilled, cased hole ..... 77

Figure 3-15. Removal of casing section and threading of instrument wires through casing ..... 77

Figure 3-16. First row of nails completed, second bench excavated ..... 78

Figure 3-17. Nail installation complete ..... 78

Figure 3-18. Detail showing load cell placement ..... 79

Figure 3-19. Completed concrete facing wall, rain gutters, and traffic barrier ..... 79

Figure 3-20. Profile view of load cell and wall connections ..... 80

Figure 3-21. Sloughing failure on non-instrumented wall ..... 92

Figure 4-1. Strain gage stress vs. time for Gage 1, 0.9 m (3 ft) from exposed end of nail ..... 103

Figure 4-2. Strain gage stress vs. time for Gage 2, 0.9 m (3 ft) from exposed end of nail ..... 104

Figure 4-3. Strain gage stress vs. time for Gage 3, 1.5 m (5 ft) from exposed end of nail ..... 105

Figure 4-4. Strain gage stress vs. time for Gage 4, 1.5 m (5 ft) from exposed end of nail ..... 106

Figure 4-5. Strain gage stress vs. time for Gage 5, 2.4 m (8 ft) from exposed end of nail ..... 107

Figure 4-6. Strain gage stress vs. time for Gage 6, 3.6 m (12 ft) from exposed end of nail ..... 108

Figure 4-7. Strain gage stress vs. time for Gage 7, 5.5 m (18 ft) from exposed end of nail ..... 109

Figure 4-8. Load vs. time in load cells ..... 112

Figure 4-9. Stress vs. time in concrete strain gages ..... 114

Figure 4-10. Stress vs. time in total pressure cell (TPC) ..... 116

Figure 4-11. Thermocouple temperatures vs. time, Nail C2-9 ..... 118

Figure 4-12. Thermocouple temperatures vs. time, Nail C2-13 ..... 119
Figure 4-13. Thermocouple temperatures vs. time, Nail C3-10 ..... 120
Figure 4-14. Thermocouple temperatures vs. time, Nail C3-16 ..... 121
Figure 4-15. Thermocouple temperatures vs. time, Nail C4-13 ..... 122
Figure 4-16. Thermocouple temperatures vs. time between nails C2-9 and C3-10 ..... 123
Figure 4-17. Thermocouple temperatures vs. time between nails C2-13 and C3-14 ..... 124
Figure 4-18. Thermocouple temperatures vs. time between nails C3-10 and C4-12 ..... 125
Figure 4-19. Thermocouple temperatures vs. time between nails C3-16 and C4-18 ..... 126
Figure 4-20. Thermocouple temperatures vs. time between nails C4-13 and C4-14 ..... 127
Figure 4-21. Ambient air temperatures vs. time ..... 128
Figure 4-22. Changes in X-Y-Z space and locations of survey points ..... 131
Figure 5-1. Stress in soil nails on November 3, 1996 ..... 140
Figure 5-2. Stress in soil nails on December 6, 1996 ..... 141
Figure 5-3. Stress in soil nails on January 6, 1997 ..... 142
Figure 5-4. Stress in soil nails on February 6, 1997 ..... 143
Figure 5-5. Stress in soil nails on March 8, 1997 ..... 144
Figure 5-6. Stress in soil nails on April 3, 1997 ..... 145

# CHAPTER 1

# INTRODUCTION

## 1.1. Overview

Soil nailing has been used in Europe and in warmer regions of the United States for nearly three decades. It is particularly appropriate for constructing retaining walls beneath highway bridge underpasses, and in areas where limited construction access or the proximity of adjacent structures would make it difficult to construct and backfill a traditional retaining wall (Chassie, 1992). The soil nailing technique uses long metal or fiberglass rods to reinforce soil in situ, proceeding in a series of vertical or near-vertical benches excavated from the top of an existing soil mass. The nails are drilled and grouted (or driven) into the soil at close intervals to form a composite structure with increased shear strength. A shotcrete facing, applied either immediately after excavation or after nails are installed, retains the exposed soil surrounding the nails and may be used as the final wall surface in some applications. Most designers add an additional facing wall for weather protection and aesthetic considerations (usually cast-in-place concrete, although timberwork and modular wall facing systems have also been used).

There is little documentation about the effects of frost heave on soil nail structures, and this has undoubtedly limited the use of soil nailing in areas with severe winter climates (like Maine). The combination of freezing temperatures, frost susceptible soils, and a source of water can lead to the formation of ice lenses, which increase the volume occupied by the soil mass. As the lenses continue to form and increase in size,

they exert a force upward and outward against the wall face. This can lead to additional (and possibly excessive) tensile stresses on the nails. In the spring, thawing of the ice lenses can produce a loss of volume and corresponding settlement of the soil mass, leading to cracks along the wall facing. In addition, soil nails may exacerbate the intensity of frost heave because their high conductivity (10 to 25 times that of a typical soil) may introduce frost more quickly and more deeply into the surrounding soil behind the wall.

While only a few soil nail wall failures have been attributed to frost heave, more knowledge is needed about soil nail performance in cold weather climates and frost susceptible soils. Some design manuals recommend avoiding the use of soil nails under these conditions. In other cases the wall facing is insulated to prevent or reduce frost penetration, resulting in additional construction costs. These actions are probably overly conservative, but they reflect the current lack of engineering knowledge about the potential for damage due to frost action in soil nail walls.

The Brunswick-Topsham Route 1 Bypass Project was the first known application of soil nailing technology in the state of Maine. Near-vertical soil nail walls were installed in the railroad bridge embankments on the existing Route 1 corridor, in order to create exit ramps for a new bypass bridge to Route I-95. The wall on the northbound side of Route 1 was instrumented to observe the effects of frost during the winter of 1996-97. If soil nailing can be demonstrated to be feasible in areas with severe winter climates,

the economic and logistical advantages offered by soil nailing could result in a substantial cost savings to clients (in this case, the Maine taxpayers).

### 1.2. Objectives of this research

The objectives of the University of Maine research on the Brunswick soil nail wall were as follows:

* Determine the effects of freezing and frost heave on wall performance;
* Determine the magnitude and rate of freezing penetration into the wall;
* Determine the effect of the soil nails on freezing penetration;
* Determine the magnitude of stresses on the nails and wall facing during the course of the seasonal freeze-thaw cycle;
*Develop recommendations for incorporating frost effects into soil nail wall design.

### 1.3 Organization of the thesis

The thesis is presented in seven chapters. Chapter 2 is a review of relevant literature on soil nail walls and the observed effects of frost heave on soils reinforced in situ, including anchored tieback and reinforced earth walls as well as soil nail walls. Chapter 3 provides the construction details for this project and describes the instrumentation that was installed along the nails and wall facing. Chapter 4 presents the results from the instrumentation, which show the behavior of the soil nail wall during the first year following construction. Chapter 5 presents an analysis of the field results with respect to the objectives of the research and issues raised during the year of monitoring. A

summary of results and conclusions from the research are described in Chapter 6. Chapter 7 presents recommendations for future research, as well as some recommended guidelines for soil nail design in cold-weather climates.

# CHAPTER 2

# LITERATURE REVIEW

## 2.1. Introduction

Soil nailing techniques have been used since the early 1970s in Europe and North America. Many articles and design manuals have been published on the subject of soil nail wall design and construction, but few address frost effects or incorporate frost protection within a design methodology. This deficiency was noted in the findings of the French National Research Project CLOUTERRE (translation: SOIL NAIL) as an area for further research (FNRP, 1991), and many questions remain unanswered. In addition, there are few case histories of frost effects on soil nail projects. Therefore, case histories of frost heave in other types of retaining walls and in pile systems have also been examined to obtain insights which may apply to soil nail walls.

Presented below is a synopsis of existing literature on soil nail technology and design, models for heat transfer in soils and in the nails, and case histories illustrating the potential effects of frost and other cyclic seasonal movements on wall performance.

## 2.2. Soil nail wall design

### 2.2.1. Mechanisms and construction

Soil nail walls use tension-resisting inclusions, such as steel bars or (rarely) fiberglass rods, to reinforce and anchor an in situ soil mass and increase its stability. The reinforcing elements are typically placed in drilled boreholes and grouted along their

entire length, although some firms drive the nails into the natural earth (Byrne et al., 1993). Drilled nails tend to have a higher capacity (Sieczkowski, 1989). Also, because of the mandated corrosion protection in most major transportation projects, drilling and grouting is the vastly preferred technique in North America (Byrne et al., 1996).

The use of in situ soil distinguishes soil nailing from mechanically stabilized earth (MSE) techniques in which the native soil, which may be frost susceptible, is usually replaced with clean fill sandwiched between layers of free-draining geotextile or strip inclusions. Because the in situ soil remains in place around the metal-grout annulus of the nails in soil nailing, frost susceptibility may result in heaving and the subsequent loss of soil strength during the spring thaw. This action can act to increase the tension on the inclusions and the wall facing, in some cases to near or above the design values (Byrne et al., 1996).

In addition, soil nail construction proceeds in a "top-down" fashion, as opposed to the "bottom-up" construction of MSE walls. In soil nailing, the top of the embankment is benched vertically to a depth of 1 to 2 m (3 to 6 ft) from top of slope, depending on the soil type and its short-term stability. After a reinforced shotcrete facing is applied, the nails are driven or drilled and grouted into the in situ soil, with the exposed ends tied into the facing. In a soil with a more stable vertical face, nail installation may occur prior to shotcreting. Successive cuts are nailed following the same procedure of working down in benches, until the entire wall has been nailed and faced (Byrne et al., 1996).

The completed soil nailed mass behaves as a composite gravity structure. However, it is still possible for a failure surface to develop through the nails, particularly through the low-capacity inclusions typical of driven soil nail walls (Sieczkowski, 1989). Frost heave-thaw effects conceivably could induce a weakening of the soil between the nails (resulting in internail facing rupture or nail head pullout), although no specific reports of this type of failure were found. This implies that the design spacings now in use are adequate to protect against frost failure in the soil surrounding the nails. However, this inference cannot be confirmed without more data on soil nail wall performance in frost-prone areas.

Slopes ranging from 50° to 90° have been retained using soil nailing, with nails placed at 0° to 30° inclination below horizontal; most designs place the nails between 10° and 20° below horizontal. One nail per 1.4 to 5.6 $m^2$ (15 to 60 $ft^2$), or 1.2 to 2.4 m (4 to 8 ft) on center, is typical for drilled and grouted nails. Smaller spacings, on the order of one nail per 1.5 $m^2$ (5 $ft^2$), are used for driven nails. Parametric analysis has shown that increasing the number of nails in a wall increases the factor of safety, by forcing the failure surface further back into the soil mass (Sieczkowski, 1989).

### 2.2.2. Design Methods

**2.2.2.1. Major methods.** Over thirty years of practice, three major design methods have predominated. All are based on a limit equilibrium analysis of potential failure surfaces passing through or behind the nailed soil mass and exiting at the toe of the wall. The Davis method, developed at the University of California at Davis (Shen et

al., 1981; Bang, 1979) assumes a parabolic failure surface through the nailed soil and the toe of the wall, in which the nails provide both tensile and pullout resistance. The German method (Stocker et al., 1979; Gassler and Gudehus, 1981) assumes an angular two-component failure surface, which occurs at the interface of the soil-nail "gravity wall" and an active earth pressure wedge behind it; since the failure surface occurs behind the full nail length, nail pullout resistance is moot and the nails are assumed to provide tensile resistance only. The French method (Schlosser, 1983) assumes a circular failure surface and permits the designer to consider the nail's resistance against shear and bending in addition to tension and pullout. The French method is therefore considered slightly less conservative than other methods (Byrne et al., 1996).

**2.2.2.2. Alternative methodologies and recent innovations.** Other design approaches are worthy of mention. Juran et al. (1984) adapted a reinforced earth design approach to perform an equilibrium analysis on an active zone defined by a circular failure surface, with the assumption that failure would result from a progressive breaking of the nails and resultant shearing of the soil mass. This approach can be used to obtain maximum values for tensile and shear strength in the nails, but only in cases where the soil is homogeneous and the geometry is simple to analyze (Mitchell and Villet, 1987).

Newer limit equilibrium designs in the United States include the SNAIL design method developed by the California Department of Transportation, and the GoldNail method of Golder Associates, Redmond, Washington (both cited in Byrne et al., 1996). These methods include the wall facing as a functional component in the nailed soil mass

system. This permits consideration of the structural strength of the facing as a factor in the analysis. The newer methods also consider the pullout capacity of the nails against the wall and non-wall sides of the failure surface (Byrne et al., 1996).

In order to mesh with existing AASHTO Bridge Design Specifications (1992, 1994), Byrne et al. (1996) adapted the limit equilibrium method for FHWA using design approaches based on service load condition (SLC) and load and resistance factor design (LRFD). The FHWA method also incorporates the benefits of the SNAIL and GoldNail methods by giving some weight to the strength of the wall facing elements and connections.

**2.2.2.3. Accommodations for frost in soil nail wall design.** None of the common design methods provide explicit guidelines for soil nail walls placed in frost-susceptible soils. To the extent that the topic is addressed at all, most authorities recommend avoidance or minimization of the potential for frost heave, either by selecting a different construction method if the in situ soil is highly frost susceptible (FNRP, 1991; Byrne et al., 1993) or by using insulation to reduce the depth of frost penetration (FNRP, 1991; Byrne et al., 1996; Kingsbury, 1999; Bahner, unpublished article). After five years of intensive research on the design and construction of soil nail walls, which culminated in a large volume of design recommendations, FNRP (1991) notes only in passing that frost heave can be a potential source of wall failure in frost-susceptible soils. The same researchers observe that high tensile forces can develop in the region behind the wall facing as the frost front progresses. This effect was noted on a few soil nail

projects in the mountains (not further specified or referenced; presumably in France), where some facing damage resulted. If the facing is made rigid to prevent such damage, the nails may break in tension or the connection between the wall and the facing may be lost. The authors suggest that damage due to frost action may be minimized or prevented by insulating along the face, but offer no specific guidelines.

Elias and Juran (1991) surveyed a number of soil nail projects and reported substantial temporary stress increases in soil nail walls subjected to freezing temperatures. They postulated that the magnitude of stress increase was dependent on the depth of frost penetration, intensity and duration of the freezing season, and the relative position of the groundwater table or proximity of other water sources – in other words, the greater the frost heave, the greater the seasonal tensile stress in the nails. In a few cases, stress increases to nearly twice the initial post-construction values were observed at depths of 0 to 4 m (0 to 13 feet) behind the face of soil nail walls. Noting that similar behavior had been observed in anchored tieback walls (Guilloux et al., 1983), Elias and Juran recommend insulating the wall facing when walls are constructed in frost-susceptible soils close to the water table or other water source. However, no guidelines were provided for insulation design.

Eric Bahner, P.E. , a practicing engineer with Woodward-Clyde, reported that he routinely insulated the face in his soil nail wall designs in the Madison, Wisconsin area (unpublished article). No specific insulating guidelines were given. Byrne et al. (1996) suggested using a granular or synthetic insulating layer along the face of walls placed in

frost-susceptible soils, with the insulation of sufficient thickness to prevent frost from penetrating into the subsoil. While the authors provided no guidelines for determining this thickness, it can presumably be accomplished using standard frost penetration prediction models for the given soil and climate conditions of the construction site. Several of these models are discussed in greater detail later in this chapter.

Kingsbury (1999) studied the performance of an approximately 9 m (30 ft) soil-nail wall in Moscow, Maine over the course of two years, 1997-1999. Although the weather during both freezing seasons turned out to be milder than both the mean and design winters for that region, he obtained sufficient data to demonstrate through finite element analysis that insulating the top as well as the face of a wall can significantly reduce overall frost penetration and the resulting cumulative stress increases, particularly for the topmost nails which fall within the bi-directional frost fronts. Kingsbury also recommended sizing up the nails in the top rows of a wall to accommodate the effects of permanent cumulative tensile loads, as these nails are already subjected to the highest levels of sustained soil shear mobilization and then accumulate additional seasonal tensions in the nail heads due to bi-directional frost penetration and heave. This more conservative approach can help to extend the design life of a wall constructed in cold climates and frost-susceptible soils.

Kingsbury et al. (2002), in a followup study on the wall in Moscow, Maine as described above, determined that the magnitude of cumulative nail head tension buildup in each succeeding season is predictably less than that of the previous season, probably

due to the development of passive earth pressure resistance over time in response to cyclical loading. The permanent residual tension in each successive freezing season can be modeled as an exponential limit decay function,

$$P = e^{-(t-1)/n} \tag{2.1}$$

where P = percentage of seasonal maximum rise that remains permanent,
e = limit as $n \rightarrow \infty$ for $(1+1/n)^n$, usually expressed as 2.71828...,
t = number of winter seasons after wall construction, and
n = calibration constant for rate of decrease.

In the case of the Moscow wall, with n=2 determined as the best fit for data taken during the first three years, this observed tendency toward equilibrium over time produced a reasonable prediction of lifetime accumulated tension in the nail heads of about 2.5 times the maximum increase in the first winter season (Kingsbury et al., 2002).

Byrne et al. (1993) reported that the second phase of CLOUTERRE (the follow-on project to FNRP, 1991) would study the performance of soil nail walls under frost loading, probably under controlled monitoring conditions in a full-scale test facility, to develop design specifications. The French researchers were concerned about potential facing problems in severe frost regions. Some of these French researchers (not further specified by the authors) believed that the post-construction failure of a 500 $m^2$ (5380 $ft^2$) wall section on the Paris to Bordeaux TGV rail line, Lot 21, was due to frost action compounded by weak soils (Byrne et al., 1993). The findings of CLOUTERRE II were issued in 1993 as an internal laboratory report only; however, much of the CLOUTERRE research on frost effects was published in the doctoral dissertation of Unterreiner (1994), who served as one of the principal researchers for CLOUTERRE I and II. Juran (1997) directed me to this untranslated dissertation, and CERMES ENPC

(the national civil engineering research institution of France) mailed a copy in response to my written request. This dissertation is unique in that it provides specific recommendations for frost heave prevention in soil nail walls, so it is described in some detail below.

Unterreiner (1994) created a detailed model of frost displacement in a soil nail wall, which he calibrated and checked against actual measurements of frost displacement at La Clusaz (previously reported by Guilloux et al., 1981) and the FNRP CLOUTERRE full-scale demonstration walls. Based on the model results, he proposed two practical design modifications to accommodate the increased seasonal stresses in soil nail walls:

1) installing short nails, 2 m (6.6 ft) long, at regular intervals between structural nails of 9 m (30 ft) length, thus providing additional reinforcement for the nail-soil mass structure; or

2) providing an additional free (ungrouted) length of nail equal to the predicted frost penetration depth at the head of the nail, so that the freezing front does not affect the grouted design length. Depending on the length and severity of the freezing season, this free length can be as short as 0.5 m (1.6 ft) or as long as 9 m (30 ft) added to the design length of each soil nail. Unterreiner found that the free-length technique can reduce tensions in the nails by 21%. He obtained approximately the same improvement using the short-nail method; therefore, the designer should select whichever is the most economical approach for the predicted frost penetration conditions. This will be the free length method as long as the additional length per nail is relatively small, and the short nail method as the required free length becomes larger (Unterreiner, 1994).

Alston (1991) designed a soil nail wall faced with flexible, permeable geotextile and geogrid to accommodate frost heave in Ontario. More details are provided in the case history included in this chapter.

## 2.3. Heat transfer in soil nail walls

### 2.3.1. Overview

Theoretical predictive models for frost penetration typically assume a one-dimensional, uniform front proceeding downward from the ground surface, as the warmer temperatures deeper within the soil lose heat toward the below-freezing air temperatures. In the case of a retaining wall, a second quasi-linear front also advances horizontally inward from the face of the wall. The materials involved in the heat transfer model for soil nail walls are not only the soil, but also the wall facing, nail grout, steel nails, flowing groundwater, and in the Brunswick case even the steel H-piles on which the bridge abutment rests. These elements all provide potential routes for freezing temperatures to enter the subsoil at different rates over the course of a freezing season, resulting in a nonlinear freezing front and possibly in a higher degree of heave. One of the objectives of this research was to determine whether the materials used in soil nailing can significantly influence the depth of frost penetration behind a retaining wall, or the rate at which frost penetration occurs. The literature of heat transfer and frost penetration models was examined for indications of how these elements might influence subsoil freezing patterns behind the wall.

### 2.3.2. Heat transfer in soil, grout, and nails

Heat transfer occurs through conduction, convection, or radiation, or through a combination of several or all of these methods (Small, 1959). Soil, a porous solid, is subject primarily to heat transfer by conduction, although some convection and solar radiation may occur where the soil is in contact with groundwater or air. While convection and radiation transfer additional heat as the porosity of a soil is increased, this effect is more than offset by a decrease in conduction between the more widely spaced soil grains; hence, conduction controls total heat transfer in soils, and denser soils transfer more total heat than looser soils (Yanagisawa and Park, 1997). For solid steel nails and surrounding grout, as well as for a concrete abutment and supporting H-piles, heat transfer occurs by conduction almost exclusively (Jumikis, 1977).

Current analytic methods for thermal soil mechanics ignore convection and radiation, although these mechanisms may influence the final calculation slightly under special climatic and soil conditions. Geothermal heat transfer is also neglected, as it typically provides only $10^{-4}$ of the magnitude of atmospheric heating and cooling at the ground surface (Jumikis, 1977). For the majority of real-world problems, in fact, conduction is the sole or primary method of heat transfer; attempting to quantify convection, radiation, and geothermal effects makes the calculation much more complex without significantly changing the outcome (Jumikis, 1977). In the case of the Brunswick soil nail wall, flowing groundwater was not a major factor, as the wall was constructed in a fill embankment above the water table (although some of the lower nails extended into groundwater due to their angle of inclination). Ignoring convection,

radiation, and geothermal heat transfer therefore appears to be a rational approach to this problem.

Conductivity relationships between the facing, soil, and nail-grout system will therefore be the focus of the heat transfer analysis for this thesis. Conduction through the abutment and the H-piles undoubtedly contributed to heat transfer and limited frost penetration in Brunswick, probably even more than the nails since the piles contain much more steel than the soil nails. However, their effects cannot be quantified since the piles and abutment were not instrumented.

### 2.3.3. Conductivity of soil, grout, and nails

Fourier's Law, based on Newton's basic theory of heat transfer, is the fundamental building block for thermal soil mechanics. Fourier's Law of one-dimensional heat transfer through conduction, for a homogeneous and isotropic material, is written in equation form as

$$Q = K\, dT/dz \qquad (2.2)$$

where $Q$ = heat flow

$K$ = thermal conductivity coefficient of the material

$dT/dz$ = temperature gradient (Jumikis, 1977; Lunardini, 1981).

Following the Second Law of Thermodynamics, heat transfer always occurs from higher to lower heat; i.e., the hotter body continuously loses energy to the cooler body, until an equilibrium is reached and a gradient no longer exists. In thermal soil mechanics, as the air temperature cools and the surface soil freezes, the warmer soil at

depth will lose heat toward the surface. Local sources of porewater and groundwater also may flow along the thermal gradient toward the frozen surface soil (Jumikis, 1977). As the cold season progresses, more and more of the soil achieves freezing temperatures, and the "frost front" (e.g., the 0° C isotherm within the soil mass) moves gradually deeper below the surface. However, a thermal gradient remains with respect to the unfrozen soils and groundwater at depth. Over the course of a winter, an unlimited supply of unfrozen water moving into the freezing zone can lead to the formation of large ice lenses in frost-susceptible soils. The lenses in turn cause frost heave in winter, followed by deformations due to loss of strength as the soil thaws in the spring (Mitchell, 1993).

The thermal conductivity, K, for steel at 0° C is approximately 10 to 25 times that of soil, while concrete and grout have a thermal conductivity slightly higher than that of most soils (Ingersoll et al., 1954). Since heat flow is directly related to conductivity according to Fourier's Law, it follows that freezing temperatures will conduct more quickly along the nail-grout annulus than along the quasi-linear frost front penetrating into the soil between the nails. Conduction of freezing temperatures along the nails may also cause frost to form in the soil immediately surrounding the nails, at depths which would normally be considered beyond the frost zone. Lunardini (1980) presents several approximate solutions for predicting the depth of frost penetration around a cylinder, using various assumptions and boundary conditions to locate the distance of the phase change interface from the center of the cylinder.

### 2.3.4. Frost penetration prediction models

Numerous methods exist for determining the rate of frost penetration in soils. In general, these can be divided into two categories: empirical (direct observation and measurement of frost depths in test pits or drill holes), and analytical modeling (Jumikis, 1977). Empirical data have been compiled into charts and maps such as Figure 2-1, which shows the design air-freezing index across New England. These isotherms were constructed based on the averaged cumulative freezing degree-days from the three coldest years in 30 years of recorded winter temperatures, as measured at each of approximately 85 weather stations throughout the region. Analytical models attempt to quantify and predict depth of frost penetration based on the intensity and duration of the freezing season, temperature variations in the air and soil (and in any intervening media, such as road surface layers or a concrete wall facing), and the proximity of groundwater or other continuous water sources (Jumikis, 1977). The primary differences between the analytical models are their assumptions and boundary conditions. A survey of the more commonly used models is provided below.

The earliest analytical model of frost penetration was presented by Neumann (ca. 1860). It was originally designed to study the progression of ice buildup on a still lake, but Berggren (1943) fit thermal soil properties into the theory and was the first to apply it to frost penetration in soils (Jumikis, 1977; Lunardini, 1981). Neumann's solution assumes a homogeneous, isotropic, semi-infinite moist body at constant temperature $T_o$, which is above the fusion temperature of water, $T_f$. The air temperature at the surface suddenly drops (as a step change function) to a value $T_s < T_f$, and is held constant at that

value. An exact solution to the problem can be obtained by writing the differential equations for heat balance at the boundaries and applying a transformation using the Gaussian error function (Lunardini, 1981). However, there are several drawbacks to Neumann's method; it assumes constant density of water as it is converted to ice, assumes the surface soil temperature constant and equal to the surface air temperature, assumes the deep soil temperature constant and unaffected by surface temperature, and provides only particular solutions to the balance equations (Jumikis, 1977). Because it depends on similarity to the error function, the Neumann solution cannot be used for many real-world applications, such as finite spaces, mixed ice-water-soil initial states, temperature fluctuations with time, and non-uniform initial temperatures (Lunardini, 1981). Finally, the Neumann method predicts frost penetration most accurately in cases where the thermal properties of both the frozen and unfrozen soil are well-known (Jumikis, 1977). On the other hand, it has provided a stepping stone for later, more practical methods.

Stefan's solution, which is really a special case of the Neumann solution, was originally designed to predict ice sheet formation on still water in the polar regions (Jumikis, 1977). However, it can easily be adapted to the frost penetration problem in soils. It assumes the soil temperature at and below the frozen boundary to be equal to the fusion temperature, defined as $T_f = 0°$ C. The surface temperature is assumed constant at a value below $T_f$, and the temperature in the frozen zone increases linearly from the surface to the boundary. As with Neumann's solution, the density of ice is assumed to be the same as that of water. An approximate solution can be obtained using the Gaussian

error integral (Jumikis, 1977). Although Stefan's solution is simple to calculate, it does not account for the volumetric heat capacity of the frozen and unfrozen soil as in Neumann's method, and thus will overestimate frost penetration depth. However, in northern climates and soils with high water content, the difference will rarely exceed 10% (Aldrich, 1956).

The modified Berggren solution (Aldrich and Paynter, 1953) closely follows Stefan's solution but uses a correction coefficient, based on the local freezing index and known or estimated thermal properties of the soil, to account for volumetric heat capacity. For a multilayered soil, the weighted volumetric heat capacity and latent heat capacity values for each layer are used to develop the correction coefficient $\lambda$ (Jumikis, 1977).

Portnov's solution (Portnov, 1962) follows Stefan's solution in taking the initial soil temperature equal to 0° C; like Stefan, it ignores the volumetric heat capacity of the soil and will overestimate the depth of frost penetration (Unterreiner, 1994). However, it allows surface temperatures to change over time within a range below or equal to 0° C. Lefur et al. (1964) generalized Portnov's solution to permit an initial soil temperature greater than or equal to 0° C. A more general solution by the same authors does not assume the fusion temperature $T_f$ as a constant (Unterreiner, 1994). While Stefan's solution predicts a more rapid frost penetration rate at the beginning of the freezing season, Portnov's gives a more rapid rate at the end of the freezing season. Since the

initial heave effect on the nail heads causes the largest increase in nail tensions, Unterreiner (1994) feels that Stefan's solution is the more conservative for use in soil nail walls.

### 2.3.5. Frost penetration modeling for walls

Most frost penetration models are one-dimensional, showing the progression of a vertical frost front through parallel horizontal layers of soil. These models have only limited application for a retaining wall, in which frost penetration and heaving occur in at least two dimensions with a complex interplay between thermal, mechanical, and hydraulic processes.

Li et al. (1989) used a finite element program developed by Blanchard and Fremond (1985) to simulate two-dimensional frost heave in a retaining wall. The program uses Fourier's Law to model heat flow throughout the soil-water-ice mixture. Movement of water to the freezing front is governed by Darcy's Law and is strongly temperature-dependent, decreasing sharply when the temperature drops below freezing. The concentration of unfrozen water is assumed to be 100% above 0° C, discontinuous at 0° C, and diminishing rapidly to zero at a temperature between -3° and -4° C, although in actuality some unfrozen water may remain in clays and silts to temperatures as low as -30° C (Jumikis, 1977; Tsytovich, 1960). The temperature in the model was decreased linearly from +10° C to -10° C over 30 days, held constant from day 30 to day 90, and then increased linearly back to +10°C at day 120. The initial mesh geometry and the deformed mesh after 60 and 120 days are shown in Figures 2-2, 2-3, and 2-4 respectively.

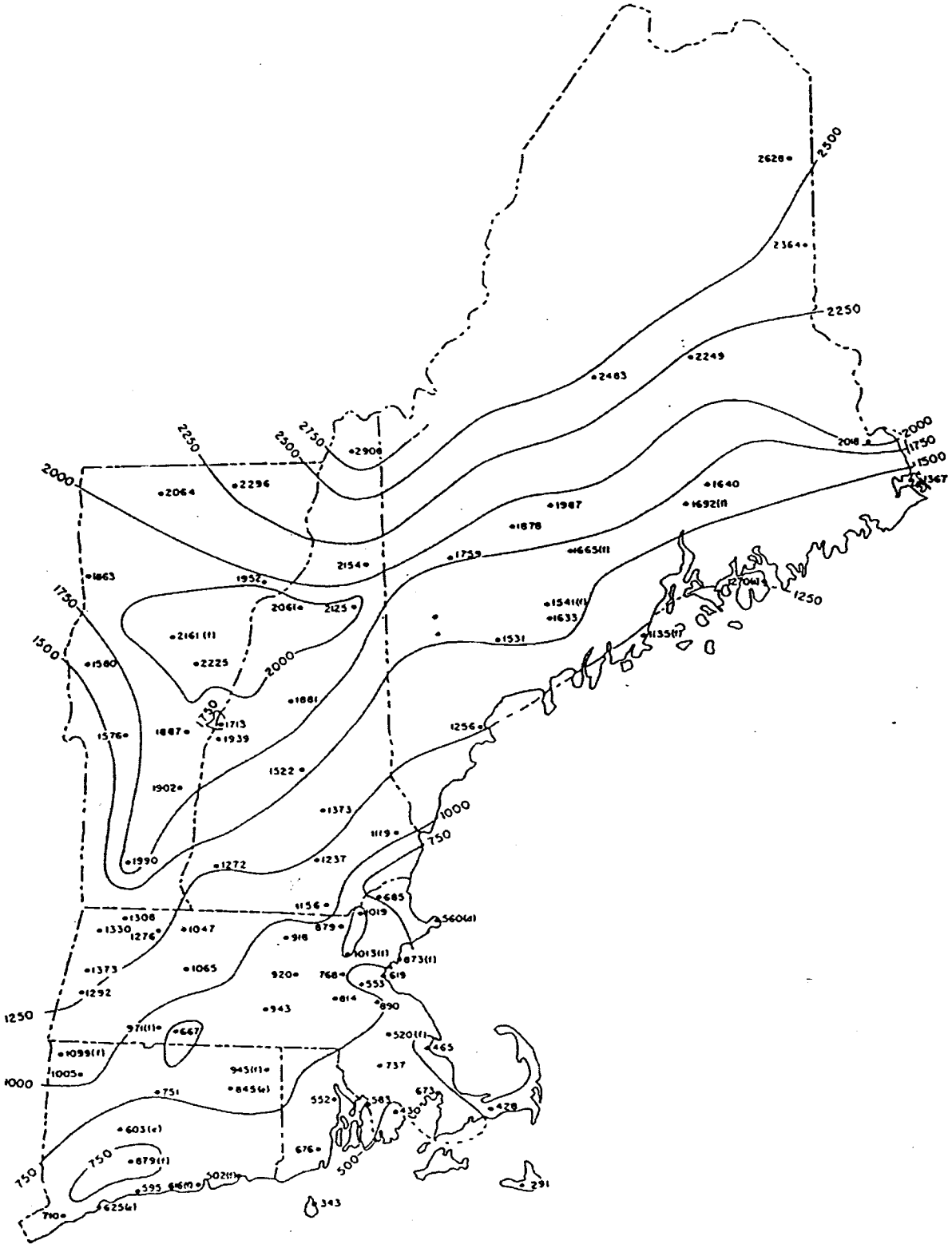


Figure 2-1: Design air-freezing index values in New England (after Bigelow, 1969; average 30-year heating degree days 1938-1968, degrees given in Fahrenheit)

The figures demonstrate the two aspects of frost action which can most damage a retaining structure: upward and outward heave and rotation about the toe during the freezing season, and settlement during the thawing season as the ice lenses melt and increase the water content in the soil, thereby decreasing its effective stress (Jumikis, 1977).

Unterreiner (1994) noted that the actual deformation of a soil nail wall is three-dimensional, with a coupling of the thermal, mechanical, and hydraulic processes. No existing finite element program is capable of this complex coupling. However, the program GEL 2D (Fremond and Williams, 1979) is capable of coupling the hydraulic and thermal characteristics, and was used for this purpose to predict the deformations in a soil nail wall designed for the bobsled run at La Plagne, France, for the 1992 Winter Olympics in Albertville (Vengeon, 1989). The 2-dimensional mesh for this wall is shown in Figure 2-5. Unterreiner (1994) noted that the hydraulic gradients, thermal flux, and deformational fields obtained from this effort (Figures 2-6, 2-7, and 2-8 respectively) were practically unidimensional through the center part of the wall. He concluded that it was indeed valid to use a one-dimensional analysis along one row of nails behind a concrete facing to simplify the frost-penetration problem.

The soil nail walls chosen for the analysis were La Clusaz, previously reported by Guilloux et al. (1981), and the full-scale demonstration walls used in Project CLOUTERRE (FNRP, 1991). Using the known soil parameters and weather conditions, Unterreiner (1994) estimated the frost depth, temperature profile with depth, and

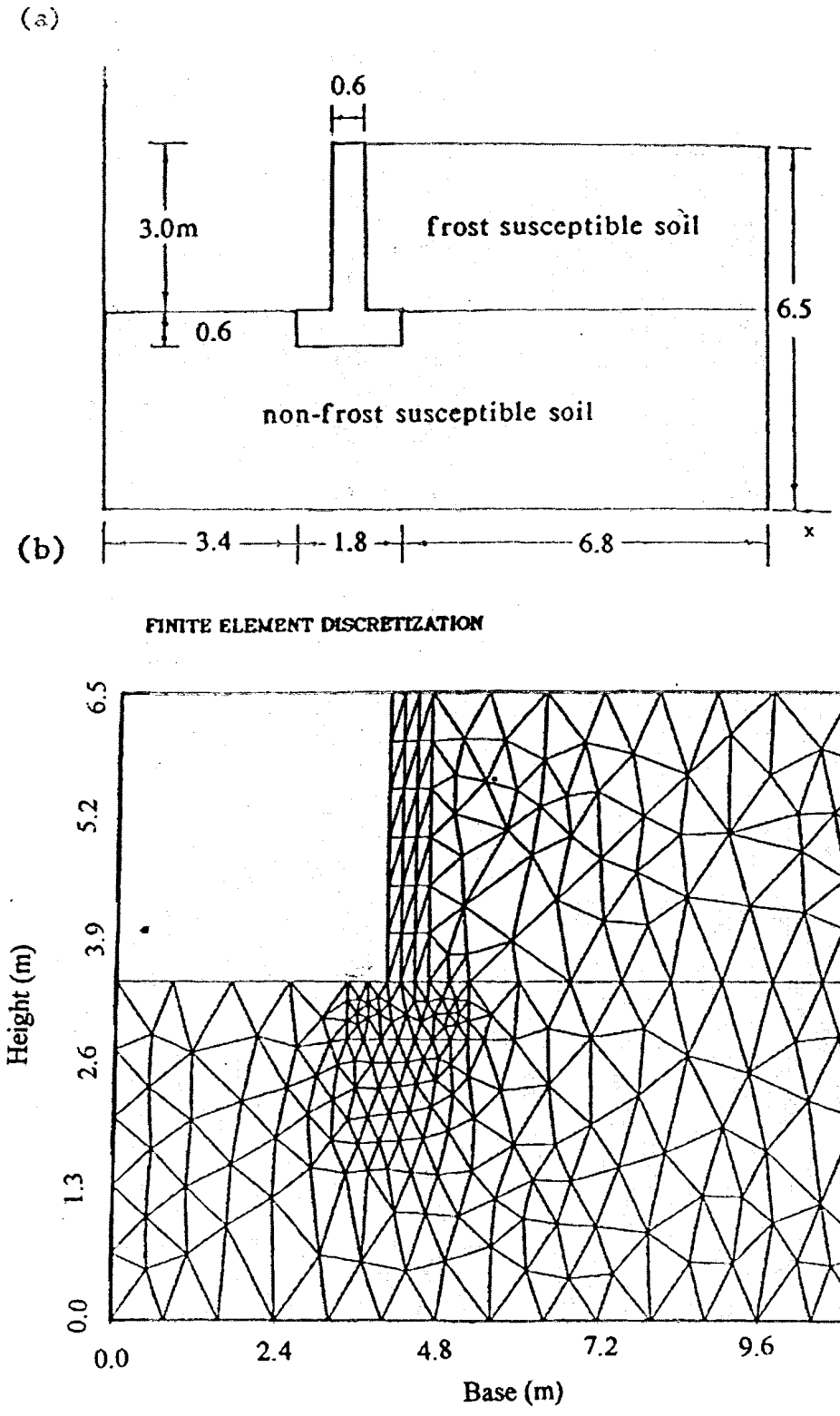


Figure 2-2: (a) Geometry of the retaining wall; (b) Mesh created using FEM (after Li et al., 1989)

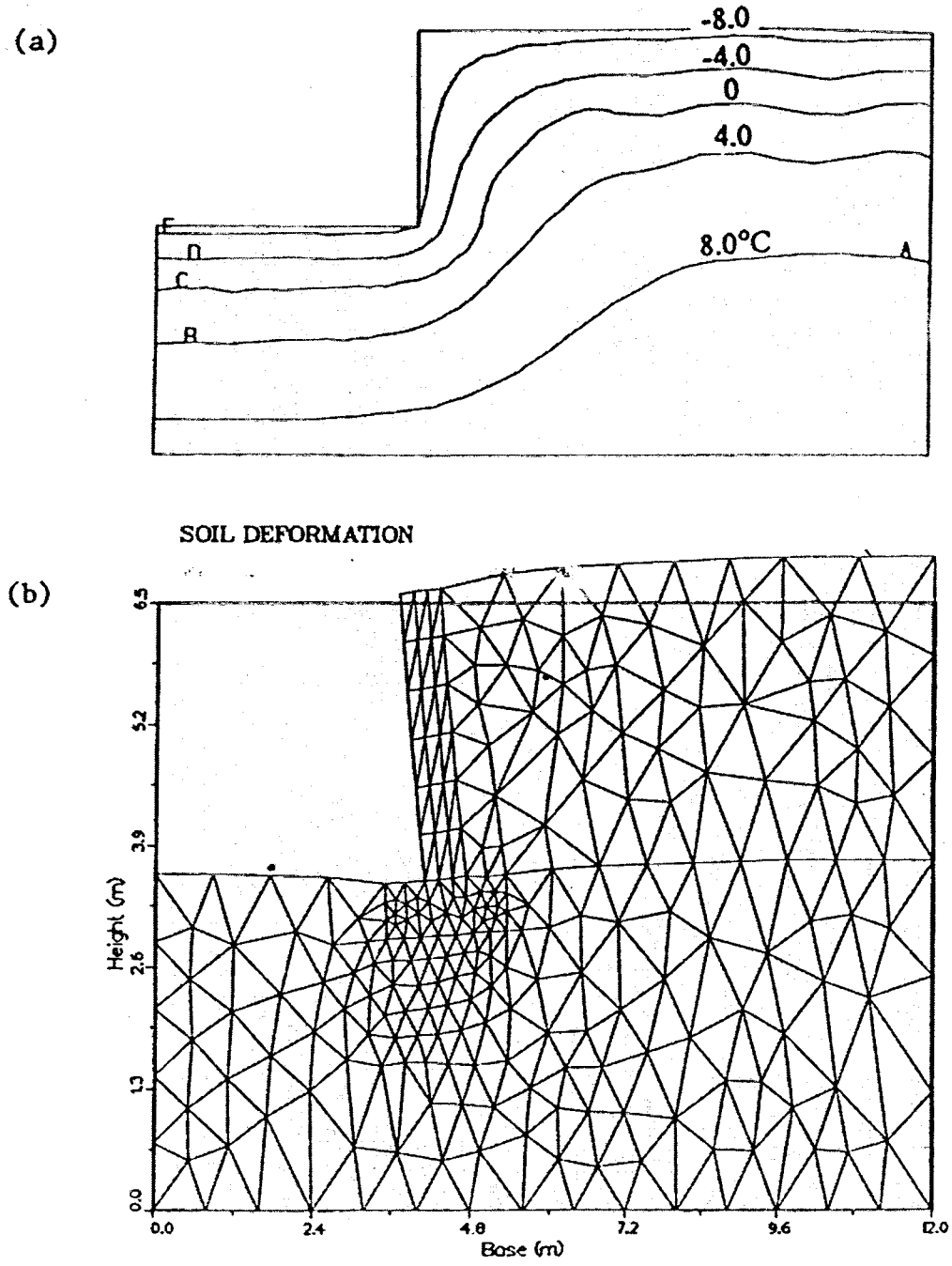


Figure 2-3: (a) Isotherms after 60 days; (b) Deformed FEM mesh (after Li et al., 1989)

(a)

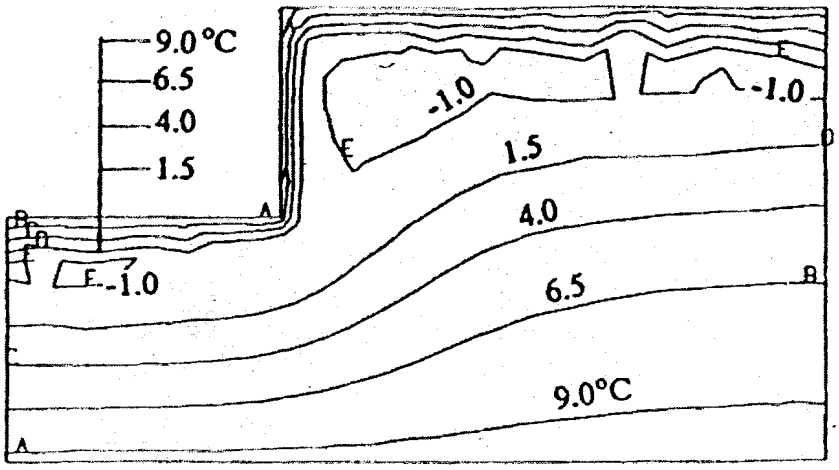


SOIL DEFORMATION

(b)

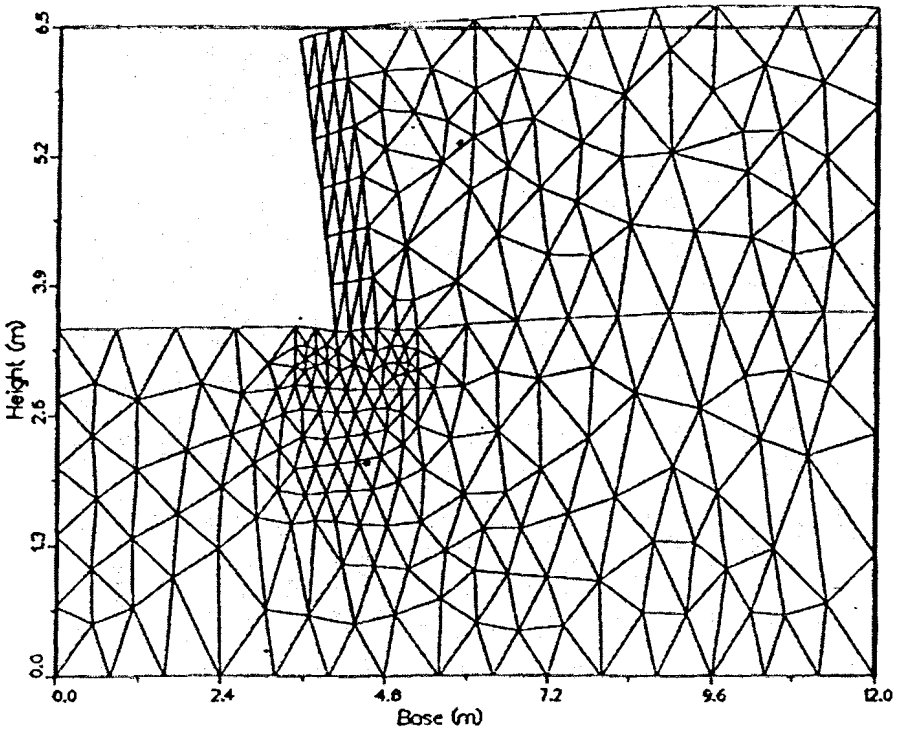


Figure 2-4: (a) Isotherms after 120 days; (b) Deformed FEM mesh (after Li et al., 1989)

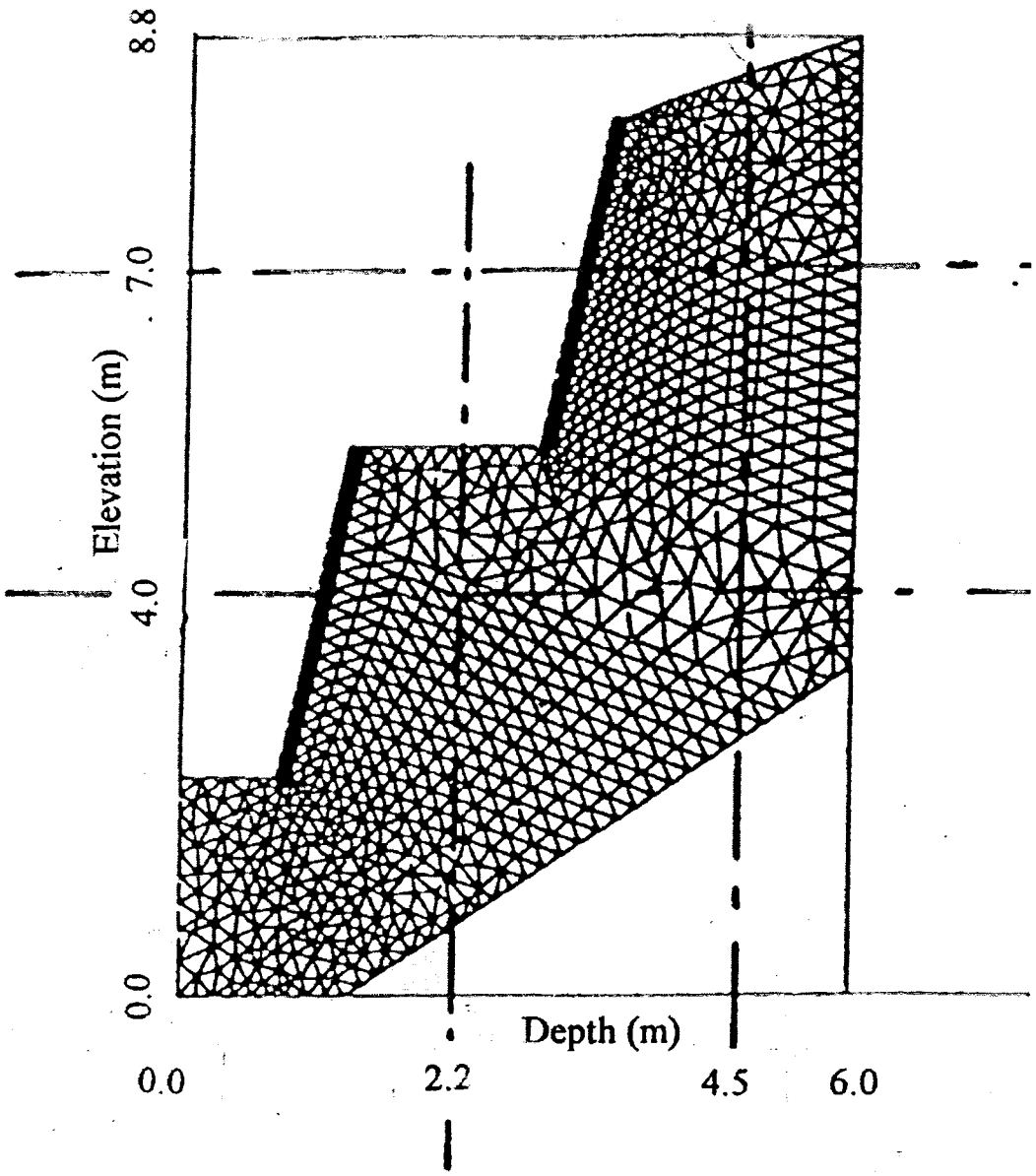


Figure 2-5: FEM mesh used for GEL 2D modeling of soil nail wall at La Plagne, France, subjected to frost during the winter of 1988-1989 (after Vengeon, 1989)

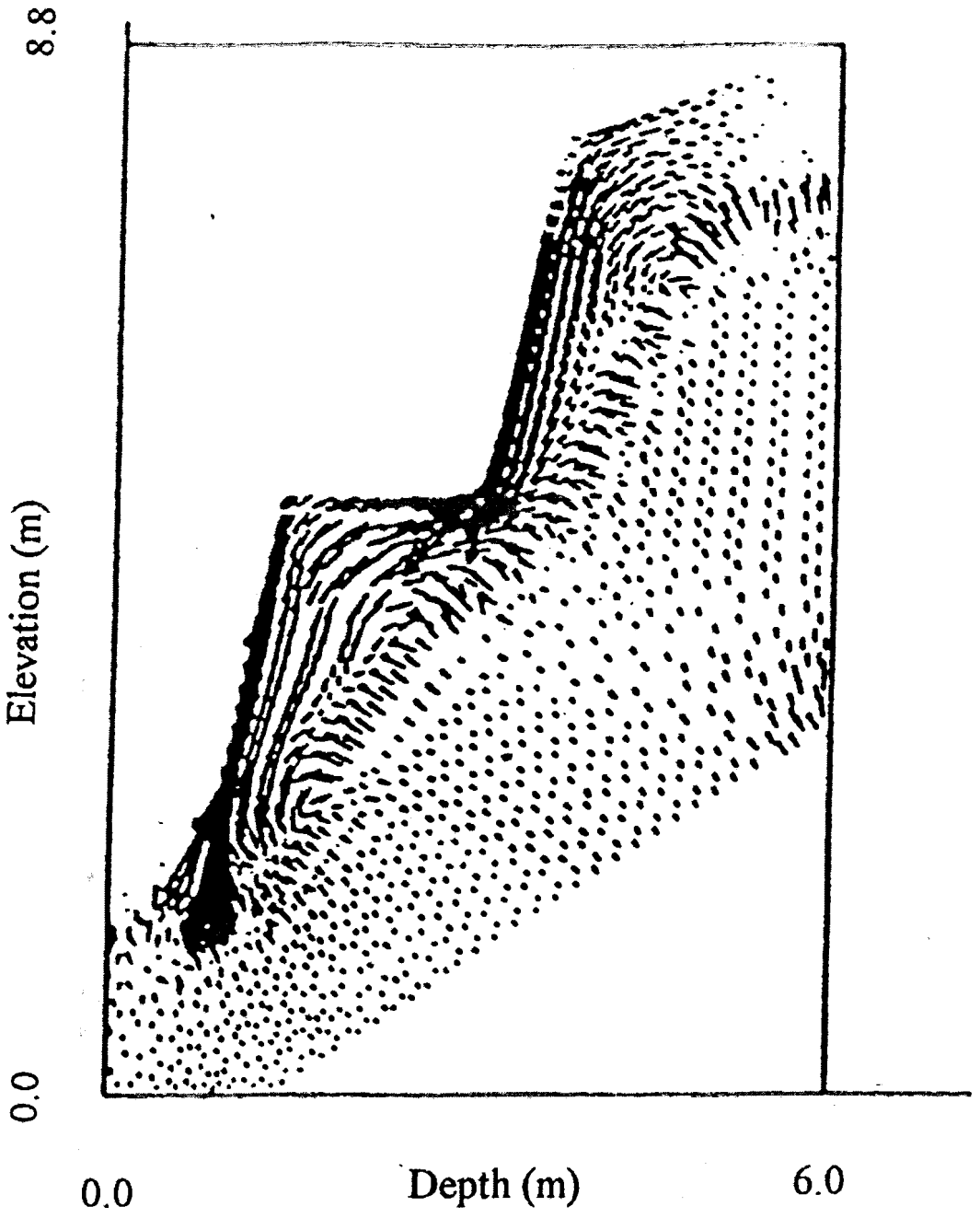


Figure 2-6: Hydraulic gradient field: GEL 2D simulations on wall at La Plagne. (after Vengeon, 1989)

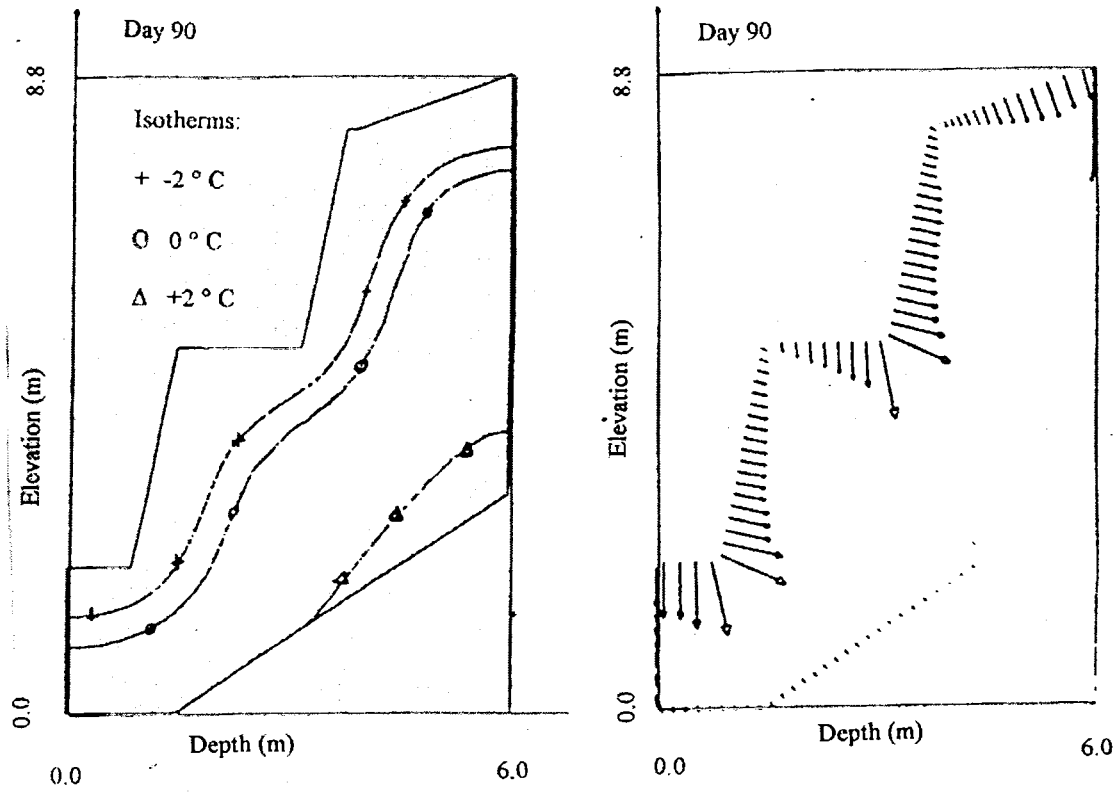


Figure 2-7: GEL 2D simulations for wall at La Plagne: (a) Isotherms, (b) Thermal flux (after Vengeon, 1989)

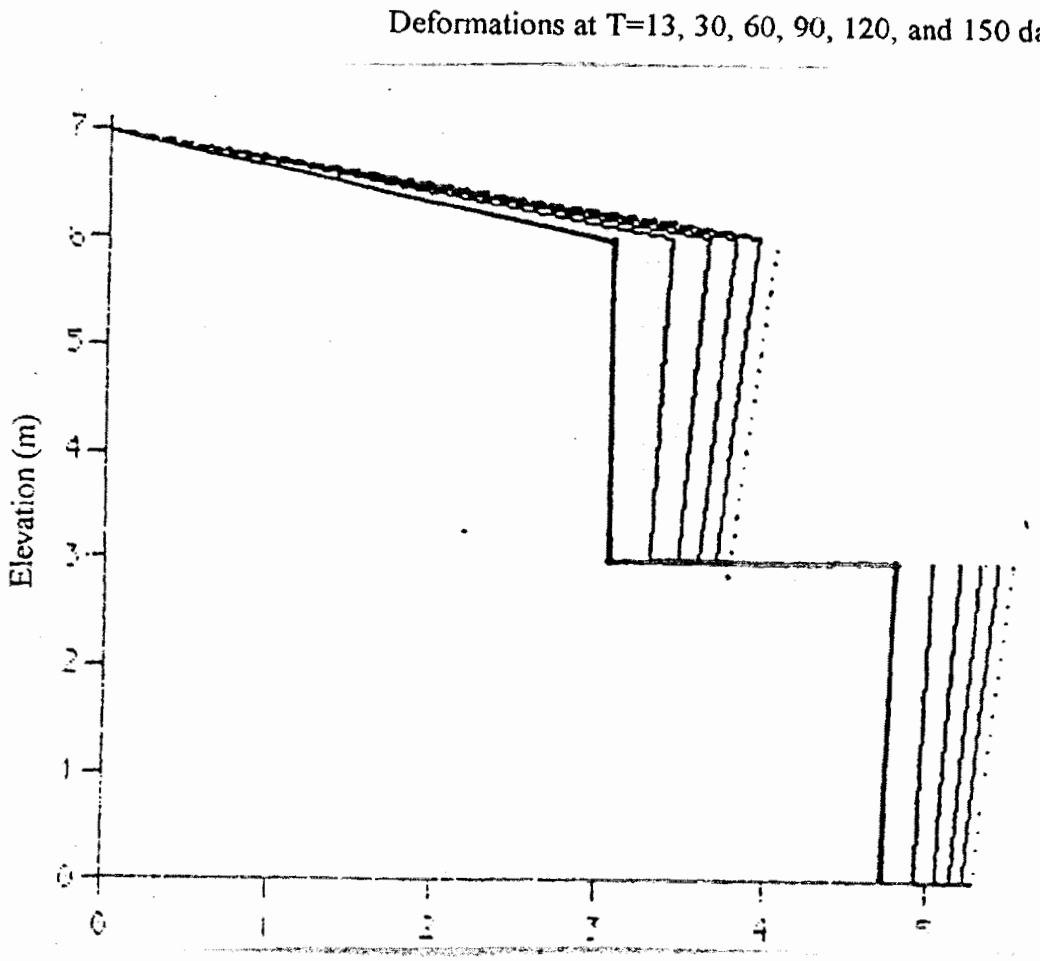


Figure 2-8: GEL 2D simulation of wall deformations at La Plagne (after Vengeon, 1989)

expected deformations induced by frost heave. For the second pass, the new conditions were imposed as the initial conditions in the soil and facing and the equilibrium state around the nail was redetermined. In this way, the thermal and hydraulic aspects of the problem were tied in with the mechanical action. Since the coupled behavior was strongly non-linear, the problem was resolved iteratively and incrementally. A finite element program called INGEL (INclusion soumis au GEL – translation: inclusion subjected to frost) was developed from an existing pile-loading program, specifically to obtain a numerical solution for this problem; the results were very close to the measured results. An analytic solution gave slightly higher deformations and frost penetrations than were measured in the field, and hence was conservative (Unterreiner, 1994). The other interesting finding by Unterreiner is that allowing temperature to vary with time over the winter (Portnov's method) provides essentially the same solution as using the mean seasonal temperature with Stefan's method, as long as the surface freezing index is used rather than the air freezing index; in other words, the freezing index must be estimated using the surface soil temperature rather than the ambient air temperature, which is normally measured at a height of 1.2 m (4 ft) from the ground surface. The surface freezing index can be obtained using empirical formulas to convert air freezing index values, if actual surface data is not available (for example, see Jumikis, 1977). The use of a seasonal freezing index, rather than daily average temperatures, simplifies the calculation considerably and does not affect the result by more than a few percentage points (Unterreiner, 1994).

Kingsbury (1999) used finite element analysis modeling to predict frost penetration depths under varying thermal regimes, using the TEMP/W version 3.01 program developed by Geo-Slope. It permits the solution of two-dimensional transient heat flow problems, using time-dependent boundary conditions and temperature-dependent boundary modifiers. By extending the finite element mesh beyond the actual dimensions of the wall, he was able to reduce localized inaccuracies near the imposed boundary conditions. The model was calibrated using actual data taken from an instrumented soil nail wall in Moscow, Maine during the winter of 1998-1999, and was then used to predict wall performance under a variety of air temperatures, insulation thicknesses, and placements (insulated top of wall plus wall face, insulated wall face only, and uninsulated). The finite element analysis demonstrated that, while facial insulation certainly contributes to the overall reduction of frost penetration along a wall, colder winters will induce deeper frost penetration from the top of the wall which can significantly elevate the stresses in nails within its frost front. Therefore it is prudent to insulate both the top and face of the wall. Kingsbury's conclusions from the finite element analysis, showing the relationships between frost penetration and seasonal temperatures (as measured by freezing degree-days) under various R-values and placements of insulation, are shown in Figure 2-9.

## 2.4. Case Histories

Although it is generally accepted that frost can have a detrimental effect on soil nail walls – in fact, several soil nail wall failures have been partially attributed to frost action (e.g., Schlosser, 1982; Byrne et al., 1993) – only a few case histories document the behavior of

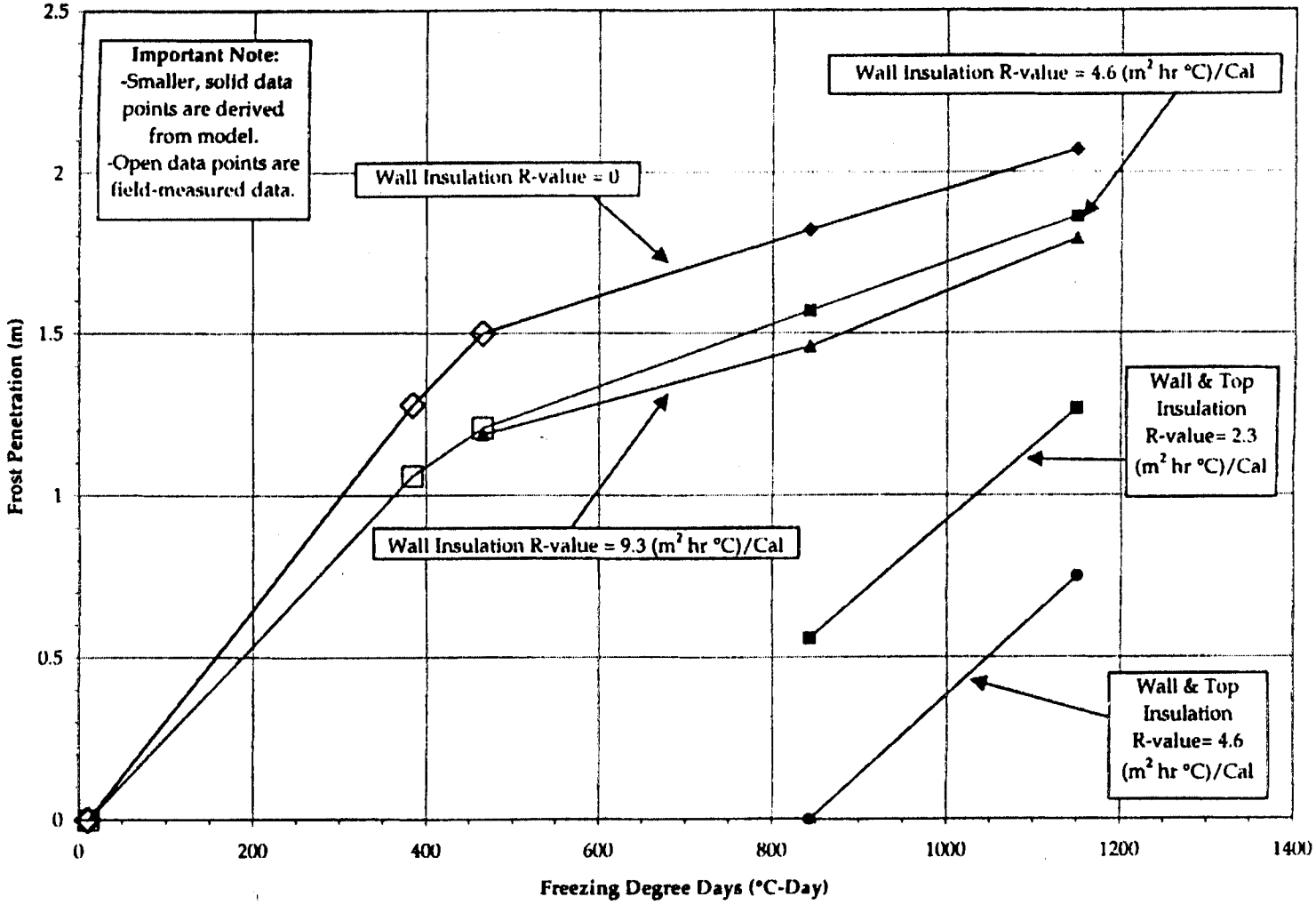


Figure 2-9: Results of finite-element modeling of frost penetration in a Maine soil-nail wall under varying thermal regimes (Kingsbury, 1999)

soil nail walls in cold weather and frost susceptible soils. However, well-documented measurements of seasonal stress cycles in other retaining wall systems may provide a model for understanding the seasonal stress increases in a soil nail wall. For example, Smoltczyk et al. (1977) measured the earth pressures against ship hoists in German locks over a number of years. They found that wall deformations closely corresponded to seasonal temperature changes, with warmer temperatures causing expansion of the concrete and outward wall movements, and cooler temperatures causing contraction with corresponding inward wall movements. It was also apparent from the measurements that the backfill became increasingly resistant to seasonal deformation with each new cycle, but that over time the toe of each wall would move continuously toward the outer backfill. In a double U-frame lock, constrained by a narrow strip of increasingly compacted backfill between the walls, the soil experienced an increase in earth pressure with each new summer cycle. In a single U-frame structure, however, the seasonal minimum and maximum earth pressures achieved relatively constant values after only a few years. Similar behavior had been noted by Broms and Ingelson (1971) in earlier research on cyclical earth movements in the abutments constrained by a rigid frame bridge in Sweden. Soil nail walls can be seen as more analogous to the double ship hoist, since the earth between the nails is constrained from movement by the nail-grout system and the entire active earth pressure wedge is constrained by the anchoring of the nails behind the wedge. This case history indicates that cyclical pressures in a soil nail wall can be expected to increase over time with each successive season, although a soil nail wall will experience its highest tensions in the nails during the colder months whereas the double ship hoist experiences highest soil stresses during the warmer months. However,

it is possible to have both winter and summer cyclical stresses in a single structure. Soil pressure monitoring in a steel frame bridge at The Forks, Maine, originally intended to monitor the pressure increases behind the abutment due to bridge deck expansion during summer heating, also revealed significant cyclical pressure increases between January and March in a supposedly "frost-free" backfill material. These unexpected winter pressure increases were attributed to frost heaving in the 1-2 m (3-6 ft) of soil between the normal river level and the daily dam-release high water line, due to the continuous seasonal ice buildup in this region (Sandford, 1997).

Similarly, frost-induced stresses in other types of anchored walls may provide valuable insight into the general behavior of frost susceptible soil under the influence of steel insertions. Some of the case histories which follow describe anchored tieback and reinforced earth walls rather than soil nail walls. Although the observed magnitude of deformation is much smaller in soil nail walls, the seasonal stress patterns in other anchored wall systems are remarkably similar.

### 2.4.1. Seasonal stresses in anchored tieback walls, Canada

Morgenstern and Sego (1981) reported on the effects of frost on an anchored tieback wall in Edmonton, Alberta. Cognizant of previous failures of tieback walls due to frost action (Sandegren et al., 1972; Stille, 1976), the authors instrumented a temporary wall constructed during the winter of 1976-77 for the Canadian Pacific Railway. The 7-m wall was constructed in stiff fissured Lake Edmonton clay overlying dense glacial till. A conservative design approach was used due to the uncertainties of developed earth

pressures in the clay and the lateral earth pressure component anticipated from the adjacent train tracks. Readings on load cells, temperature gages, and wall deflection were taken from December 1976 through July 1977. A cyclical pattern was clearly established, in which the anchors experienced high stresses as temperatures dropped below freezing and lower stresses as temperatures warmed. At peak loading during mid-February, the anchors were carrying 120% of the design load: approximately 600 kN (134 kips) compared to a design load of 498 kN (111 kips) in the lower anchors, and 380 to 400 kN (84.8 to 89.2 kips) compared to a design load of 334 kN (74.5 kips) in the upper anchors. By April 10, the loads in the anchors had leveled off, apparently indicating that the soil had thawed; they showed no more reaction to temperature variation. At the end of the monitoring period in July 1977, the tension in the upper anchors averaged 33% less than the design load, while the lower anchors averaged 58% less. Because ground movements were minimal and the design load was conservative, wall performance was deemed acceptable; however, the authors point out that in situations where it is critical to maintain transfer of the initial design loads into the ground, anchors installed in winter should be restressed after spring thaw (and possibly relaxed again before the onset of winter).

### 2.4.2. Seasonal stresses on temporary soil nail walls, French Alps

Guilloux et al. (1983) discussed the use of soil nailing to construct temporary retaining walls for an underground carpark at La Clusaz in the French Alps, at an elevation above 1000 m (3300 ft). The soil was described as moraine, i.e. compacted glacial till, with a density of 22 kN/m$^3$ (139 pcf). The density of the soil and the presence

of large boulders made it difficult to place the soldier piles for a Berlin wall as originally specified, so soil nailing was proposed as an alternative in order to complete construction before the onset of winter. Ultimately, the Berlin wall technique was used for the east wall while soil nails were used for the north and south walls, to a maximum height of 14 m (46 ft). At the client's request, the engineers installed a wall monitoring system. This consisted of surveying measurements of wall movements at 24 points across the entire excavation, and welded strain gages placed at four locations along each of four nails. The winter of 1980-81 was particularly severe, with frost penetrating to 0.4 m (1.3 ft) behind the shotcrete facing, or approximately 0.55 m (1.8 ft) from the exposed surface of the wall. The following observations were made:

1) The distribution of stresses along the soil nails were not uniform with depth, but reached a maximum at a short distance behind the facing. The engineers were able to trace a pattern of maximum forces in the strain gages along the nails, which roughly corresponded to the development of a wedge-shaped zone of active earth pressure at the back of the shotcrete facing. They postulated that this wedge was held in place by the friction between the soil and the nails. The gages placed furthest from the shotcrete exhibited very little increased stress even during the peak frost months of February and March.

2) The mobilized loading in tension for *most* nails remained low in comparison to their capacity, generally less than ¼ of the yield strength of the steel, *except in the region immediately behind the facing*. Here, some of the nails experienced tensile stresses approaching the yield strength. On one nail, the force behind the facing increased from 20 kN (4.5 kips) at installation to 400 kN (89.2 kips) in late February. At that

point, fearing the potential for plastic deformation if the nail stresses continued to increase, the engineers relaxed the tension in all of the nails. Thus an assessment of the total seasonal magnitude of frost-induced stresses was not possible.

3) Horizontal wall displacements were 1 to 2 cm (0.4 to 0.8 in) or approximately 0.1% of wall height, within the expected range for a soil nail wall.
4) While displacements did not increase significantly after installation was completed, the tensile forces on the nails increased regularly from December to the end of February, when the anchors on the nails were released and rebolted to reduce stresses. By late April, the stresses on the nails had decreased to approximately the same values observed before the onset of frost conditions.

The measurements taken by Guilloux et al. at La Clusaz in 1980-81 were later used by Unterreiner (1994) to refine and check his model for frost deformation, as described earlier in this section.

### 2.4.3. Winter failure of reinforced earth wall with successful soil nail reconstruction, France

Another French case history from the winter of 1980-81 was presented by Long et al. (1984). In this case, a section of a reinforced earth wall along the access road to Frejus Tunnel, elevation 1200 m (3900 ft), failed in March 1981 after a defective manhole seeped and caused excessive frost expansion of the soil behind the wall facing. The frost action ruptured several tie strips at their connections in the failure zone and created a bulging deformation of adjacent facing units. The wall was repaired in situ,

without disrupting traffic, by reconnecting the tie strips to a new poured concrete facing in the ruptured areas and soil nailing through the centers of existing concrete facing blocks in the deformed areas of the wall. The wall was also instrumented at this time to gain a better understanding of its behavior under frost conditions during the following winter, using temperature gages along the back of the facing and on top of the wall, load cells on the end of three of the soil nails, and LCPC leveling gages on the concrete facing panels. Data from the winter of 1981-82 showed that the frost penetrated the wall to a maximum depth of 4.2 m (14 ft) behind the facing near the top of the wall (influenced by a two-way frost front progressing from the top as well as the front of the wall), decreasing to about 1.5 m (4.9 ft) along the lower wall area. The highest stresses on the soil nails were observed on 23 February, when air temperatures had already begun to rise, but prior to maximum frost penetration (early March). Rotation of facing elements was minimal, even at the maximum observed tensile loading. The observed nail stresses at the center of the facing blocks were used to back-calculate approximate values for maximum stresses on the reinforced earth strips at the time of the previous year's failure (i.e., before the nails were placed). These forces were determined to be less than the shear strength of the tie-strips, but greater than the yield strength of the steel in the connections. This calculation helped to confirm the cause of the wall's failure and indicated that, without the soil nails in place, the wall might have been subject to another failure of the same type during the winter of 1981-82, especially since seepage continued throughout the second winter despite additional drainage control measures.

### 2.4.4. Seasonal stresses in FHWA demonstration soil nail wall, Cumberland Gap, Kentucky

Nicholson (1986a, 1986b) described the performance of a soil nail wall in a tunnel project through the Cumberland Gap on the Kentucky-Tennessee border. The 12-m (39-ft) high wall was constructed in a soil of unspecified grain size derived from weathered shale and sandstone, underlain by the weathered bedrock. Because the wall was contracted as a demonstration project for FHWA, it was instrumented with slope inclinometers, strain gages, load cells, and electronic distance measuring (EDM) survey points on selected nails. The wall facing was a second 7.6 cm (3 in) of shotcrete.

During the winter months, seepage through the shotcrete face caused an ice buildup in the wall. Drainage strips had been placed during construction on 4.6 m (15 ft) centers, but these proved inadequate for the actual quantity of seepage. The author recommended 1.5 m (5 ft) centers for drainage strips on future soil nail projects. During January and February 1986 (four months following installation), the loads on instrumented nails increased from 2000-2400 kN (450 to 540 kips) to 4000-5000 kN (899 to 1120 kips), apparently as a result of frost heave behind the wall. Following the spring thaw, the loads dropped off again. (Note, however, the comments of Juran and Elias (1987) with regards to this case history, summarized in the next paragraph.) The nails, which had been sized conservatively for this design, handled the higher seasonal loads without problems.

Deformations of the Cumberland Gap wall were on the order of 0.5 to 1 cm (0.2 to 0.4 in), less than 0.1% of wall height. Juran and Elias (1987) surveyed performance criteria for several instrumented soil nail projects (including Cumberland Gap) and observed that displacements and ground movements in soil nail walls normally do not exceed 0.2 to 0.3% of wall height in nonplastic soils, since very little movement is required to mobilize the nail tension. They also noted that, although the Cumberland Gap nail loads all decreased noticeably following the spring thaw, tension in sections closest to the facing remained permanently elevated over initial values. For example, strain gage data for a point 7.6 cm (3 in) from the wall face, with a post-construction load of 20 kN (4.5 kips) and a maximum observed load of 70 kN (16 kips) in February 1986, decreased to a constant load of about 50 kN (11 kips) in the spring of 1986. The authors attributed this increased tension near the wall face to local dislocations and volumetric strains in the soil, induced by frost movements and restrained by the nail friction. This is similar to the gradual yearly increase of earth pressure noted by Smoltczyk et al. (1977) in the Lunenburg double ship hoist, although at Cumberland Gap the cyclic strain cycles were induced by winter frost rather than summer heat.

### 2.4.5. Seasonal stresses on a terraced highway wall, Germany

Schwing and Gudehus (1988) examined the effects of frost on a 7-m (23-ft) soil nail wall with a 70° slope, constructed for a road project in West Germany. The wall was constructed in three terraced sections, and the terraces were filled with topsoil and planted to disguise the shotcreted surface of the wall. The soil type was described as several meters of loam, unit weight 20 kN/m$^3$ (126 pcf), underlain by weathered Keuper

marl (*Gipskeuper*). The wall was instrumented with four "pressuremeters" (sic; author is apparently referring to load cells) to measure nail head forces and four extensometers to measure wall displacement, and it was monitored for 2½ years to determine the effects of repeated freeze-thaw cycles. The results proved conclusively that both force and displacement increased with frost duration, with nail head forces rising to about double their initial values during winter months. The forces decreased again in the spring but remained elevated over their initial values, as with the Cumberland Gap wall. In the second year's freeze-thaw cycle, nail head forces achieved approximately the same winter maximums and summer minimums as in the previous year. Maximum wall displacements ranged from 0.26 to 0.32 mm (0.01 to 0.0125 in) in the bottom terrace and from 0.13 to 0.20 mm (0.005 to 0.008 in) in the center terrace. These movements, while very small, correlated very strongly with freezing conditions behind the wall. During summer months, as with the nail head forces, the displacements diminished but were not entirely reversed. Schwing and Gudehus's research also seems to confirm Juran and Elias's theory that freezing causes volumetric strains in the soil which mobilize additional resistance in the nails, resulting in cyclic stress increases accompanied by small but measureable permanent displacements. Similar cyclical displacement behavior was also noted by Kuzevanov and Shulyatyev (1997) in short piles subjected to frost heave.

### 2.4.6. Design to accommodate severe frost heave in soil nail walls, Canada

Alston (1991) designed a soil nailed slope reinforcement project in Cambridge, Ontario, in which a naturally stable hillside was reshaped from a grade of 1v:2h to 3v:1h (approximately 72°) to permit construction of a luxury highrise condominium in a river

valley. The original plans for the 18-m (59-ft) wall called for two separate retaining structures: a temporary support wall of soldier piles and lagging in the basement levels, and a permanent reinforced concrete gravity wall from the main floor level to the top of slope. This plan was scrapped when adjacent property owners refused to provide access or excavation easements for construction, so a soil nail alternative was developed. The soil nail wall also resulted in a 40% cost savings over the original design.

The soil at the site was a very dense glacial till, with a unit weight of 22.5 $kN/m^3$ (142 pcf). It was known to be highly frost susceptible, with mostly silt sizes and numerous clay lenses, which created numerous perched water tables throughout the area to be nailed. Using a design based on the German limit-equilibrium method described in Stocker et al. (1979), the nails were placed on a 1.8 by 1.5 m (5.9 by 4.9 ft) grid with three graduated nail lengths ranging from 6.5 to 12 m (21 to 39 ft) depending on the height of slope. Shotcreting was not required for face stability – the soil could stand unsupported at near-vertical inclinations for 1 to 2 weeks – and the drainage qualities and aesthetics of shotcrete were considered less than optimum for this project. Instead, the wall was designed with a flexible, permeable facing to accommodate the anticipated cyclic volume changes and load variations due to frost, as well as to facilitate drainage from saturated zones along the face of the wall. A system of geotextile (for drainage, surface erosion control, and fines retention) with geogrid overlay (to transfer earth pressures to the soil nails) was used over most of the wall, with a slurry of sand, topsoil, and water injected between the geotextile and the native soil to fill any voids.

In one area of the wall construction, severe and chronic seepage problems at the face (later determined to be caused by a leaky water main at the top of the slope) caused continual and progressive slumping which could not be stabilized before the onset of winter. Further damage occurred during the winter season, which was marked by numerous freeze-thaw cycles and heavy rains alternating with snow. During the spring thaw, this portion of the wall was protected from further slumping by a restraining geotextile membrane, held in place by a timber grillage connected to the soil nails. The area was reconstructed with a geogrid-reinforced "pillow" of granular fill placed in the slumped area between the scarp slope and the rest of the wall, with a facing of geocomposite (Geoweb filled with sand). The design assumption here was that the soil nails would continue to retain the soil behind the scarp slope, while the geocomposite facing would resist any forces developed in the active pressure wedge formed by the pillow of reinforced fill. Horizontally placed strips of geogrid were used to sculpt the reconstructed elements into conformation with the rest of the wall and to tie the new elements into angle bars attached to the soil nails, thus transferring much of the loading back onto the nails. This arrangement is illustrated in Figure 2-10.

In the basement area, a temporary soil nail wall was constructed with an 80° slope, covered only with a lightweight geotextile for drainage and erosion control. It was designed for a 2-month lifespan ending with construction of the permanent basement, which was scheduled for completion prior to the onset of winter. Because of major delays on the project, the temporary wall in fact remained in place throughout the first winter, and experienced some surface sloughing as a result of repeated freezing and

thawing. A timber grillage tied into the nails provided the necessary support to maintain this wall and extend its life. In all other aspects, the wall performed well during its first two years of operation. The author noted that the post-construction monitoring program would consist of two detailed visual inspections per year, one after spring thaw and one before winter onset.

### 2.4.7. Use of insulation to reduce the effects of frost heave in soil nail walls, Maine

The mountainous western interior of Maine is noted for its severe winter climate and highly frost susceptible, glacially deposited soils. Kingsbury (1999) performed extensive research on a soil nail wall that was constructed in this region in 1997. A followup paper, focusing on the long-term cumulative effects of seasonal frost heave on this wall, was later presented by Kingsbury et al. (2002).

A perennially high groundwater table, combined with downward-sloping shallow and exposed bedrock that channels groundwater and early spring snowmelt toward the river from the surrounding mountains, provides a constant water source through highly frost-susceptible sandy silt—the worst-case combination in the dense glacial till of mixed sand, gravel, silt, and clay which characterizes the construction site, due to the potential for sustained capillary action through the silt-size particles to form large ice lenses behind the wall. Because of the high potential for damaging frost heave under these conditions, Moscow was designed as one of the first well-documented soil nail projects in the U.S. to incorporate insulation materials at the face.

To accommodate variable depth to bedrock, some of the nails were drilled and grouted into rock while others were grouted into soil. The wall was heavily instrumented for research and monitoring, featuring vibrating wire strain gages, piezometers, load cells, tiltmeters, total pressure cells, concrete strain gages, thermocouples, an inclinometer, and survey points to gage overall settlement during construction. Strain gages and thermocouples were tied into an automated datalogging system to permit remote downloads by modem 12 times per day. To further understanding of the principles of soil nail wall behavior under severe frost conditions, one small section of wall was instrumented but left uninsulated to serve as a control for comparison against the insulated sections.

Despite the climate and soil conditions, frost loads were not incorporated into the design of the nails and wall components. It was assumed that the use of 10 cm (4 in) of polystyrene board insulation and geocomposite drainage strips behind the wall face would be adequate to protect the wall against damage from frost heave. In the first winter of observation (1997), all peak nail head tensile forces stayed considerably below the design force of 68 KN (15 kips). However, by the third winter of the study, peak seasonal nail head tensions in the topmost nail rows in both the insulated and uninsulated sections had quadrupled, exceeded the design value (Kingsbury et al, 2002), despite the fact that all three freezing seasons were milder than both the design winter and the mean historical winter for the region. One upper nail head registered a peak tensile force

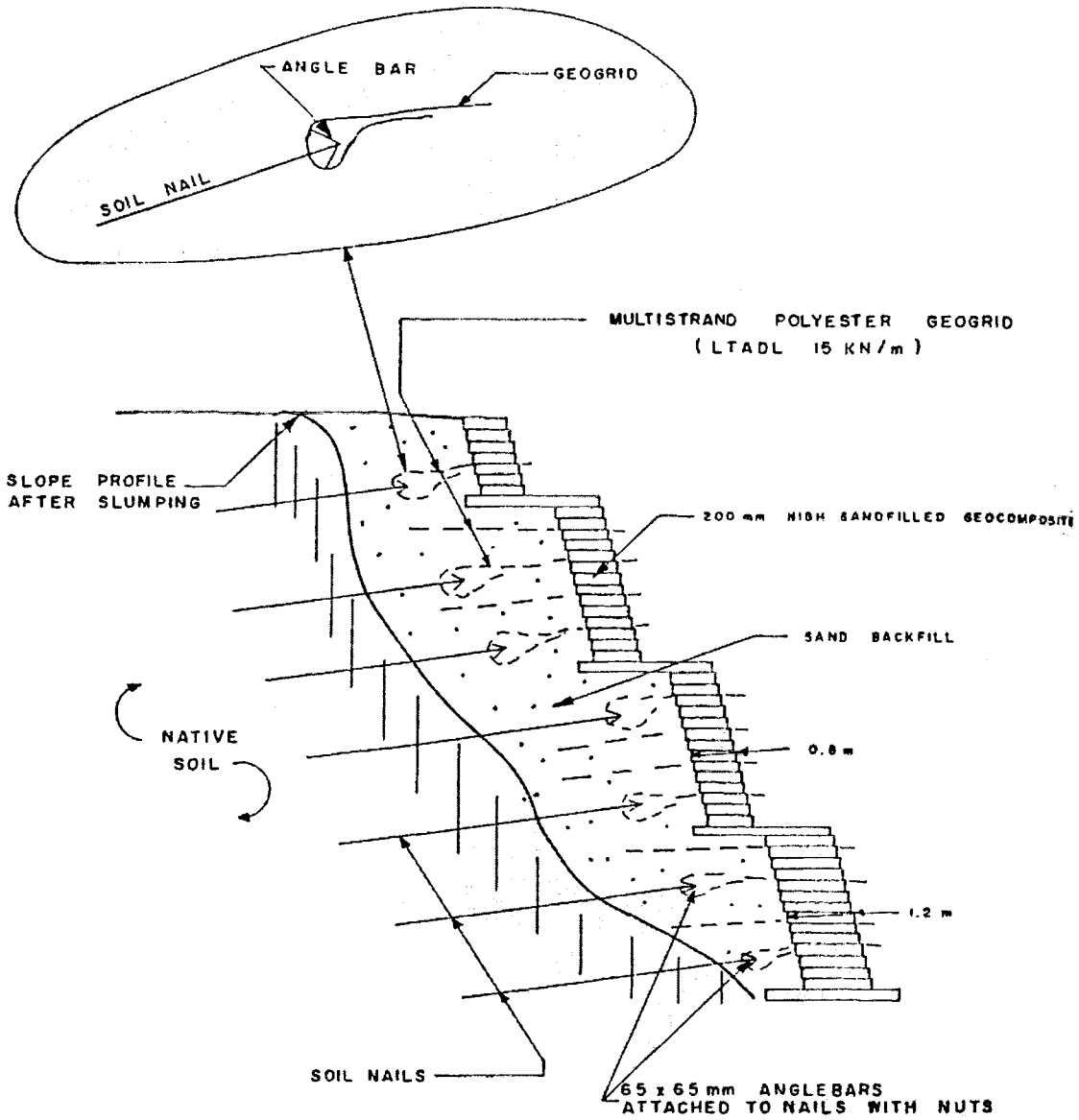


Figure 2-10: Schematic representation of slope facing reconstruction using geosynthetics (after Alston, 1994)

increase due to frost heave in the third season that was 73 KN (16 kips) above post-construction, fully-mobilized soil shear values, and the load cell on an uninsulated upper nail head failed in the second observation season shortly after spiking to over twice the peak tensile value noted during the first winter (Kingsbury et al., 2002). An additional finding of the long-term study was that the magnitude of residual seasonal tension decreased in accordance with an exponential decay function in each successive season, as described earlier in this chapter.

Through finite element analysis modeling of different temperature regimes up to and including the design winter condition, Kingsbury (1999) was able to conclude that insulating the top of the wall in addition to the face would not only have reduced the peak nail head tensions and cumulative seasonal tensile forces in nails located within the bi-directional frost front near the top of the wall, but would have reduced the thickness of insulation required at the face of this particular wall by approximately half.

## 2.5. Summary

Severe winter conditions in frost susceptible soils can increase the tensile stresses in soil nails, in some cases to near or above the yield strength of the steel. Even before the yield value is reached, frost heaving close to the face of the wall can cause facing cracks or connection failures. Although the tensile stress values drop after the soil thaws, several well-instrumented case histories have shown that some residual stress remains in the nails. Thus each successive cold cycle causes increasingly higher stresses, unless the tension in the nails is mechanically relieved by loosening the end nuts after each winter

season (a difficult undertaking if a reinforced concrete facing has been applied over the shotcrete). For dense glacial tills, a reasonable estimate of lifetime residual seasonal stress due to frost heave is approximately 2.5 times the maximum (first-year) seasonal increase, as each season the increase will be progressively less and it can be modeled using an exponential decay function. Design measures to prevent wall damage from frost heave include insulation along the face and top to prevent or minimize frost penetration, increasing the diameter of nails in the top rows to handle cumulative seasonal stresses, the addition of short nails in the soil spacing between design-length nails, or adding a free unbonded length to the head of each nail so that the grouted zone starts beyond the predicted frost depth. Economic considerations normally govern the selection of preventative measures.

Severe frost heave causes soil expansion and movement upward and outward from the toe of a retaining wall during the heaving phase, followed by weakened soils and consolidation as the soil thaws. In a soil nail wall, frost heave behavior is highly non-linear due to the interactive coupling of hydraulic, mechanical, and thermal factors; it must be modeled iteratively using a finite element program. However, there is no need to account for daily temperature variation in calculating the frost penetration depth, as it can be predicted equally well using the seasonal surface frost index. The modified Berggren method permits calculation of frost penetration through multiple layers (reinforced concrete, shotcrete, soil) and accounts for volumetric heat capacity, and thus it is superior to Stefan's method which overpredicts frost depth by about 10%. Frost penetration from

the nails into the soil can be estimated using approximate solutions and polar coordinates to determine distance to the phase change boundary from the center of an infinitely long cylinder.

# CHAPTER 3

# PROJECT CONSTRUCTION AND INSTRUMENTATION

## 3.1. Overview

This project was the first known use of soil nail retaining walls in the state of Maine. The walls were constructed from the existing embankments of a railroad overpass on Route 1, in order to create lane space for exit ramps to the new Brunswick-Topsham bypass bridge over the Androscoggin River. The University of Maine instrumented the north-facing wall in order to monitor the performance of the soil nails under freezing conditions.

This chapter describes the site characteristics, soil conditions, design and construction, and installation of instrumentation in the wall. Difficulties encountered during construction, and the methods used to overcome these difficulties, are also discussed.

## 3.2. Site characteristics

The site is located in southern Maine on the Route 1 Bath-Brunswick highway corridor, beneath a railroad bridge appoximately 1.0 km (0.6 mi) east of the Route 196 overpass in Brunswick. Although the highway is labeled Route 1 North/South, the roadway in this area actually runs east-west. The roadways are therefore labeled as "eastbound" (Route 1 North) and "westbound" (Route 1 South) throughout this thesis. The soil nail

wall which was instrumented for this project is also referenced in the text as the north-facing wall -- i.e., the wall adjacent to the breakdown lane of eastbound Route 1, with its face to the north.

The existing roadway was a divided highway, providing two high-speed driving lanes and a breakdown lane in each direction. The railroad bridge is approximately 55.5 m (182 ft) long and is supported on two abutments and three piers resting on embedded steel H-piles. The outer piers are located adjacent to the eastbound and westbound traffic lanes and the central pier is located in the median strip, as shown in Figure 3-1. The existing soil embankments surrounding the abutments were 4.6 to 5.5 m (15 to 18 ft) high on a 2H:1V slope from the roadway. The bridge abutments were reinforced laterally by batter piles passing through the embankments at a 1H:6V slope toward the roadway.

MDOT plans for the Brunswick-Topsham Bypass called for removing the 2H:1V slopes from the two abutments (as shown in Figure 3-2) in order to create space for new exit ramps to the bypass bridge, using retaining walls to provide lateral support as near-vertical faces were excavated directly beneath and adjacent to the abutments. The pier and abutments had to remain intact, as the bridge supported daily railroad traffic which could not be rerouted. The geotechnical consultant, Haley and Aldrich, Inc., considered three alternatives for construction of the retaining walls: soil nailing, a Berlin wall using anchored soldier piles and lagging, and in situ grouting of the embankment fill. Of these three, a permanent soil nail structure was determined to be the most cost-effective and

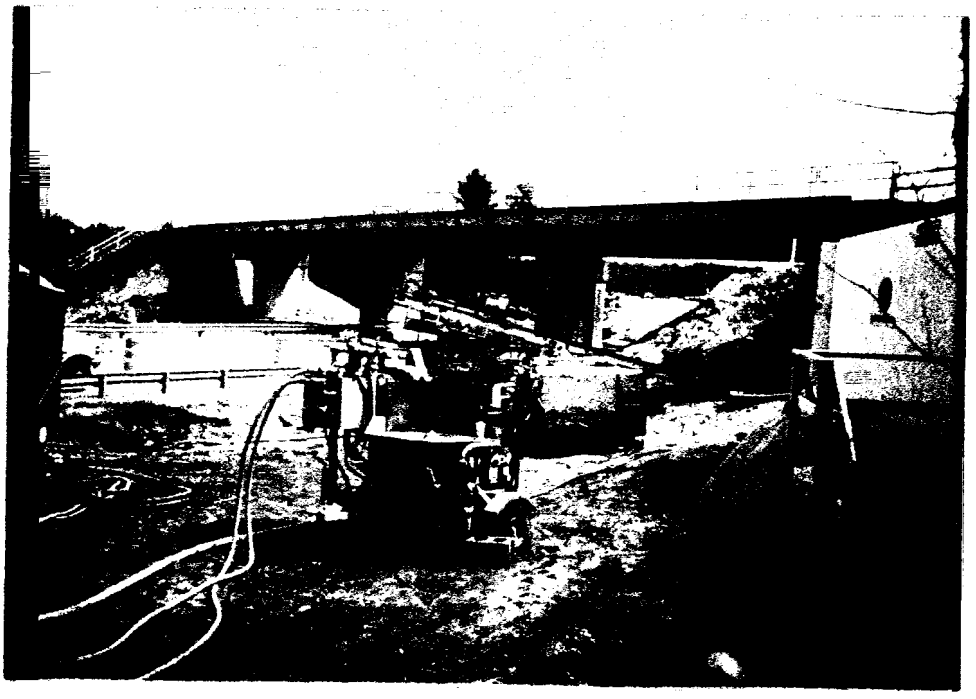

Figure 3-1: View (facing northeast ) of existing railroad bridge during initial clearing operations for soil-nail wall, showing abutments and three center piers

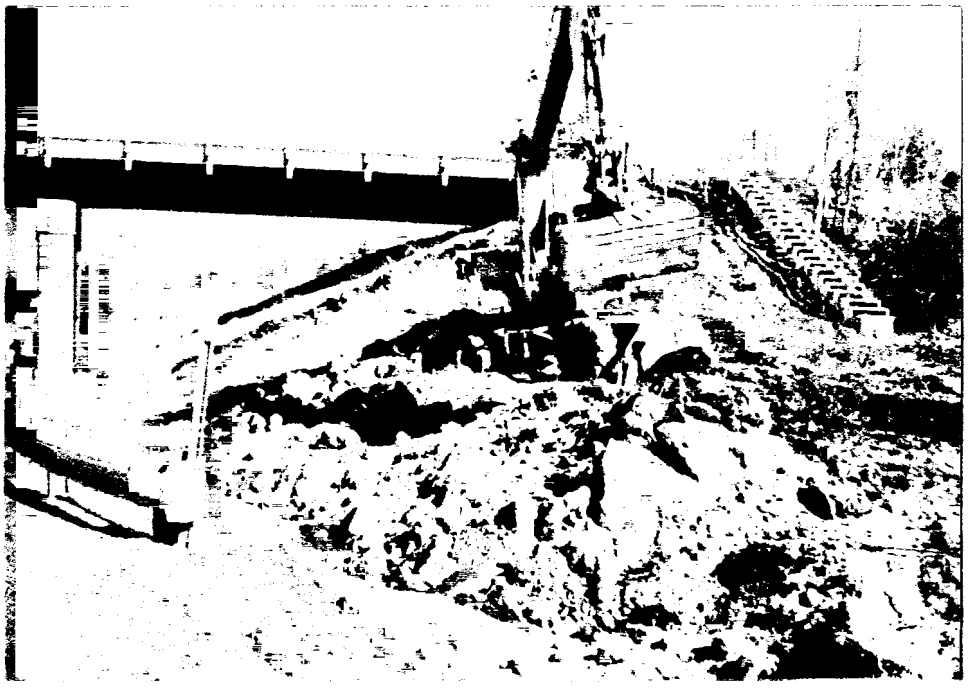

Figure 3-2: View of abutment and pier adjacent to eastbound lane of Route 1. Existing 2:1 slope (shown) was replaced with a soil-nail wall to created a new exit lane.

technically feasible method. It was easier to construct in the low-headroom conditions under the railroad bridge and would not require holes to be drilled through the bridge as with soldier piles, and it offered a higher degree of verifiable soil support than in situ grouting (Whetten and Weaver, 1995). Soil nailing also provided the engineering flexibility to reposition individual nails in the field without a total redesign. This flexibility was important because the current locations of the batter piles were approximated from the as-built drawings submitted in 1960.

Weather at the Brunswick site is typified by temperate summers and cold winters, although the nearby Atlantic Ocean provides a heat sink which keeps the winter temperatures considerably warmer than further inland. For example, the 30-year mean freezing index for this area (Bigelow, 1969) is 427 C degree-days (800 F degree-days), as compared to 994 C degree-days (1822 F degree-days) in Greenville. Freezing degree-days are calculated for each day using the following equation:

[ (average daily temperature ) - (freezing temperature, 0° C or 32° F) ] * 1 day **(3.1)**

The freezing index is then determined by plotting cumulative freezing degree days versus date. The freezing index is the difference between the maximum and minimum freezing degree-days on this plot, and the mean freezing index is calculated by taking the seasonal average based on multiple years of observations.

### 3.3. Soil conditions

Test borings from the top of the abutments (Whetten and Weaver, 1995) indicated 2.3 to 7.6 m (7.7 to 25 ft) of fill, overlying a marine outwash deposit of fine sand. The fill was typically described as loose to medium dense, brown, medium to fine sand, trace to some gravel, trace to little silt, with 60 to 150 mm (0.2 to 0.5 ft) of fine sandy silt topsoil at the surface. The groundwater table was observed at a level close to the bottom of the fill in November 1994.

Two near-vertical test pits (one on each side of Route 1), each approximately 4.6 m (15 ft) long and 1.8 m (6 ft) deep, were excavated in sections of the embankment slopes which later would be removed during construction of the soil nail walls. The test pits were left open and unsupported for one week, and exhibited very little movement or loss of soil during that time. The test pits indicated that there was sufficient apparent cohesion to favor construction of soil nail walls, which typically require the soil to remain stable in a vertical bench cut for several hours following excavation in order to to drill and grout the nails and shotcrete the face. However, noting that loose areas (SPT blow count of 5 to 10) were encountered in the lower portions of the embankment borings, the geotechnical consultants advised that contractors should anticipate caving and low soil strength in these areas and plan accordingly (Whetten and Weaver, 1995). Also, because the soil was essentially granular and cohesionless, the excellent soil standup time observed in the test pits was attributed to apparent cohesion and/or to a favorable combination of soil gradation sizes at the natural water content; the consultants cautioned that precipitation during construction could raise the water content enough to

reduce the predicted stability of the vertical cuts. Very little precipitation occurred during the week that the test pits were left open.

The subsurface investigation report of the Maine State Highway Commission Soils Division for the Route 1 Underpass, issued in January 1960, indicated that there were significant deposits of peat and other organic soils in the vicinity of the underpass. However, that report also indicated that there was no peat below the railroad embankments. Test borings in the embankments in 1994 appeared to confirm the earlier report; nonetheless, peat was encountered in two drill holes in the lowest (fourth) row of soil nails during the grouting operation. This event is described in more detail later in this chapter. Peat deposits extending (6 to 10 ft) in depth were also found in close proximity to the walls on both sides of Route 1. Because of concerns about global stability of the wall as well as heavy equipment requirements, some of the surrounding peat was excavated and replaced with granular fill during wall construction.

The groundwater table was estimated by the geotechnical consultants to be located close to the surface of the natural topography of the site, near the bottom of the placed embankment fill. This was confirmed during wall construction. Although the nails in the bottom row had to be grouted by displacing groundwater along part of their length (due to their placement at 15° below horizontal), there was no groundwater encountered at the face of the wall. Therefore no sloughing or loss of stability at the wall face occurred due to seepage.

As shown in the grain size distribution graphs in Figures 3-3 through 3-5, the soil samples taken from the abutment contained from 2% to 13% finer than 0.02 mm. Using criteria developed by the U.S. Army Corps of Engineers, the frost susceptibility of this soil would be classified as "possible" at 3% to 10% finer than 0.02 mm, "negligible to high" at 10 to 15%, and "very low to high" above 15% (Chamberlain et al., 1984). The classification of this soil is SP-SM or SM according to the USCS system, and A-2-4 in the AASHTO system. Corrosivity tests (Whetten and Weaver, 1995) indicated that the soil was non-corrosive and the groundwater was non-corrosive to marginally corrosive, so no extraordinary measures were required to protect the nails against chemical deterioration. Either fully encapsulated or epoxy-coated nails were specified (the contractor decided to use both). FHWA criteria state that: "In aggressive ground or for critical structures (e.g., walls adjacent to lifeline high volume roadways or walls in front of bridge abutments) or where field observations have indicated corrosion of existing structures, encapsulated nails should be used" (Byrne et al., 1996; emphasis mine).

The following engineering properties and loading characteristics were used for design of the soil nail walls, for both the embankment fill and the underlying marine sand (Whetten and Weaver, 1995; GeoMechanics, Inc., 1996):

Friction angle, $\varphi$: 30°

Cohesion, psf: 0

Unit Weight, pcf: 115

Seismic acceleration coefficient, a: 0.1

Surcharge loads: 120 pcf multiplied by the vertical distance from top of wall to top of embankment, plus 300 psf train load.

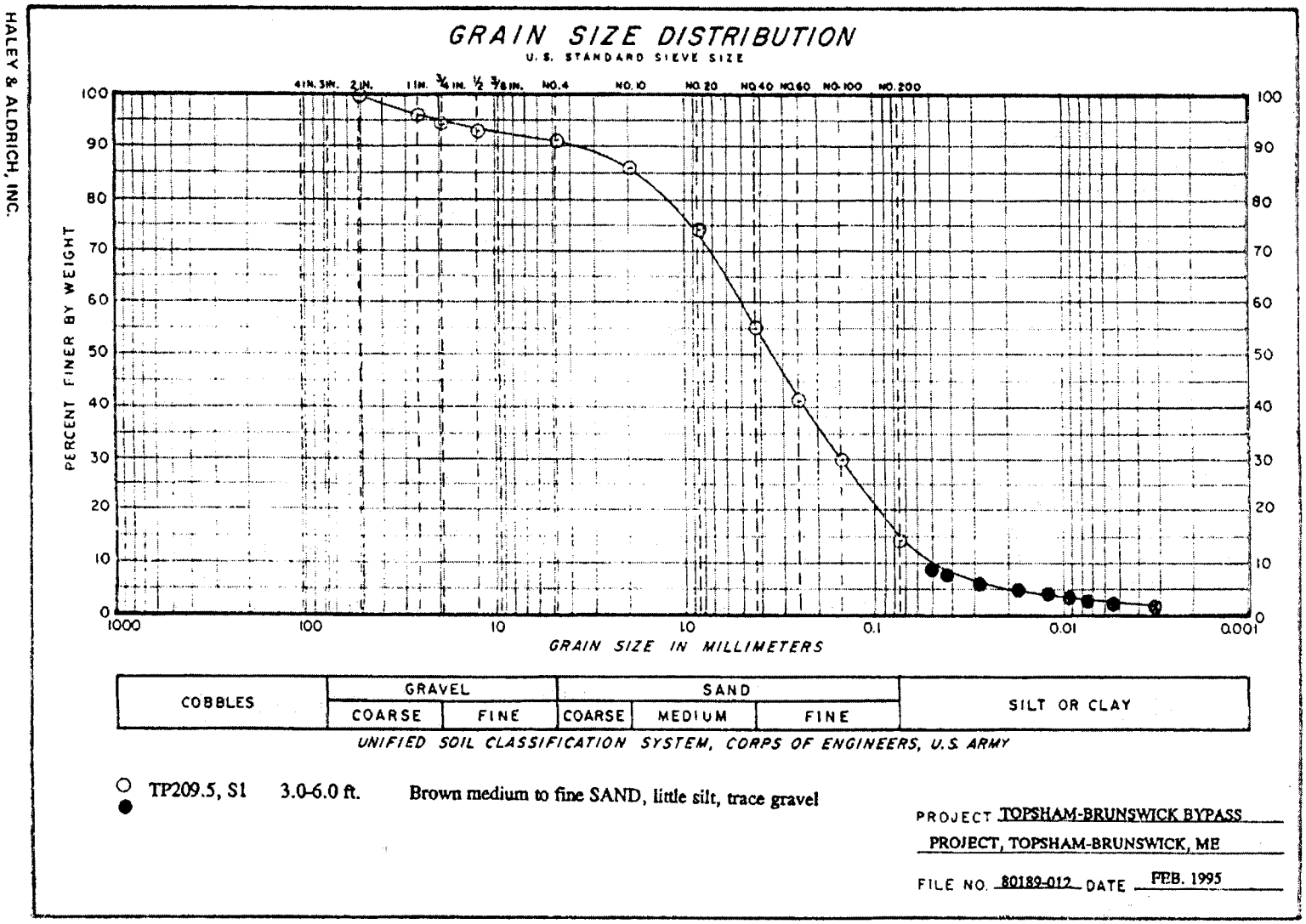


Figure 3-3: Grain size distribution curve from embankment, 0.9-1.8 m (3-6 ft) depth (after Whetten and Weaver, 1995)

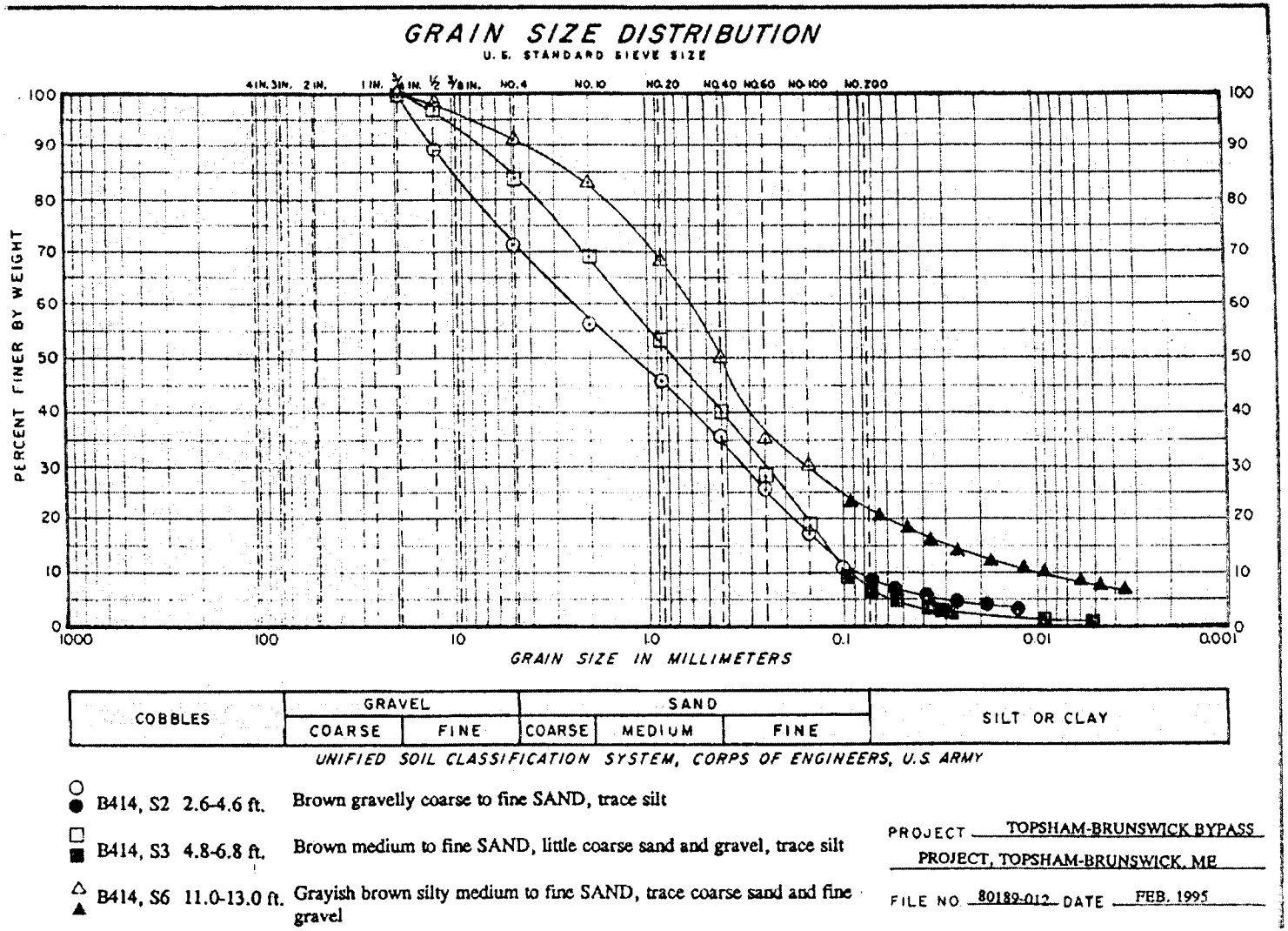


Figure 3-4: Grain size distribution from embankment, 0.8-4.0 m (2.6-13 ft) depth (after Whetten and Weaver, 1995)

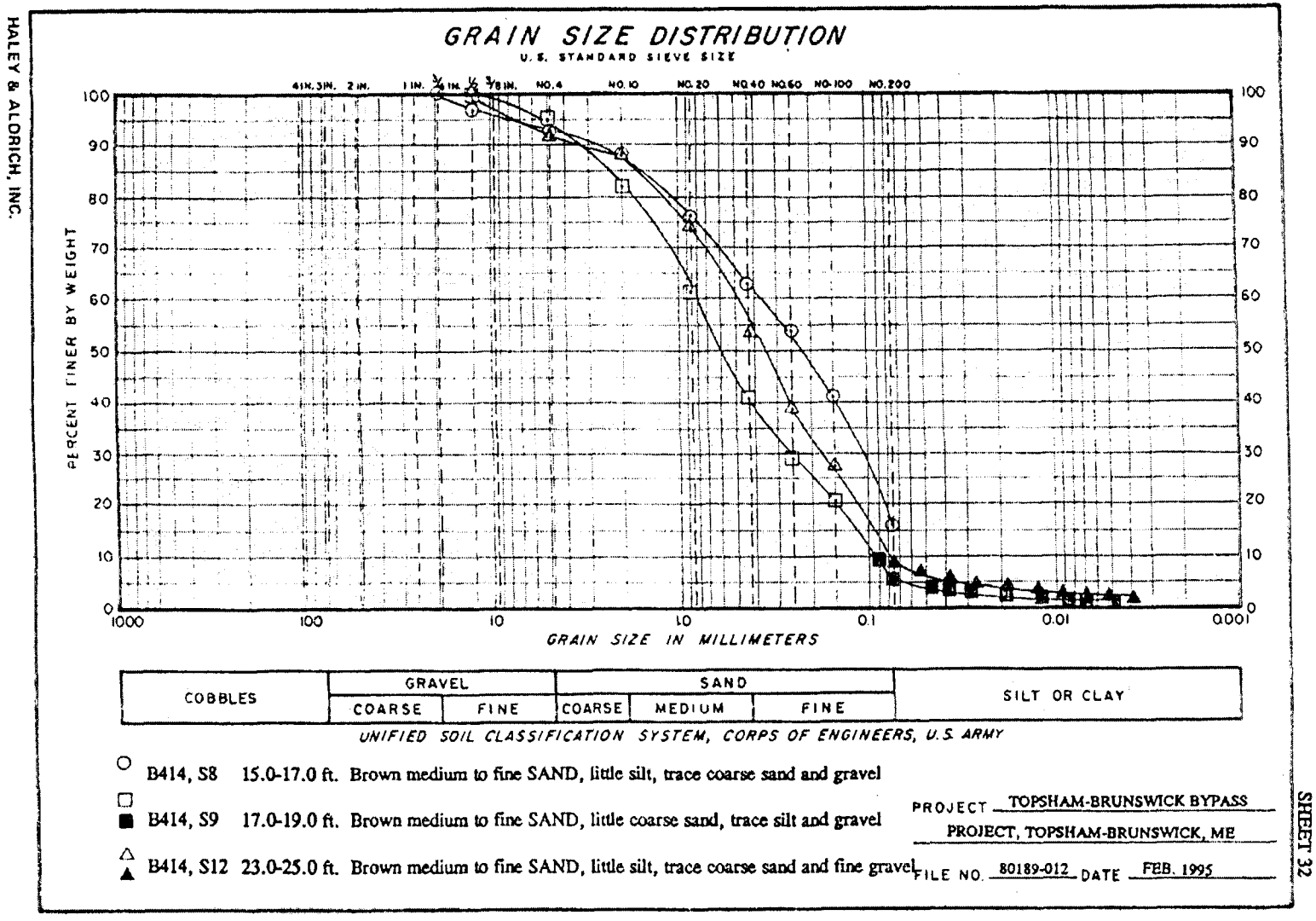


Figure 3-5: Grain size distribution from embankment, 4.6-7.6 m (15-25 ft) depth (after Whetten and Weaver, 1995)

### 3.4. Wall design and construction

Soil nail walls were recommended by the geotechnical consultant as the most economical and technically feasible technique for constructing near-vertical walls in the embankments supporting a working railroad bridge. However, the sand-silt fill presented some potential for frost heave during the winter months. Under similar climatological and geological conditions, a soil nail wall is more prone to frost heave damage than a traditional retaining wall, for two reasons: 1) the in situ soil may contain sufficient fine grain sizes to promote capillary action and the formation of ice lenses, whereas the fill placed behind a traditional wall normally contains only a small fraction of fine particles; and 2) freezing temperatures can be introduced into the soil along the highly conductive steel nails, thus penetrating more quickly and deeply than the frost front proceeding parallel to the wall facing and top of a conventional wall.

To allay concerns about frost heave and wall performance under freezing conditions, the University of Maine developed an instrumentation program for the wall on the eastbound side of Route 1. The wall face on this side of the roadway has a northern exposure which receives little sunlight, and it therefore experiences colder temperatures during winter than the south-facing wall on the westbound side. It was hoped that the results obtained from the wall instrumentation would augment the scant engineering knowlege base on soil nailed walls placed in cold-weather climates and frost susceptible soils, while providing MDOT with an "early-warning system" in case the tensile stresses behind the wall became unacceptably high. This pilot program was also a

stepping stone for a much larger MDOT instrumented soil nail wall project planned for construction on Route 201 in Moscow, Maine during the summer of 1997.

Construction started in May 1996 and was completed in September 1996. For the wall on the eastbound side of Route 1, a total of 66 nails were placed on approximately 1.2-m (4-ft) centers in four rows, as shown in Figure 3-6. Figure 3-7 is a section A-B through Figure 3-6, showing the approximate positions of the H-pile supports, batter piles, and soil nail placement within the abutment. Figure 3-8 is a plan view showing the location of the abutment, support piles, wall, and nails. This drawing shows how the nail locations were adjusted to fit between the H-piles of the abutment.

### 3.5. Instrumentation

The literature review (Chapter Two of this thesis) indicated that increased tension in the nails, potentially to a level approaching or even exceeding the yield strength of the nails or their facing connections, was sometimes observed in soil nail walls subjected to frost heave. Thus a key focus of this research was to determine the load profile along the length of the nails, at the attachments between the nails and the facing, at the soil-shotcrete interface between nails, and within the reinforced concrete facing wall itself. In order to correlate tension readings with temperatures in the soil and along the nails, temperature readout devices were also required. This section describes the types and locations of instrumentation placed within the project to gain a better understanding of wall behavior under freezing conditions.

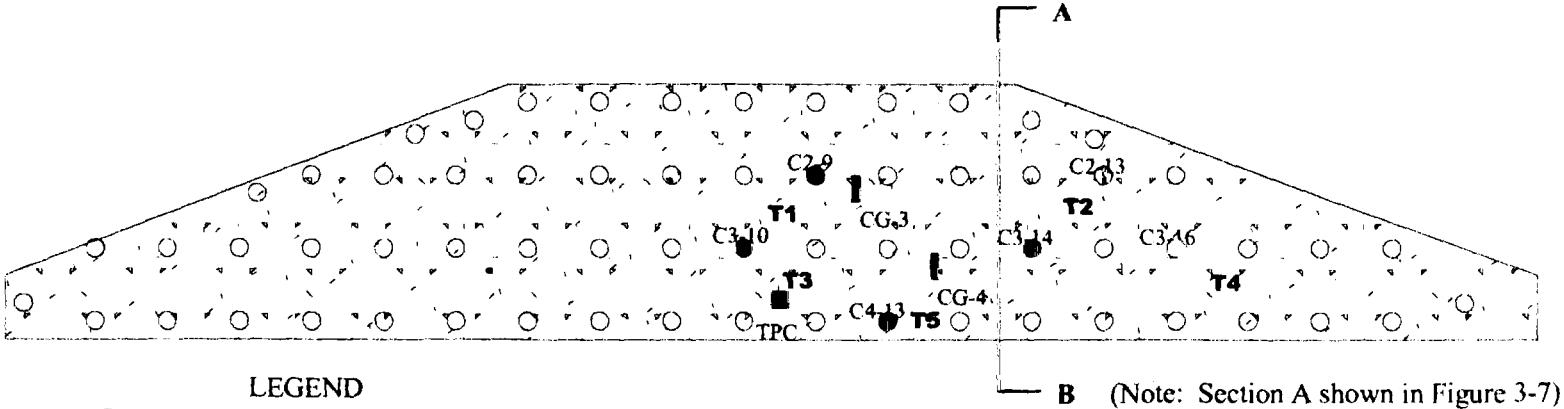


(Note: Section A shown in Figure 3-7)

LEGEND

- C2-9, Soil Nail with 7 Roc-Test Strain Gages, Load Cell, Thermocouples
- C3-10, Soil Nail with 7 Roc-Test Strain Gages, Load Cell, Thermocouples
- C2-13, Soil Nail with 7 Slope Indicator Strain Gages, Load Cell, Thermocouples
- C3-16, Soil Nail with 7 Slope Indicator Strain Gages and Thermocouples only
- C4-13, Soil Nail with 7 Geokon Strain Gages, Load Cell, Thermocouples
- C3-14, Soil Nail with Load Cell only (see Figure 3-4)
- CG-3, CG-4 -- Concrete Strain Gages, embedded in concrete facing wall
- TPC -- Total Pressure Cell, placed behind shotcrete surface between four soil nails
- T Thermocouple strand on wooden rod -- identifying numbers shown (T1, T2, etc.)

Scale: 0 1 2 3 4 5 meters

Figure 3-6: Profile of instrumented north-facing soil nail wall, Brunswick-Topsham Bypass

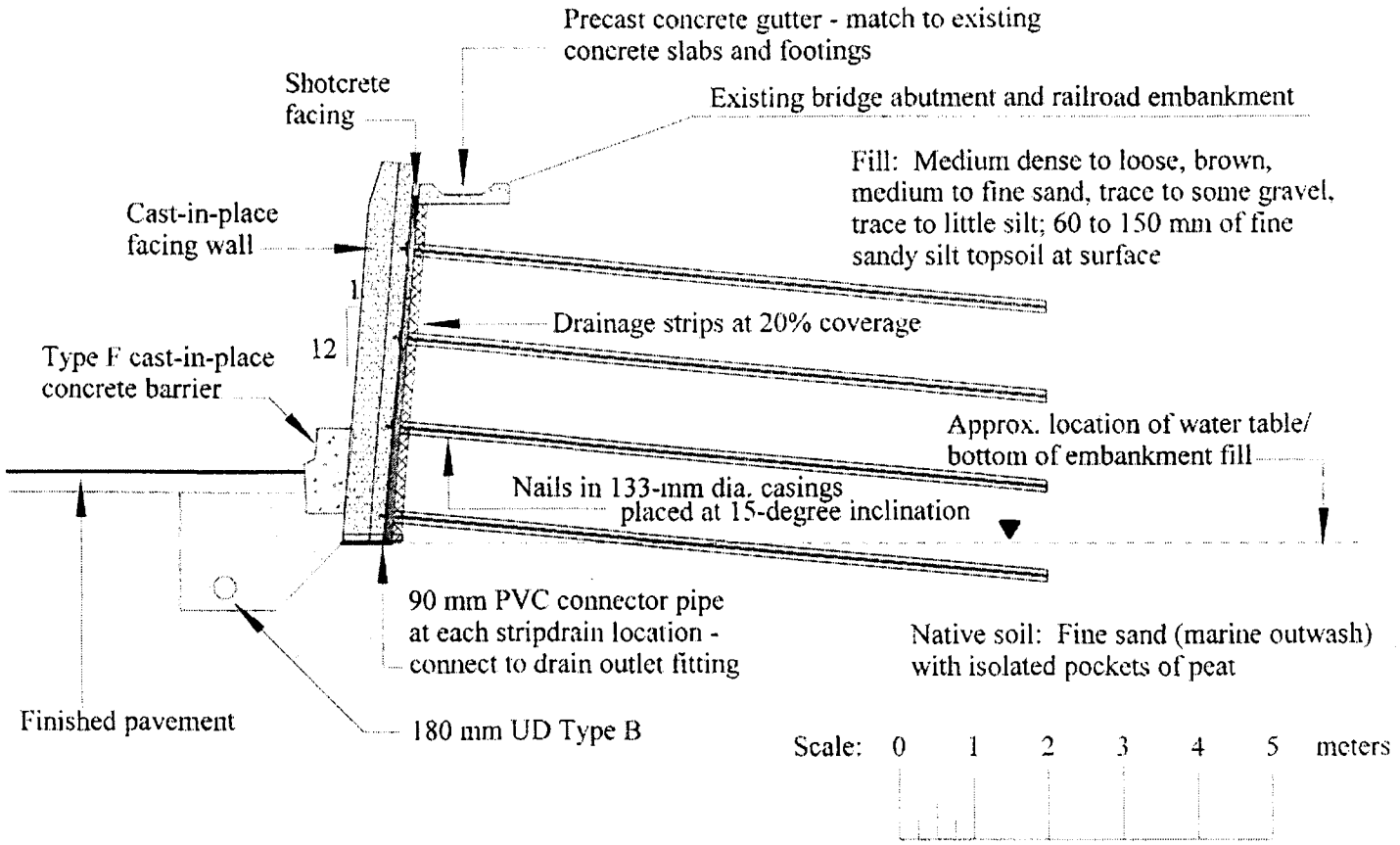


Figure 3-7: Section view A-B through north-facing abutment

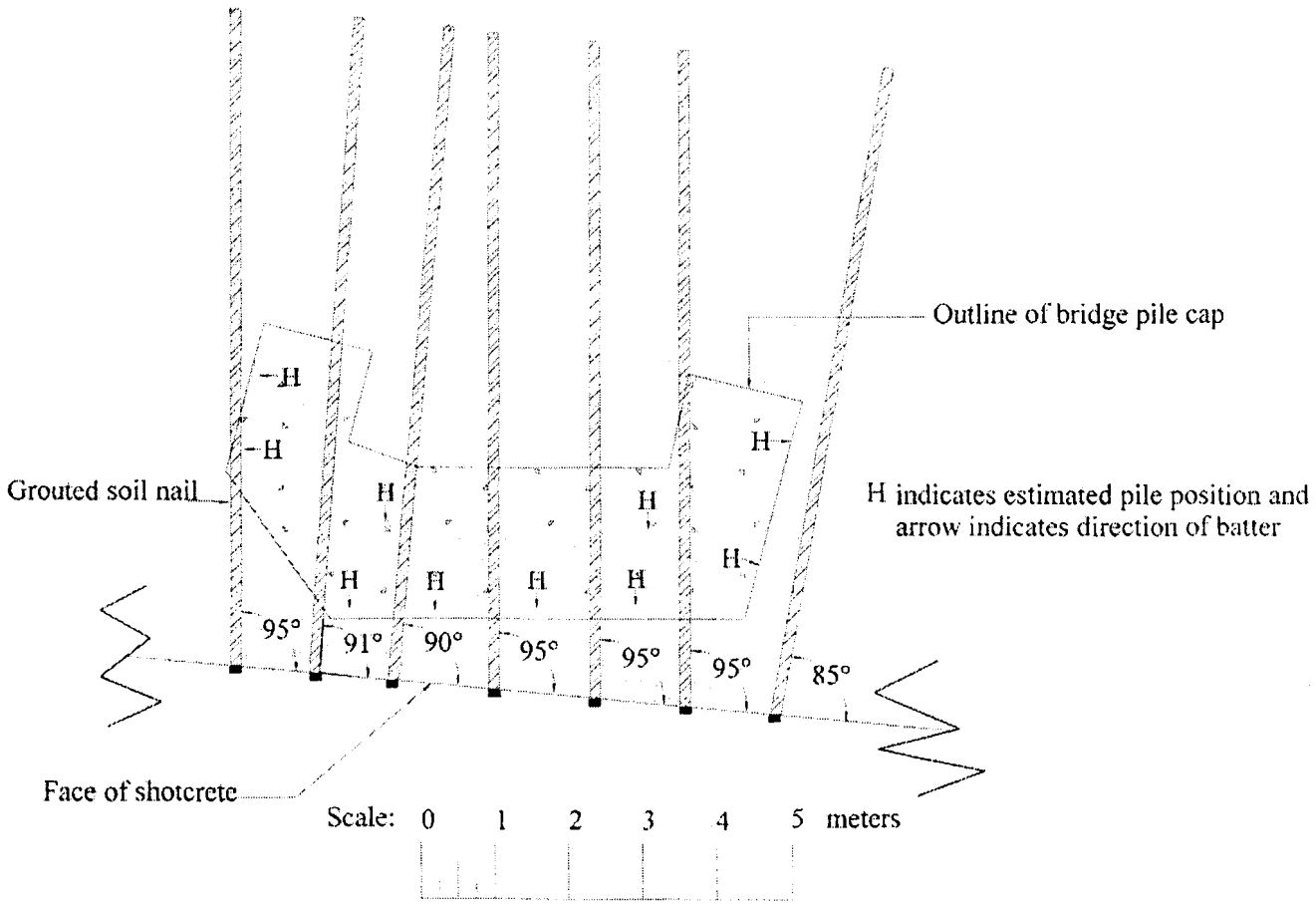


Figure 3-8: Plan view of north-facing bridge abutment, batter piles, and nail placement

Five of the soil nails were instrumented, each with seven strain gages (Figure 3-9) and twelve thermocouples (Figure 3-10) along their length. A load cell was placed behind the nut on the protruding end of each nail. The strain gages contained sensors to record temperatures corresponding to each strain gage at various depths behind the wall. Thermocouple strands were also mounted on wooden rods (12 thermocouples per rod) as shown in Figure 3-11; the rods were inserted into the soil between instrumented nails, to give a better idea of the temperature comparisons between nails and the surrounding soil. Other instrumentation included a total pressure cell, placed at the soil-shotcrete interface behind the reinforced concrete facing wall; and two concrete strain gages, also containing thermistors, which were placed within the facing wall itself. All instrumentation was installed in the north-facing wall on the eastbound side of Route 1. The south-facing wall on the westbound side of Route 1 was a similar soil nail design, but it was not instrumented.

### 3.5.1. Strain gages

Spot-weldable vibrating wire strain gages from three different vendors (RocTest, Slope Indicator, and Geokon) were selected to measure the amount of tension induced along the length of the nails. Vibrating wire strain gages contain a fine steel wire which vibrates at a given frequency, corresponding to the stress in the wire. When the strain gage is welded to another object, any deformation of the object will cause the vibrating wire to lengthen or shorten, thereby changing the frequency. Laboratory calibration factors permit the investigator to determine the change in microstrain for any measured

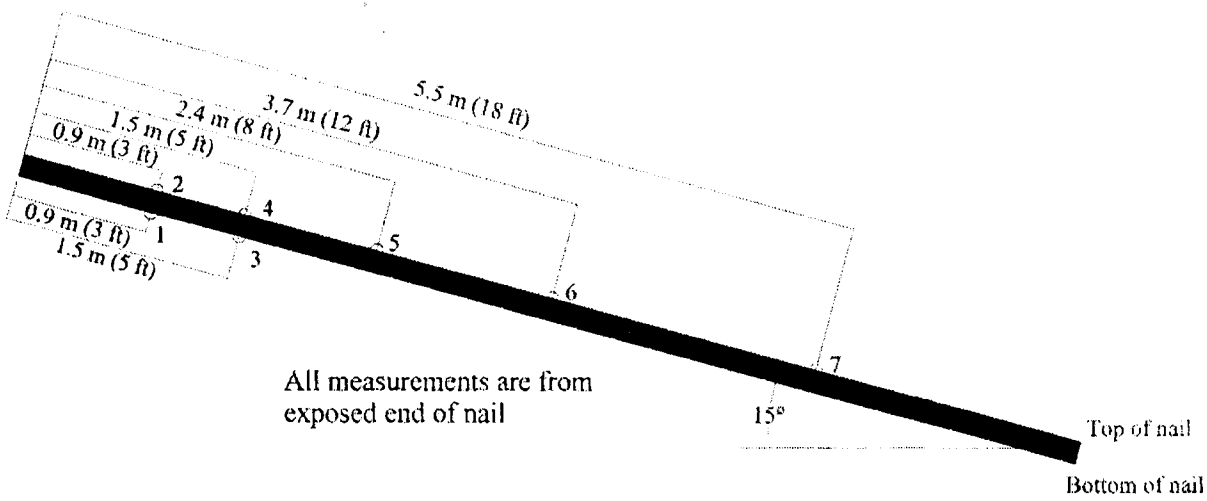


NOTES: (Refer to Figure 3-1 for nail locations on wall)

1. Top of nail C3-10 is rotated 170 degrees clockwise from vertical (vertical defined as "top of nail" in this figure).
2. Top of nail C2-13 is rotated 10 degrees counterclockwise from vertical.
3. Top of nail C3-16 is rotated 12 degrees counterclockwise from vertical.
4. Nails C2-9 and C4-13 are positioned as shown in this figure.
5. Nail C4-13 was damaged during the installation process, causing immediate loss of strain gages 5, 6, and 7. Strain gage 2 failed in December 1996, reasons unknown. Placement of strain gages 1 and 2 is reversed (1 is on top, 2 is on bottom of nail)
6. Approximately 20 cm (8 in) of each nail was left exposed beyond the shotcrete following installation.
7. All nails are Dywidag #8 rebar, approximately 2.5 cm (1 in) in diameter.

Scale: (nail and gage diameter exaggerated to show location of strain gages)

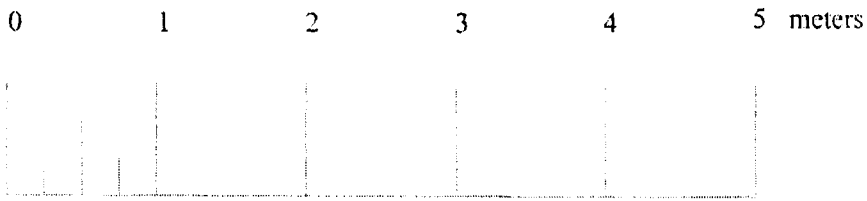


Figure 3-9: Typical layout of strain gages along soil nail

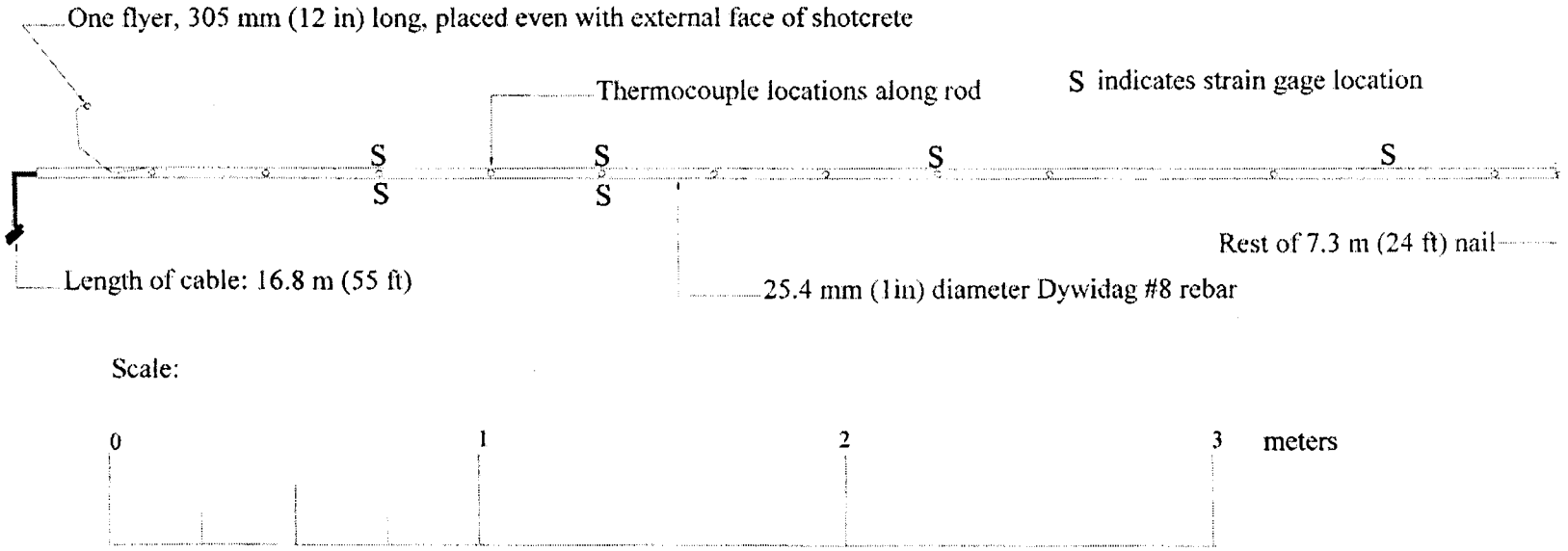


Figure 3-10: Typical layout of thermocouples along soil nail

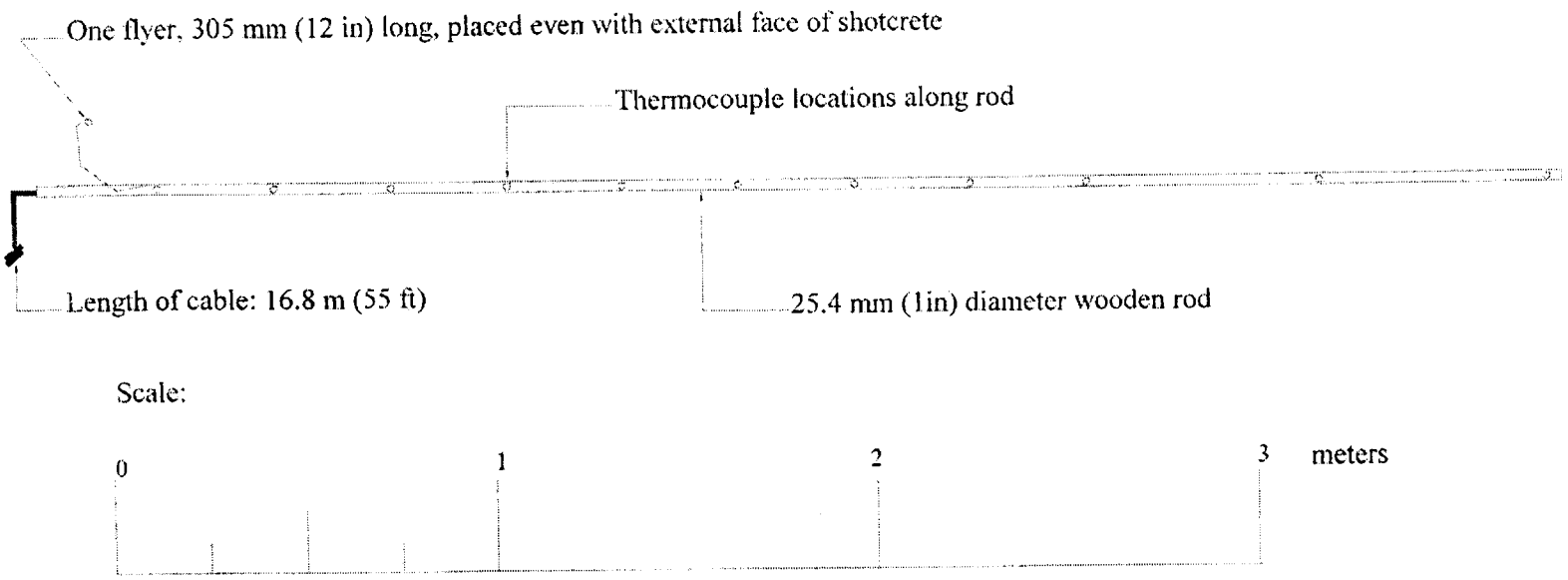


Figure 3-11: Typical layout of thermocouples along wooden rod

frequency, and stress can then be calculated by multiplying the strain value by the elastic modulus for steel, E.

All of the strain gages contained internal temperature sensors. The RocTest and Geokon strain gages used thermistors to measure temperature, while the Slope Indicator strain gage used a resistance temperature detector (RTD). The readout device, an MB-6T manufactured by RocTest, was not programmed to provide a direct temperature readout from the RTD on the Slope Indicator strain gage or the thermistor on the Geokon strain gage. For these instruments, resistance values in the temperature sensors were measured and later converted to temperature readouts on spreadsheets in the office, using calibration formulas provided by the vendors. The resistance readings became inconsistent and hard to obtain as the season became colder. On numerous occasions, particularly in extreme cold and on the Slope Indicator temperature instruments, it was impossible to obtain good readings. It is not known whether this inconsistency was due to temperature effects on the MB6T, the additional wiring required for remote sensing, the proximity of an electrical outlet and cell phone, or a combination of all these factors. Fortunately, temperature data was obtained from the redundant strand of thermocouples (which remained stable) located at approximately the same locations along the nail. This temperature data permitted a reasonable estimate of strains due to temperature fluctuation, above and beyond the strains due to bearing stresses on the nails.

Based on previous studies of frost deformations, it appeared important to place gages within the first 1.5 m (5 ft) from the exposed end of the nail, where the majority of

the tension increase was expected to occur. On the other hand, if strain gages were placed too close to the end of the nail, they could end up in the shotcrete facing or even out of the soil entirely, depending on the final installation position of the nail. Also, it was desirable to place some gages further back from the exposed end of the nail for comparison purposes and to examine the strain and temperature relationships with increased depth. Finally, the French soil nail design methods assume a small bending resistance which increases the overall capacity of the nails; by placing strain gages on both the top and bottom of a nail at a given depth, the bending moment could be calculated as well. With these considerations in mind, the final instrumentation design placed strain gages on both the top and bottom surfaces of the nail at 0.91 m (3 ft) and 1.5 m (5 ft), and on the top surface only at 2.4 m (8 ft), 3.7 m (12 ft), and 5.5 m (18 ft) from the exposed end of the nail. Approximately 0.28 m (11 in) of the exposed nail end was encased in the shotcrete and exterior concrete wall. Two of the nails (C2-9 and C3-10) were instrumented with RocTest strain gages, two (C2-13 and C3-16) with Slope Indicator strain gages, and one (C4-13) with Geokon strain gages. Results from the strain gages are provided in Chapter Four. The layout of the strain gages is shown in Figure 3-9. The nails selected for strain gage instrumentation are shown in Figure 3-6.

Five 7.3-m (24-ft) lengths of Dywidag #8 (approx. 25-mm diameter) epoxy-coated, grade 400 (grade 60) steel bar, specified for use as soil nails, were delivered to the University of Maine campus in April 1996 to be equipped with strain gages. Grade 400 (grade 60) refers to the rated tensile yield strength of the bars, 400 MPa (60 Ksi). The nails were beveled on two opposing faces. Because of the flexibility of the nails and

the finite strain capability of the strain gages, individual cradles for the nails were custom constructed from standard lumber sizes. The nails were placed in the cradles, and the epoxy corrosion protection was machine ground from the positions marked for strain gage application. The gages were spot-welded to the beveled faces of the nails according to the manufacturer's directions, and new epoxy was applied with paintbrushes to the ground areas and to the spot-welded flanges of the gages. The epoxy served to protect the spot welding from corrosion. As a quality control measure, each strain gage was tested prior to its installation on the nail, and then again after installation to determine whether any damage had occurred during the welding process. Out of the 35 strain gages installed in this fashion, one Slope Indicator gage failed after spot-welding and had to be replaced.

After the strain gages were welded, the sensor covers for the Roc-Test and Slope Indicator gages were placed over each strain gage and secured by a hose clamp and two plastic ties, as shown in Figure 3-12. The Roc-Test sensors are on the two nails in the foreground of Figure 3-12, while the Slope Indicator sensors are on the next two nails in the row and the Geokon sensors are in the row furthest from the camera. The sensor for the Geokon instrument was integral with the strain gage, but a protective cover was placed over each of the Geokon strain gages and secured with two plastic ties. The open ends of the Geokon protective covers were sealed with epoxy. Each sensor was tested after the covers were secured. Several had to be repositioned in order to obtain an accurate signal. All sensors and covers were then sealed to the bar with silicone caulk, to prevent intrusion of grout into the strain gages. The sensor wires were run up the length

of the nails and secured to the nails every 0.6 to 0.9 m (2 to 3 ft) by several plastic ties. This was done to prevent the wires from jerking the sensors, or from snapping off the sensors during installation.

For transport to the field, the instrumented nails in their cradles were stabilized using soft foam pipe insulation and plastic wire ties. Figure 3-12 shows the nails supported within in their cradles by the black foam insulation, with the strain gages in place. The wooden cradles were manually hoisted onto an open-bed truck trailer and secured using ropes and tiedowns, and in this fashion were trucked approximately 110 miles to the Brunswick construction site. At the field site, 12 thermocouple leads were attached to each nail by plastic ties, at the locations shown in Figure 3-10. Four centralizers were placed on each nail (also shown in Figure 3-12), and then the instrumented nails were inserted into 10-cm (4-inch) diameter corrugated high-density polyethylene (HDPE) tubing. The tubing was secured to the nail by hose clamps placed on either end of the nail, and then several holes of approximately 2 cm (0.8 in) were cut in the polyethylene on the far end of the nail. This was done to allow injected grout to flow back to the surface from within the protective sheathing, in order to completely fill the space between the sheathing and the sides of the drilled hole and permit the nail and grout to function as a unit. More plastic centralizers were placed around the HDPE tubing in order to center the nails within each drilled hole in the wall face, as shown in Figure 3-13. Once again, readings were taken on all sensors to ensure that none had been damaged during application of the HDPE corrosion protection.

Figure 3-12: Instrumented nails in wooden carrying cradles

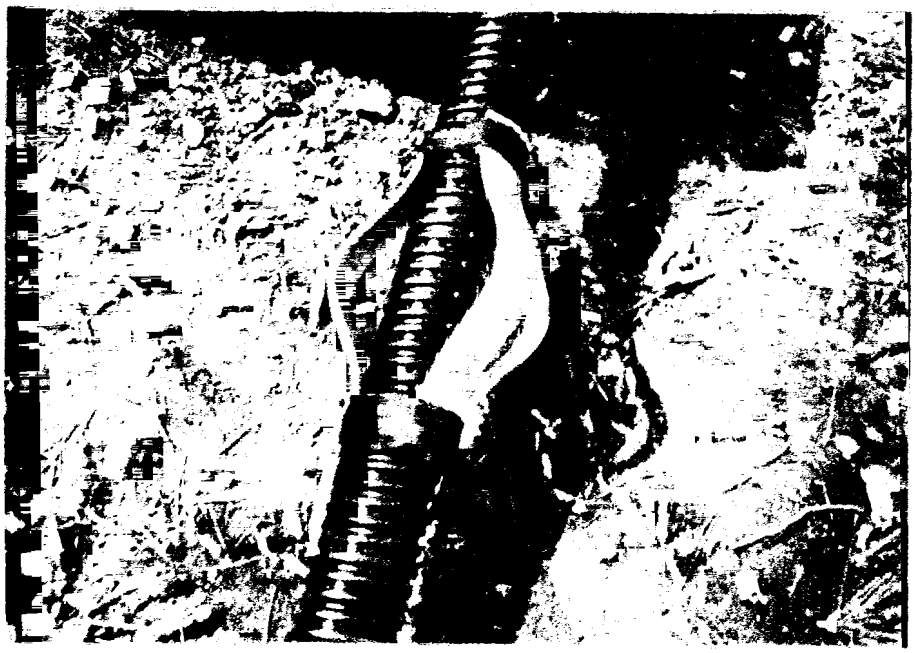

Figure 3-13: Detail showing stabilizer applied to HDPE sheathing

The nails were installed in 13.3-cm (5.25-in) diameter holes drilled through the flash-shotcrete face by the specialty soil nail contractor, Pennsylvania Earth Tech, Inc. After the nails were placed in the holes, they were grouted by attaching the grout pipe to the HDPE sheathing. Grout was pumped into the sheathing, exited through the holes at the tip, and returned to the surface along the space between the sheathing and the hole. Thus the grout filled the space between the nail and the sheathing, and between the sheathing and the drilled, cased hole. The casing was removed as the grouting progressed.

Although the non-instrumented nails were pressure grouted, the strain gages were considered too delicate to survive this procedure. The factor of safety in the overall wall design was sufficiently high to forego pressure grouting the five instrumented nails without undue risk. Figures 3-14, 3-15, 3-16, 3-17, 3-18, and 3-19 show instrumented and non-instrumented nails in various stages of the installation process.

After installation, the rotational positioning of the instrumented nails to determine if any rotation had occurred from the designated "top" and "bottom" of the bars, since this would affect the magnitude of tensile stress and bending moment calculated in the nails. This information is reflected in the notes which accompany Figure 3-6.

Some difficulties occurred during the installation of the nail to which Geokon strain gages had been attached. The encapsulating polyethylene sheath caught against the drill casing and retracted from the nail during the insertion process, and repeated efforts

by the construction crew to free it were unsuccessful. As a result, at least 4 m (13 ft) of the 7.3-m (24-ft) nail was left exposed and unprotected as it was inserted into the soil. Not surprisingly, when readings were taken immediately following the grout operation, the last two strain gages, placed at 5.5 m (18 ft) and 3.7 m (12 ft) from the exposed end of the nail, had been irreparably damaged. The strain gage at 2.4 m (8 ft) on this nail had also failed by the next reading, one week following installation. Another strain gage on this same nail, located only 0.9 m (3 ft) from the exposed end, failed in early December for presumably unrelated reasons. All other strain gages on the five nails remained operational throughout the period covered by this research.

### 3.5.2. Load cells

After the nails were installed and grouted in place, load cells were placed behind the nut at the exposed end of five nails to measure the forces exerted against the head of the nail, as shown in Figure 3-20. The original design shear connection for the nails consisted of a 200 mm by 200 mm (8 in by 8 in) plate held between two nuts near the exposed end of the nail. These extra nuts did not allow sufficient space for the load cell to be placed without interfering with the design concrete thickness of the exterior wall. Therefore, shear studs were added to the plate, and the plate was placed behind the load cell instead of in front of it, as shown in Figure 3-20. For three nails, only one plate with shear studs was placed at the wall, again because of clearance considerations. Even with the redesign, the load cell intended for instrumented nail C3-16 had to be moved to nail C3-14 (otherwise uninstrumented) to provide enough room for the facing connections.

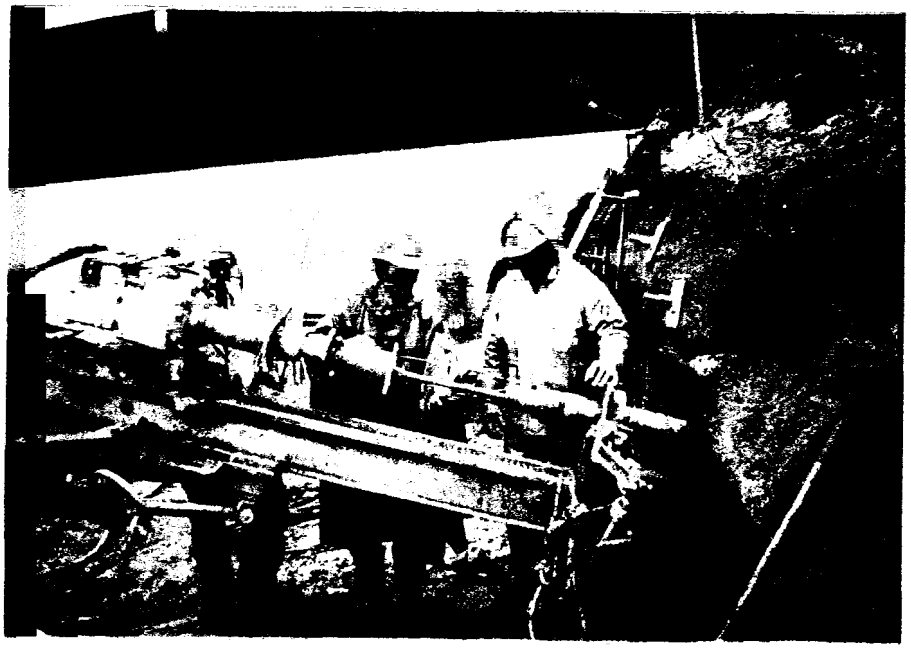

Figure 3-14: Installation of nail through drilled, cased hole (Note instrument wires held to side of hole)

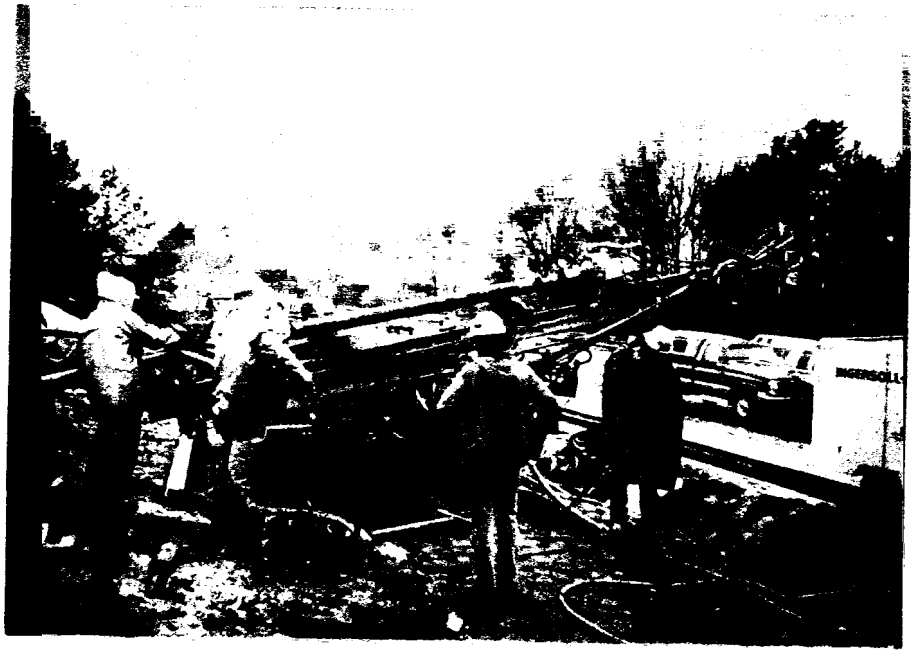

Figure 3-15: Removal of casing section and threading of instrument wires through casing

Figure 3-16: First row of nails completed, second bench excavated. Note finished shotcrete, bearing plates and end nuts on nails, vertical drainage strips, and reinforcement for shotcreting of second bench.

Figure 3-17: Nail installation complete. Note instrumented nails and conduit for instrument wires to top of wall. Formwork for footing of concrete facing wall is in progress.

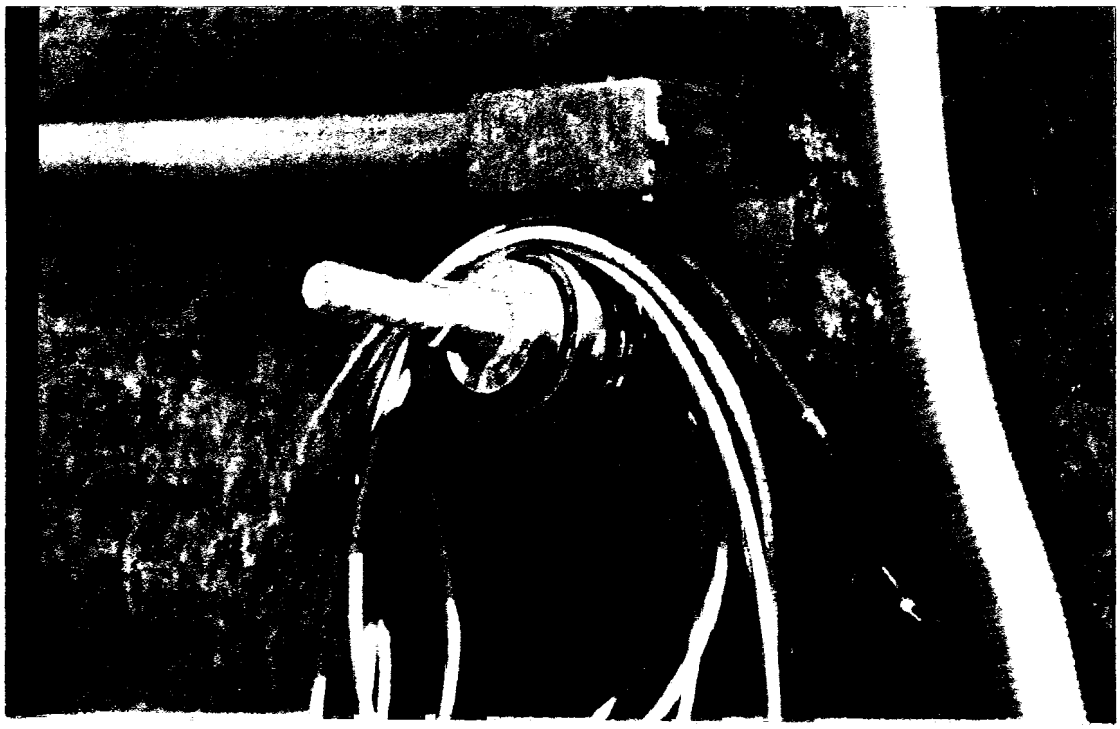

Figure 3-18: Detail showing load cell placement

Figure 3-19: Completed concrete facing wall, rain gutters, and traffic barrier. Note gray rectangular instrument boxes attached to railroad bridge at top center.

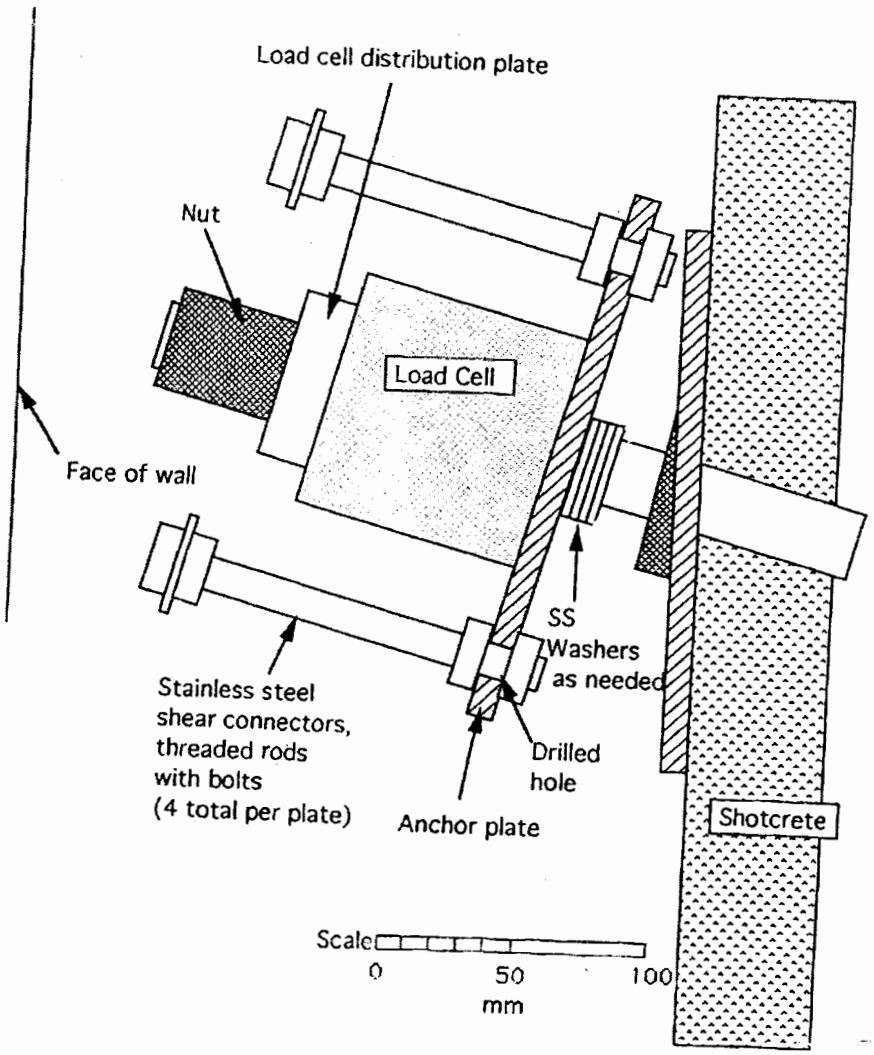


Figure 3-20: Profile view of load cell and wall connections (T. Sandford graphic)

This was because the shotcrete surface intruded too far into the area required for casting the concrete exterior wall.

Figure 3-18 shows the original load cell placement, before the addition of the bearing plate with shear studs. Figure 3-20 illustrates the redesigned load cell placement. Figure 3-6 shows the locations of the load cells along the wall.

The load cell, supplied by RocTest, consists of three vibrating wire strain gages placed 120° apart within a donut-shaped steel cell. The cell is mounted within a load ring which is securely fastened normal to the loading direction between flat plates. As load is applied to the ring (and thus to the cell), the strain gages deform and the frequency of the vibrating wire increases or decreases. An average of the three strain gage readings can then be used to obtain an average load over the surface of the load cell.

The Roc-Test load cells did not contain temperature sensors. However, temperature within the cast-in-place (CIP) concrete wall was measured using the thermistors in the two concrete strain gages, described below. There were also thermocouple sensors located within the concrete exterior wall, and at the interface between the shotcrete face and the CIP wall. The thermocouples are also described in more detail below.

Signals from all five load cells were received continuously during the period covered by this research. Results from the load cells are presented in Chapter 4.

### 3.5.3. Concrete strain gages

In order to measure stresses in the concrete due to frost heave behind the exterior wall, embedded concrete strain gages were placed in the same general area as the instrumented nails, as shown in Figure 3-6. Two embedment vibrating wire strain gages, approximately 17.1 cm (6.75 in) in length by 5.0 cm (2.0 in) in diameter, were tied into the reinforcing steel in the external CIP wall prior to the concrete pour. These gages, which worked according to the same principles as the smaller gages spot-welded to the nails, were used to gain an understanding of the deformations within the wall as the temperatures dropped. The gages had built-in thermistors so temperature and microstrain could be recorded simultaneously.

The concrete strain gages were placed as shown on Figure 3-6, with the long axis fixed vertically against the concrete reinforcement. These positions are approximate, as the sensors were moved slightly by the construction crew after initial placement by UMaine researchers. Plywood forms were placed for the concrete pour before the new strain gage position could be accurately measured and recorded, but the onsite inspector provided a reasonably close estimate of their locations. The concrete strain gages were placed in the approximate center of the wall, between instrumented nail locations.

Signals from both concrete strain gages were received continuously during the period covered by this research. Results from the concrete strain gages are provided in Chapter 4.

### 3.5.4. Total pressure cell (TPC)

A single total pressure cell was placed at the interface between the soil and the shotcrete flash facing, to measure heaving of the soil between nail locations. Figure 3-6 shows the placement of the total pressure cell on the wall.

The total pressure cell, purchased from Slope Indicator, is a thin 23-cm (9-in) diameter steel plate filled with a pressure-sensitive liquid (ethylene glycol), mounted securely between the soil and the facing wall (in our case, behind the flash shotcrete). Any change in the stress on its sensitive side (placed toward the soil) can be measured as a fluid pressure by an internal vibrating wire piezometer (pressure transducer). This value must be corrected for temperature and barometric pressure variation. The TPC contains an internal temperature sensor (an RTD, like all the Slope Indicator products), but barometric pressure data must be obtained from an external source. The author, a Lieutenant Commander in the United States Navy Reserve, requested the assistance of the Meteorological and Oceanographic Detachment (METOCDET) at Naval Air Station Brunswick and was able to obtain precise hourly readings of barometric pressure in Brunswick. These were compiled by METOCDET and sent to UMaine weekly, providing valuable data for this and other ongoing UMaine research projects in the Brunswick-Topsham area.

Although the TPC appeared to work well throughout the period covered by this research, the results (adjusted for temperature and barometric pressure) indicated virtually no pressure variation from the time of installation. This indicates that the load

plate was not firmly set in contact with the soil. This result occurred despite extra effort during installation to ensure a good contact between the plate surface and the exposed face of the wall, including packing of all visible voids and irregularities. The results are presented and discussed further in Chapter 4.

### 3.5.5. Thermocouples

The strain gages and TPC were equipped with internal temperature sensors. However, these could only record temperatures at the sensor locations. In order to see and compare how the frost front progressed along the nails and in the areas of soil between the nails, Type-T thermocouples were installed along the nail lengths and at corresponding locations in the soil. The thermocouples were fabricated by the U.S. Army Corps of Engineers Cold Regions Research and Engineering Laboratory (CRREL). Thermocouples were placed in strands along 2.5 cm (1 in) wooden rods and grouted into drilled holes, similar to the soil nails, so that temperatures could be taken at various depths behind the wall facing. This provided more temperature locations with depth, plus a backup temperature measurement along the nails in case any of the strain gage temperature sensors failed. The data proved quite useful as the winter progressed and temperature readings from resistance values in the instrument thermistors became increasingly difficult to obtain.

Five strands of 12 thermocouples each were placed along the instrumented nails, and another five strands of 12 thermocouples were mounted on long wooden rods and

placed in the soil between the nails. Figure 3-6 shows the locations within the wall of the thermocouple strands at internail locations.

An additional thermocouple string consisted of twelve sensors along a wooden rod, which was to be placed vertically within a PVC casing approximately 3.0 m (10 ft) behind the wall. It was hoped that this thermocouple string would aid in the analysis of the three-dimensional progression of the frost front within the wall. The vertical string would show the temperature gradient from the top of the wall downward, while the other thermocouples showed the gradient from the face of the wall inward. Unfortunately, the wooden rod with attached thermocouples was accidentally removed from the site and trashed by the contractor while awaiting installation. Time and budget constraints prevented the preparation and installation of a replacement string, so this aspect of the research was eliminated.

The thermocouples were not read manually. In addition, because of problems and delays in the procurement, programming, and operation of the remote sensing program, the first thermocouple readings were not obtained until late January. The results from the thermocouples are provided in Chapter 4.

### 3.5.6. Slope indicators

Two slope indicators, one for either side of the existing railroad bridge abutment, were planned as part of the instrumentation program. Installed vertically prior to construction, slope indicators will measure any deviation from their initial position as the

wall moves forward and outward. Like mechanically reinforced earth (MRE) walls, soil nail walls are "passive" retained earth structures and require small wall movements to fully develop the strength of the nail-grout-soil system.

Unfortunately, the prime contractor's initial clearing and grubbing operations were so extensive that the top of slope on the embankment could no longer support the heavy drilling equipment that MDOT had designated for this purpose. Therefore this instrumentation also had to be eliminated from the research plan.

### 3.5.7. Survey points

A survey program was undertaken with two objectives in mind. The first was to ensure the integrity of the working railroad bridge, since soil nailing was still an unproven technology in the state of Maine. Any large movements in the embankment as a result of excavation would have been cause to temporarily stop the project and consider other means of shoring up the bridge. The second objective was to give researchers a better understanding of the magnitude and sequence of wall deformations as construction progressed. The wall was surveyed from March 27 (prior to start of construction) to July 31, at which point the construction was finished except for rain gutters and finish work. No further data was received from the surveying firm after that date, although MDOT planned to continue the survey through the first winter. The results from the survey are given in Chapter 4.

### 3.5.8. Data acquisition system

The data acquisition system used for this project consisted of two Campbell Scientific CR10X programmable dataloggers, one for the thermocouples and one for the vibrating wire strain gages, concrete strain gages, TPC, and load cells. Auxiliary processing equipment, also from Campbell Scientific, included an AVW4 Vibrating Wire Interface (for additional signal conditioning and noise reduction), AM416 Relay Multiplexer (permitting 64 individual signals to be measured and recorded in each datalogger cycle), AM25T thermocouple multiplexers, and a DC112 modem connected to a standard cellular telephone. Measurement data from each sensor is recorded and stored every two hours on a daily basis, then downloaded directly into a computer at the University of Maine by initiating a phone call to the cellular phone at the site.

The instrumentation was mounted in two rectangular electrical boxes, approximately 0.9 m high and 0.6 m wide (3 ft high by 2 ft wide), as shown in Figure 3-17. Wires from the various sensors were threaded through electrical conduit up the wall and into the bottom of the box, then individually stripped and inserted into the appropriate junction slots in the multiplexer. 110V power supply was extended to the site via an underground trench from a power pole approximately 180 m (600 ft) away. In an attempt to shield the vibrating wire processor unit from additional electrical noise, the electrical power was brought into the box containing the thermocouples, with only a cable connection to the box containing the strain gage sensors. The thermocouple box also contained light bulbs and foam insulation in order to maintain a fairly constant

temperature as the temperature dropped, since serious fluctuations could have affected the thermocouple readings.

There were numerous difficulties in getting the automated system to function as planned, starting with an eight week delay between ordering and receiving the various components from Campbell Scientific. Then, with winter fast approaching, the system was installed and programmed in the field rather than in the laboratory. This created more problems since the field site was approximately two hours away from the research offices at the University of Maine, and difficult weather and electrical conditions frequently prevailed. Also, although the multiplexer is designed to handle up to 64 different signals, it quickly became obvious that using strain gages from different vendors would complicate the programming tremendously; the datalogger had to be reset multiple times during each sample period to adjust for the parameters of each individual sensor type. Eventually, the researchers obtained additional sensors and another Campbell Scientific remote datalogger system (which would be used for a followon soil nail project in Moscow, Maine) and did the bulk of the programming and debugging in the civil engineering laboratory at the University of Maine. Even so, the work was difficult and slow. In particular, the Slope Indicator program required weeks of debugging before it worked successfully.

Despite close interaction over a period of almost six months with technical representatives from the various vendors as well as from Campbell Scientific, the datalogger was not successfully programmed to work reliably for all sensors until April

1997, although the first usable measurements were received in mid-January 1997. For most of the period of research, therefore, sensor measurements were taken manually using the Roc-Test MB-6T as described previously. The exception was the thermocouples, which were monitored only via the automated datalogger (starting in mid-January).

The automated datalogger continued to take sensor readings at two-hour intervals from the soil nail wall until June 1998. The data from the following winter season may be the topic of a follow-on research project.

### 3.6. Construction sequence

The following is a summary of significant events during the soil nail wall construction. With the exception of the large-scale failure on the south-facing wall on May 13 and the end-of-construction dates, the summary focuses solely on the north-facing (instrumented) soil nail wall. MDOT field inspector Debbie Coffin kept meticulous daily construction logs, which greatly augmented the author's own notes and limited observations in establishing this sequence of events.

April 1, 1996: H.E. Sargent (HES) started work on project, clearing and grubbing site. MDOT survey crew set control points for wall surveying during construction.

April 9, 1996: Contractor's clearing and grubbing operations have disturbed the site to the point that planned slope indicator instrumentation cannot be safely installed by UMaine as originally planned.

April 11, 1996: HES drilled and placed 3" PVC pipe in top of slope (presumably for the vertical thermocouple string that was never installed).

April 15, 1996: Pennsylvania Earth Tech (PET), the soil nail specialty contractor, arrived to inspect site prior to start of soil nail construction.

April 16, 1996: PET discussed technical problems with existing design: due to limited work space and the locations of the battered piles, PET wanted to install the top row of nails at a lower angle than the specified 15°. This would affect wall strength and stability, so the design engineer asked to see revised and approved shop drawings first (never received). PET also asked permission to excavate ground for two rows of nails at a time (denied), and to use casing when drilling holes in the loose soil (accepted).

April 19-21, 1996: PET drilled and placed two test nails, one 8.8 m (29 ft) long #9 Dywidag bar (39-mm diameter), and one 7.3 m (24-ft) #8 bar (25-mm diameter). Equipment problems caused significant and prolonged delays.

April 23-24, 1996: HES excavated the first bench for the soil nail wall. Test nails #1 and #2 failed pullout verification tests. Design engineer L. Krusinski (MDOT) and D. Cotton of Golder Associates (technical consultant) met with PET personnel to discuss the failures. They agreed to repeat the test using pressure grouting.

April 25-26, 1996: PET drilled and placed two new test nails, #3 and #4, using pressure grouting in place of gravity grouting.

April 26, 1996: University of Maine delivered five nails instrumented with strain gages and thermocouples to site.

April 28, 1996: Test nails #3 and #4 passed verification testing.

April 29-30, 1996: PET began drilling and placing first production nails. Almost immediately, they hit the concrete bridge abutment and remove a 15-cm (6-in) piece of rebar. A cross-check of plans revealed a design error: the bottom edge of the existing abutment was directly in the installation path of the inclined nails. The design engineer approved recentering the row of nails from elevation 41.0 to elevation 39.9, which eliminated the problem.

May 7, 1996: Excavation of the second bench caused significant sloughing at the face. Shotcreting exacerbated the sloughing, prompting the specialty subcontractor to pump in additional shotcrete for stabilization. However, the weight of the excess shotcrete caused the entire joint between the first and second benches to give way, pulling soil with it. The first bench of nails remained in place. HES required the excess shotcrete to be removed after it set up, as the thickness was out of tolerance in several locations.

May 10, 1996: The first two instrumented production nails (C2-9 and C2-13) were installed, using gravity grout in place of pressure grouting. While drilling for (non-instrumented) nail C2-6, workers hit a battered pile; the center position for this nail was moved slightly, permitting successful installation.

May 13, 1996: The small sloughing failure on the north-facing wall was reenacted as a major failure on the south-facing, uninstrumented wall. The second bench of the south-facing (westbound Route 1) wall sloughed along its entire length at approximately 10:15 am, shortly after excavation. The slough created large voids in the soil behind the shotcrete face of the first bench of installed nails, and the undermining process initiated failure within the soil-nail mass. The wall collapsed,

starting at the west side and proceeding toward the east side of the wall, as shown in Figure 3-20. Work on the project was stopped for the day at around 10:30 am.

Figure 3-21: Sloughing failure on non-instrumented wall

Rainy conditions had prevailed for several days preceeding the excavation and failure, possibly contributing to a loss of apparent cohesion in the essentially granular fill.

May 14, 1996: MDOT, HES, and PET representatives met to discuss the failure and various options for stabilizing the soil and rebuilding the failed wall. Until further notice, PET would work on the north-facing wall only. (The south-facing wall was ultimately repaired using a permeation grout curtain in two near-vertical layers of columns, plus several "false walls" of plywood along the excavated face. A similar

grout curtain, placed prophylactically in the north-facing wall, was sufficient to prevent further sloughing.)

May 15, 1996: PET repaired the joint between the first and second benches on the northbound wall, using several lifts of CR740 overhead mortar.

May 18, 1996: Liquidated damages began for construction delays. Work continued on the grout curtain, placed to avoid any future sloughing problems.

May 20, 1996: Third bench was excavated. The grout curtain did not interfere with face stability during excavation, and no further sloughing was noted (even when a train passed over the bridge and a vibratory roller operated adjacent to the site while the face was exposed and unshotcreted).

May 21, 1996: Attempts to drill for an instrumented nail (C3-10) were halted when a battered pile was encountered in the hole; the position for this nail was moved slightly.

May 22, 1996: Two more instrumented nails (C3-10 and C3-16) were installed, using gravity grouting.

May 23, 1996: Thermocouple strings were inserted in holes drilled between nail locations; wires from nails and thermocouples were threaded through conduits to the top of the wall for connection in an electrical box.

May 28, 1996: Excavation, shotcreting, and nail installation began along the fourth (final) bench.

May 29, 1996: Problems occurred during nail installation at the lowest level, when groundwater and peat were encountered in some of the holes. Nail C4-18 pulled out with the casing; C4-8 experienced grout blowout and contamination by flowing sand while C4-10 was being air flushed, causing it to pull out with the casing; and C4-14 suffered a combination of nail pullout and separation of the encapsulating sheath. All were removed and reinstalled. Peat was encountered in the drill hole for C4-10 at 6.1 to 7.3 m (20 to 24 ft) and in C4-14 at about 3.7 m (12 ft).

May 30, 1996: The final instrumented nail (C4-13) was installed and gravity grouted; approximately half of the sheathing around the nail pulled off as the drill casing was removed, but the nail remained in place and it was judged to be acceptable. Groundwater and peat were encountered during installation of nail C4-16, causing operation to be abandoned for the day. The drill hole was pressure grouted to stabilize voids, and the nail was reinstalled through the set grout the next day.

May 31, 1996: Three more nails pulled out during installation and will have to be reinstalled through set grout. Three more thermocouple strings were installed in the spaces between nails; wires from the instrumented nails and the thermocouples were threaded through conduit to the top of wall for connection to an electrical box.

June 1, 1996: One of the nails, C4-15, could not be installed even through the set grout; the hole was abandoned. The design engineer requested a pullout test on nail C4-11, even though it passed the verification test. This meant that an additional production nail had to be installed 0.6 m (2 ft) above and 0.3 m (1 ft) to the left of the sacrificial nail.

June 2, 1996: C4-15 and the new production nail, C4-11A, were successfully installed.

June 3, 1996: Nail C4-21 was rejected by the design engineer; a new nail, C4-21A, was successfully installed. Installation of nails on the north-facing wall was completed as of this date.

June 5, 1996: Placement of load cells on the exposed ends of instrumented nails concerned the HES carpenter foreman, who believed that the planned placement would not provide enough space for the nail-facing connections within the cast-in-place concrete facing wall. T. Sandford of the University of Maine agreed to redesign the placement of the load cells. The foreman was also concerned about the conduit for electrical wires from the instrumentation, which he felt should have been placed along the planned CIP construction joints to prevent concrete cracking along the conduit lines.

June 12, 1996: UMaine personnel relocated conduit along planned concrete joints and install load cells according to the new plan (see Figure 3-4). The load cell planned for nail C3-16 could not be installed due to insufficient exposed length on the end of the nail, so instead the load cell was placed on nail C3-14, which was otherwise uninstrumented. The other four load cells were placed on the ends of the remaining four instrumented nails in the wall.

June 14, 1996: Rebar construction and forming for the CIP facing wall is well underway. Concrete strain gages were tied into the rebar with baling wire.

June 21, 1996: Concrete strain gages were relocated and attached to rebar by HES using metal clamps, as the previous wire tying had produced unreliable readings in the

sensors. This method yielded appropriate readings. Wooden forms were then erected along the front of the planned CIP wall in preparation for the concrete pour.

June 25, 1996: Equipment for remote monitoring of instrumentation was installed in two junction boxes, located at the top of slope, which were bolted into the concrete at the side of the railroad bridge abutment.

June 27, 1996: UMaine personnel used a ditchwitch and manual labor to dig a trench and place electrical line approximately 600 ft from an existing electrical pole to the junction boxes atop the soil nail wall. HES received a call after 4:30 pm, ordering them to cancel the concrete pour planned for the next morning.

July 2, 1996: HES checked and straightened concrete forms, waiting for the go-ahead for the concrete pour.

July 10, 1996: The concrete pour, rescheduled for July 11, was again canceled unexpectedly at 4:00 pm.

July 11, 1996: HES drilled holes in external wooden forms at nail locations, in order to access the second plate assembly for removal and modification. This was because the CIP wall designer at the HES home office had reviewed and rejected the original configuration. The next week was spent modifying the plate assemblies with Nelson studs, re-epoxying the drill holes, and patching the holes in the forms.

July 18, 1996: Concrete pour for the facing wall. UMaine took sensor readings before and after the pour to check for any damage to sensors.

July 19, 1996: Strongbacks and walers were removed from newly poured wall, revealing a large void in the top of the wall. The inspector believed the void occurred because workers could not see what they were vibrating between the narrow forms,

resulting in poorly vibrated concrete. She provided them with a flashlight, but it was only marginally helpful.

July 22, 1996: Forms were stripped from the CIP wall. In addition to the large void noted above, there was a another small void and several rough spots throughout. M. Steele, MDOT Bridge Inspector, was called in to check the wall. He pronounced it structurally sound, but in need of considerable finish work (chipping and rubbing).

July 23-24, 1996: UMaine personnel soldered instrument wires into junction boxes at the top of slope.

July 31, 1996: Another modification from the HES home office, this time to the placement of bolts on the bearing plates, required HES to drill holes in the new concrete, cut out the improperly placed bolts, drill holes and grout in new bolts, and repatch the wall.

August 7, 1996: Construction joints on wall were sealed using Sika-Flex 1A. Patching of holes and concrete finish work continued. M. Steele of MDOT made a site visit to check the concrete work.

August 9, 1996: Finish work on wall was completed. Two coats of 50% linseed oil/ 50% mineral spirits were applied to the face as a protective coating and to add sheen.

August 20, 1996: Concrete gutters at top of wall were completed and forms were removed. The site was cleaned up and excess materials were moved to the westbound side of Route 1, where work on the other wall continued.

August 23, 1996: UMaine personnel worked on programming the remote data collection system for wall instrumentation.

August 26, 1996: Work on instrumented wall was substantially completed as of this date.

September 12, 1996: Work on uninstrumented wall was substantially completed as of this date.

September 20, 1996: All work on this project was completed as of this date.

# CHAPTER 4

# INSTRUMENTATION RESULTS

## 4.1. Introduction

Most of the instrumentation in the soil nail wall was monitored from time of installation in May 1996 through May 1997. Thermocouples were monitored from mid-January through May 1997. University of Maine researchers continued to collect performance data from the wall for another year, and future analysis of the additional winter freezing cycles may provide additional insights. However, that work falls outside the scope of this research effort.

The original intent was to provide continuous cold-weather monitoring of all sensors using an automated remote data collection system, the Campbell DataLogger, which could be accessed by modem from the University of Maine campus in Orono to download and process data. The automated system could be programmed to take multiple readings over the course of a day, thus minimizing the effect of a single bad reading on the overall results. Automated systems are more convenient and potentially more accurate than manual monitoring in a climate with severe winters, as cold weather tends to degrade the operating efficiency of the battery-powered portable monitoring gauges. Winter weather also complicates site access and creates uncomfortable and unsafe monitoring conditions for the human observer.

Unfortunately, due to procurement and installation delays and programming difficulties, only the thermocouple measurements could be automatically collected and downloaded during the 1996-97 winter season. The collection of thermocouple data began in mid-January and continued (with some breaks due to equipment malfunction and programming errors) through the research period. All other instruments were manually monitored on a weekly to biweekly basis throughout most of the period of investigation. These other instruments – 35 nail strain gages, two concrete strain gages, one total pressure cell, and five load cells – were finally connected into the automated data system in May 1997, close to the end of the period of interest for this research. The automated system continued to collect readings from the instrumentation in the wall for another year, with the exception of the temperature sensors in the Slope Indicator strain gages (which were backed up by working thermocouples along the same nail) and the strain and temperature sensors in the total pressure cell (which provided unusable data, as described below). Automated readings were taken every two hours and downloaded to the University of Maine on a weekly basis.

### 4.2. Strain gages

Figures 4-1 through 4-7 show the stress vs. time relationships by gage for each of the five instrumented nails. Refer back to Figures 3-1 and 3-3 respectively for the placement of nails in the wall and placement of strain gages along the nail. The results confirm the findings of previous researchers, showing a large increase in tension during the initial period following installation, a more gradual increase over the course of the cold weather

season, and a gradual loss of tension as the soil warms (though nails remain permanently stressed beyond their initial values).

Previous researchers (e.g., Juran and Elias, 1987) have reported that the highest stresses due to frost occur in a zone approximately 1 to 2 m (3 to 6 ft) from the nail head, and this was largely the case in Brunswick as well. The largest magnitudes of stress along the nails were observed in Gage 3, 1.5 m (5 ft) from the exposed nail head, with two exceptions: C4-13, where the highest stresses occurred in Gage 1, 0.9 m (3 ft) from the nail head, and C2-9, where the highest stresses occurred in Gage 5, 2.4 m (8 ft) from the nail head. The highest stress noted in any gage was in Gage 3 for nail C3-10, which reached 146 MPa (21.2 ksi) during late February 1997. This is slightly more than 1/3 of the rated ultimate tensile stress of the nail, 400 MPa (60 ksi). By May 1997, the stress in this nail had dropped to 91.1 MPa (13.2 ksi).

All the nails showed an abrupt dip in stress values during the week from July 17 to July 24, 1996 (refer to the Day 199 and/or Day 206 reading on Figures 4-1 through 4-7). This coincided with the erection of forms and casting of the concrete facing wall on July 18. It is possible that the facing wall construction interacted with the shotcrete surface and embedded nail heads in a manner which temporarily relieved some of the tension in the nails. The effect was most pronounced in the gages closest to the face of the wall, but it was noticeable even on the deepest strain gages, located 5.5 m (18 ft) behind the exposed ends of the nails.

Because strain gages were placed on both the top and bottom of the soil nails at 0.9 m (3 ft) and 1.5 m (5 ft), it was possible to calculate an approximate extreme fiber bending stress from the measurements at these positions on each nail. To make this calculation, it was assumed that the bending stresses were isometric on either side of the nail and that the nails deformed in line with the oppositely placed strain gages. (In fact this may not have been the case, as several of the nails rotated during installation so that their strain gages were no longer at the "top" and "bottom" of the nail as intended. Thus the two opposing strain gages may not have been aligned with the maximum deflection plane along each nail. However, it would have been impossible to estimate the extreme fiber bending stresses without assuming maximum deformation in line with the strain gages.) The stress values from the two opposite gages were averaged, and the average number was subtracted from the higher gage stress value to obtain the amount of stress on either side of the "zero bending plane" (the center of the nail). Then the calculated bending stress at the gages was linearly interpolated back from the known height of each strain gage to obtain the extreme bending stress at the flattened portion of the nail. February 20, 1997 (Day 417) was selected to perform this analysis because that was the date on which almost every gage indicated the maximum seasonal stress at the 0.9 m(3 ft) and 1.5 m (5 ft) positions. The results of this analysis are discussed in Chapter Five and shown in Table 5-3.

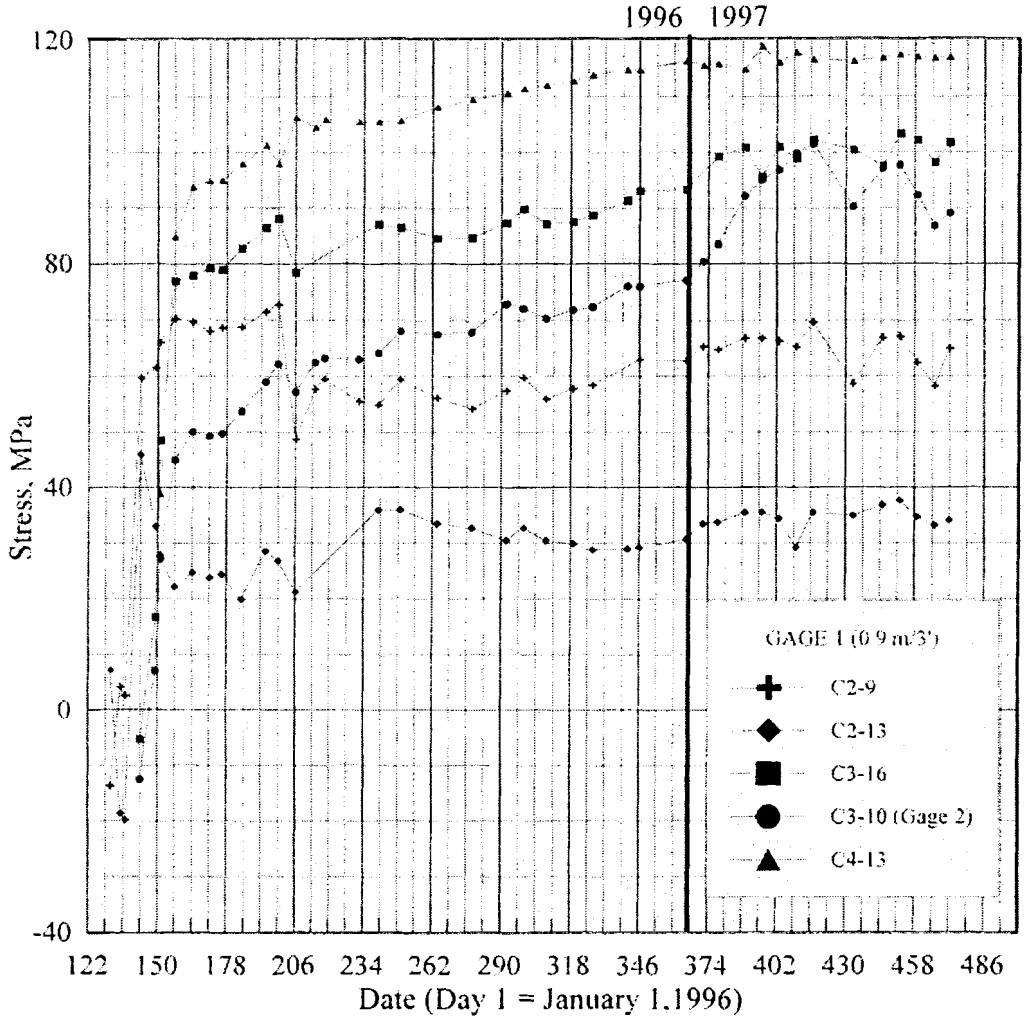


Figure 4-1: Strain gage stress vs. time for Gage 1, 0.9 m (3 ft) from exposed end of nail

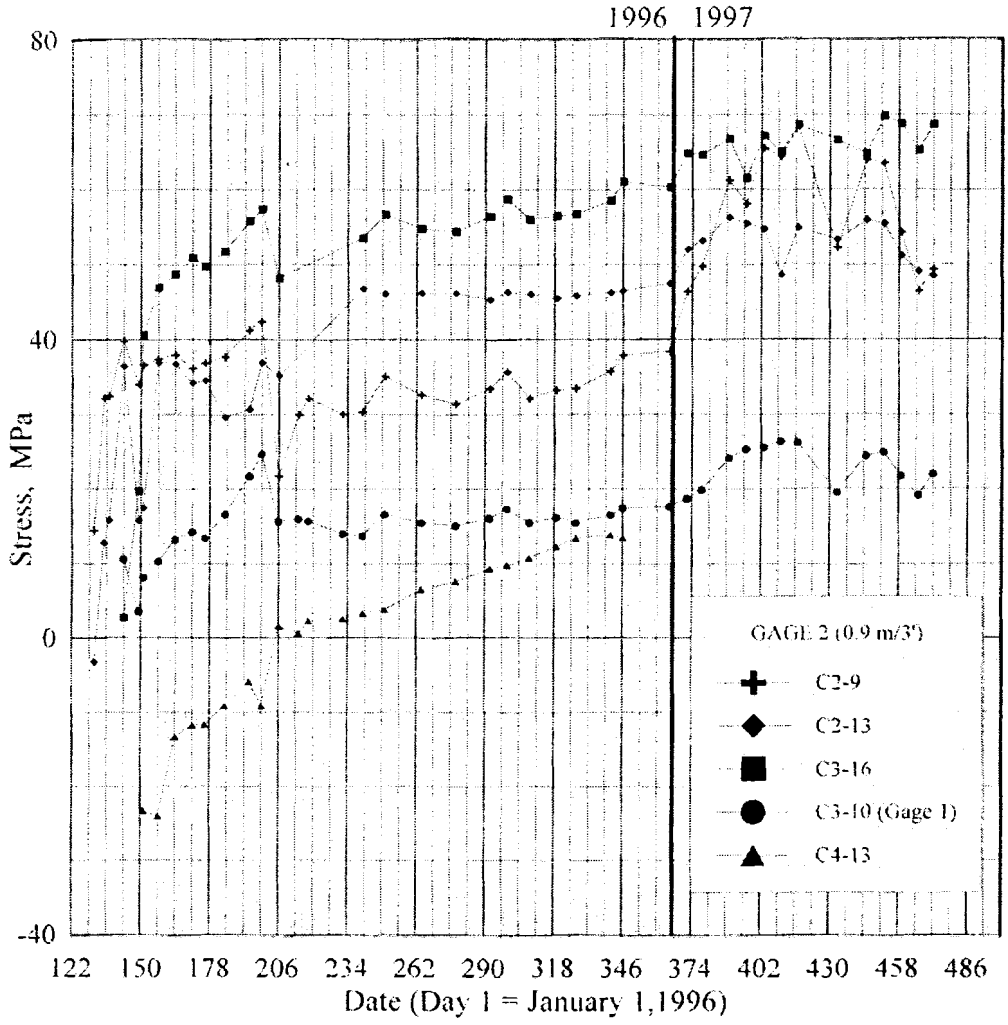


Figure 4-2: Strain gage stress vs. time for Gage 2, 0.9 m (3 ft) from exposed end of nail

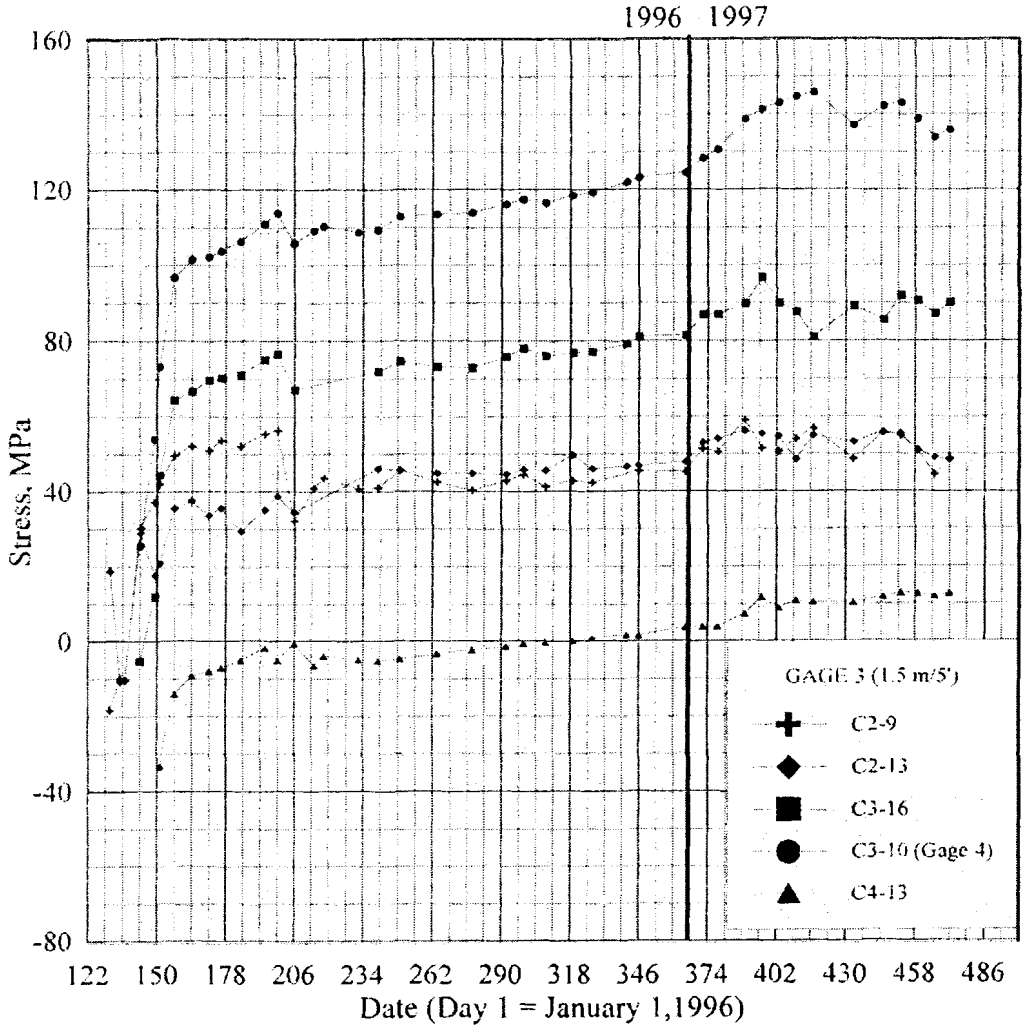


Figure 4-3: Strain gage stress vs. time for Gage 3, 1.5 m (5 ft) from exposed end of nail

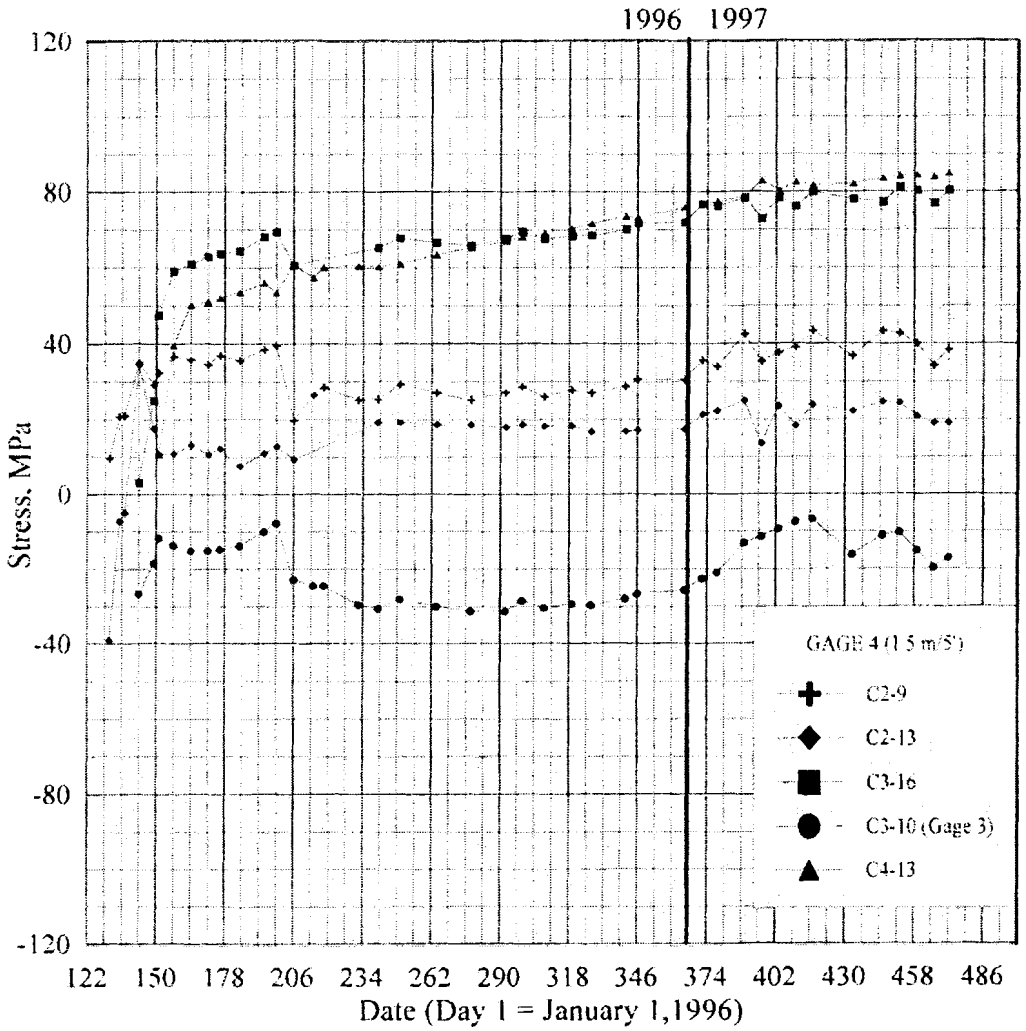


Figure 4-4: Strain gage stress vs. time for Gage 4, 1.5 m (5 ft) from exposed end of nail

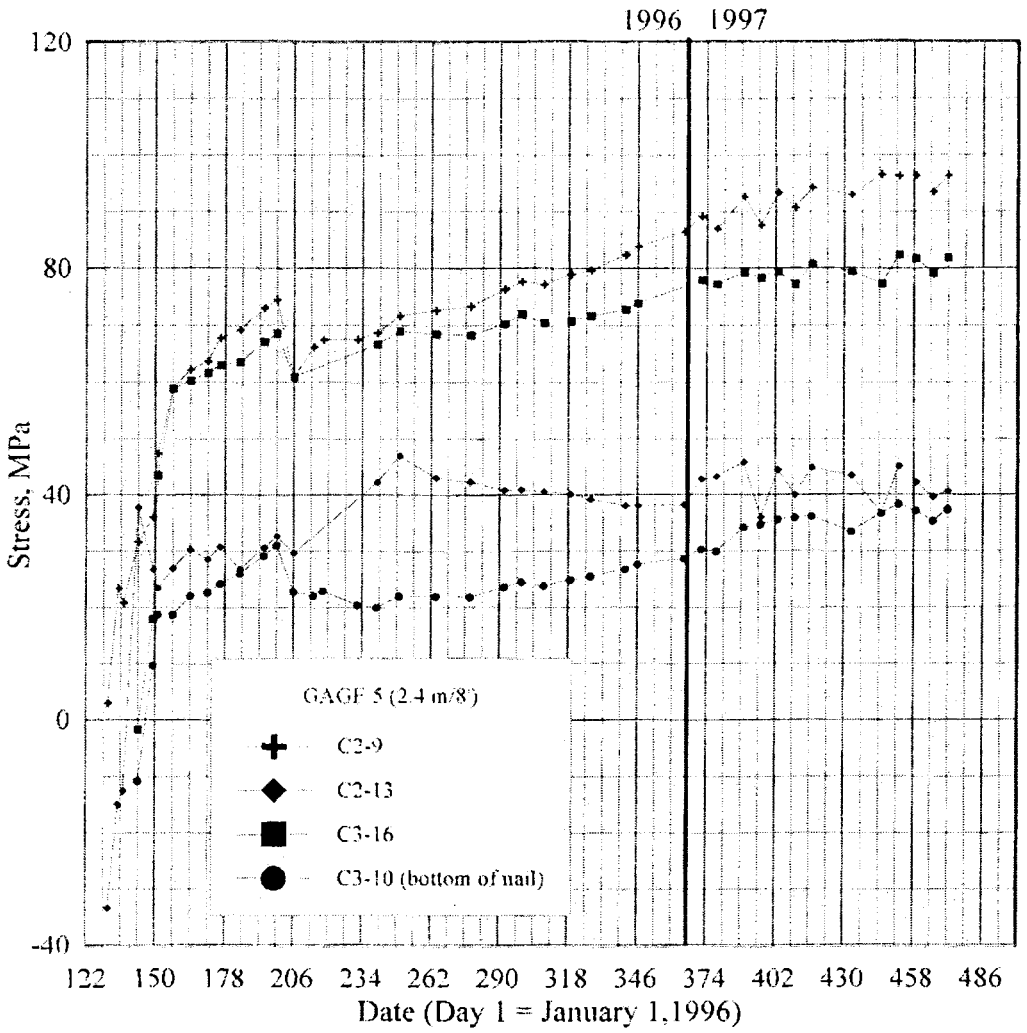


Figure 4-5: Strain gage stress vs. time for Gage 5, 2.4 m (8 ft) from exposed end of nail

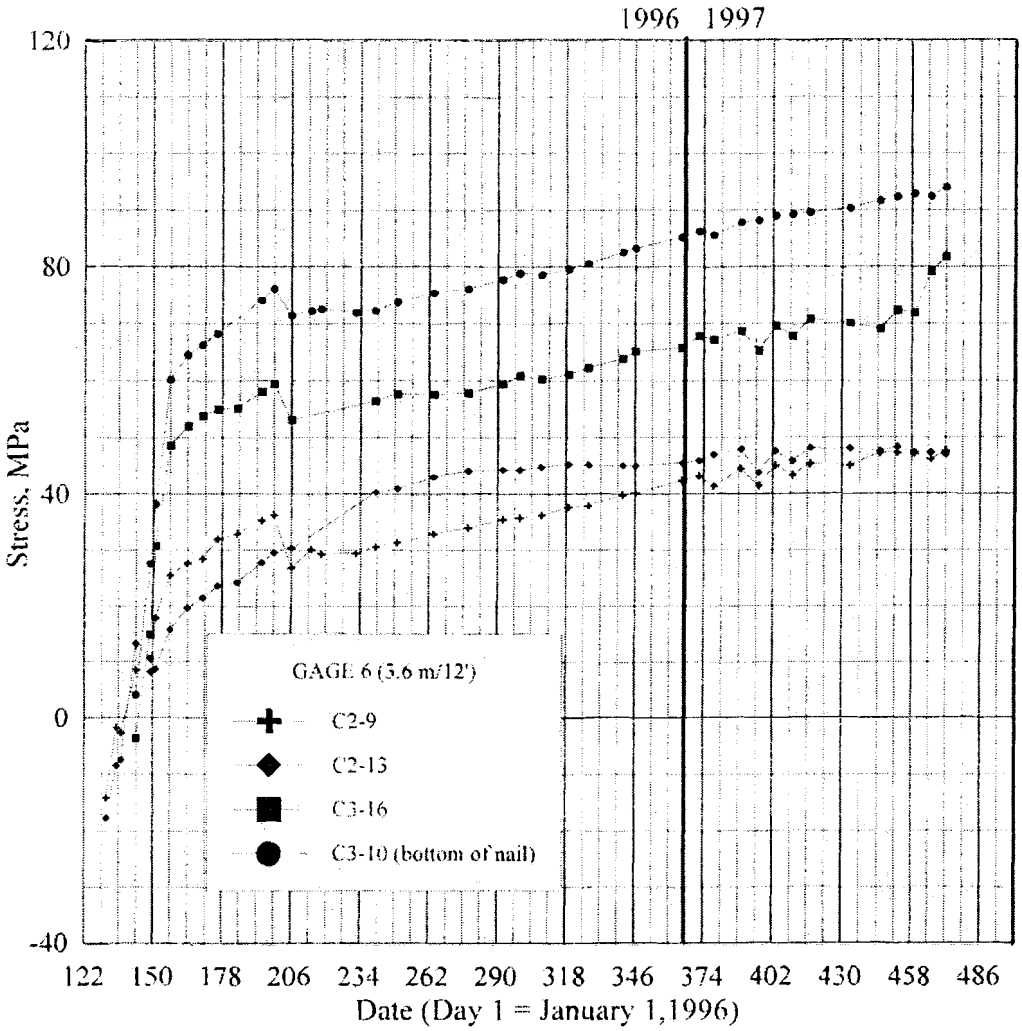


Figure 4-6: Strain gage stress vs. time for Gage 6, 3.6 m (12 ft) from exposed end of nail

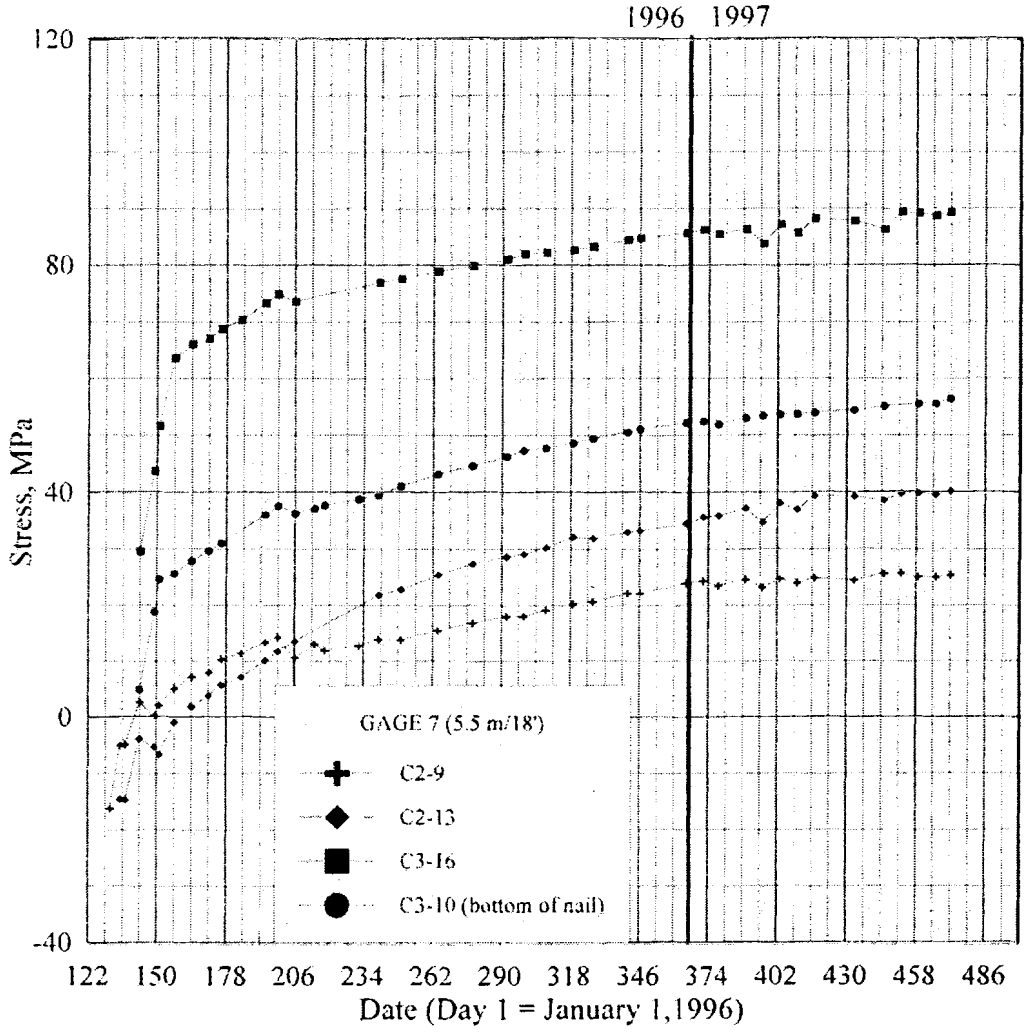


Figure 4-7: Strain gage stress vs. time for Gage 7, 5.5 m (18 ft) from exposed end of nail

### 4.3. Load cells

Figure 4-8 shows the results from load cells placed at the exposed end of instrumented nails. Most of the load cells showed a dramatic temporary stress increase during the installation of concrete storm gutters at the top of the concrete facing wall in August 1996. The effect is most marked on nails C3-10 and C2-13; it is not apparent at all in nail C4-13, which is located furthest from the storm gutters. The effect may be due to the nail-to-facing Nelson stud connections which are attached to the load cell bearing plates. Despite the tight fit of the load cells behind the end nuts on each nail, some disturbance may have occurred during the connection of the storm gutter reinforcement to facing wall reinforcement, formwork construction, or concrete vibration and curing. The highest load observed during the gutter construction was 31.0 kN (6970 lbf) in nail C2-13.

To check the validity of load cell results, selected load cell data were converted to stress measurements by dividing the load values by the cross-sectional area of the Dywidag #8 bars used as soil nails. These stress values were then compared to the averaged stress value from the two strain gages at the 0.9 m (3 ft) position on each bar. The load cell locknut on each nail was located approximately 0.2 m (8 in) from the end of each nail, embedded in the concrete facing wall. Tables 4-1 through 4.3 show a comparison of the load cell stresses and averaged strain gage stresses for each nail at three milestones in the construction project: the concrete pour for the facing wall, peak seasonal stresses as reflected in the strain gage data, and a post-frost condition. The comparisons indicate that the load cell data were consistently lower than the averaged nail. However, the load cell stresses did not vary by more than 50 MPa (7.25 ksi) from

the averaged stress values on the nail, and the literature search in Chapter Two indicates that the greatest stresses are found in a region 0.9-1.8 m (3-6 ft) from the end of the nail. Recall that the load cell on Nail C3-16 had to be moved to Nail C3-14 and that Gage 2 on Nail C4-13 failed in December, as described in Chapter Three. Taking all these factors into account, the load cell data appear reasonable compared to the strain gage data and can be considered valid. It is interesting to note that the highest load cell value in these tables, 42.6 MPa (6.18 ksi) on Nail C3-14, occurred in the post-frost condition on 4/16/97. Stress on this load cell had decreased to 22.2 MPa (3.22 ksi) by 5/22/97.

| Nail # | Load cell, 0.2 m (8 in) | Strain gages, 0.9 m (3 ft) |
|---|---|---|
| C2-9 | 17.6 MPa | 35.2 MPa |
| C2-13 | 23.4 MPa | 28.2 MPa |
| C3-10 | 21.8 MPa | 36.4 MPa |
| C3-16 (C-14 for load cell) | 16.5 MPa | 63.4 MPa |
| C4-13 | 10.4 MPa | 53.9 MPa |

Table 4-1: Load cell stress vs. averaged strain gage stress, 7/18/96

| Nail # | Load cell, 0.2 m (8 in) | Strain gages, 0.9 m (3 ft) |
|---|---|---|
| C2-9 | 26.9 MPa | 69.1 MPa |
| C2-13 | 33.1 MPa | 45.3 MPa |
| C3-10 | 34.0 MPa | 85.5 MPa |
| C3-16 (C-14 for load cell) | 27.6 MPa | 63.9 MPa |
| C4-13 | 26.8 MPa | N/A – Gage2 failed |

Table 4-2: Load cell stress vs. averaged strain gage stress, 2/20/97

| Nail # | Load cell, 0.2 m (8 in) | Strain gages, 0.9 m (3 ft) |
|---|---|---|
| C2-9 | 23.7 MPa | 57.2 MPa |
| C2-13 | 32.4 MPa | 41.3 MPa |
| C3-10 | 32.6 MPa | 85.2 MPa |
| C3-16 (C-14 for load cell) | 42.6 MPa | 55.6 MPa |
| C4-13 | 25.7 MPa | N/A – Gage2 failed |

Table 4-3: Load cell stress vs. averaged strain gage stress, 4/16/97

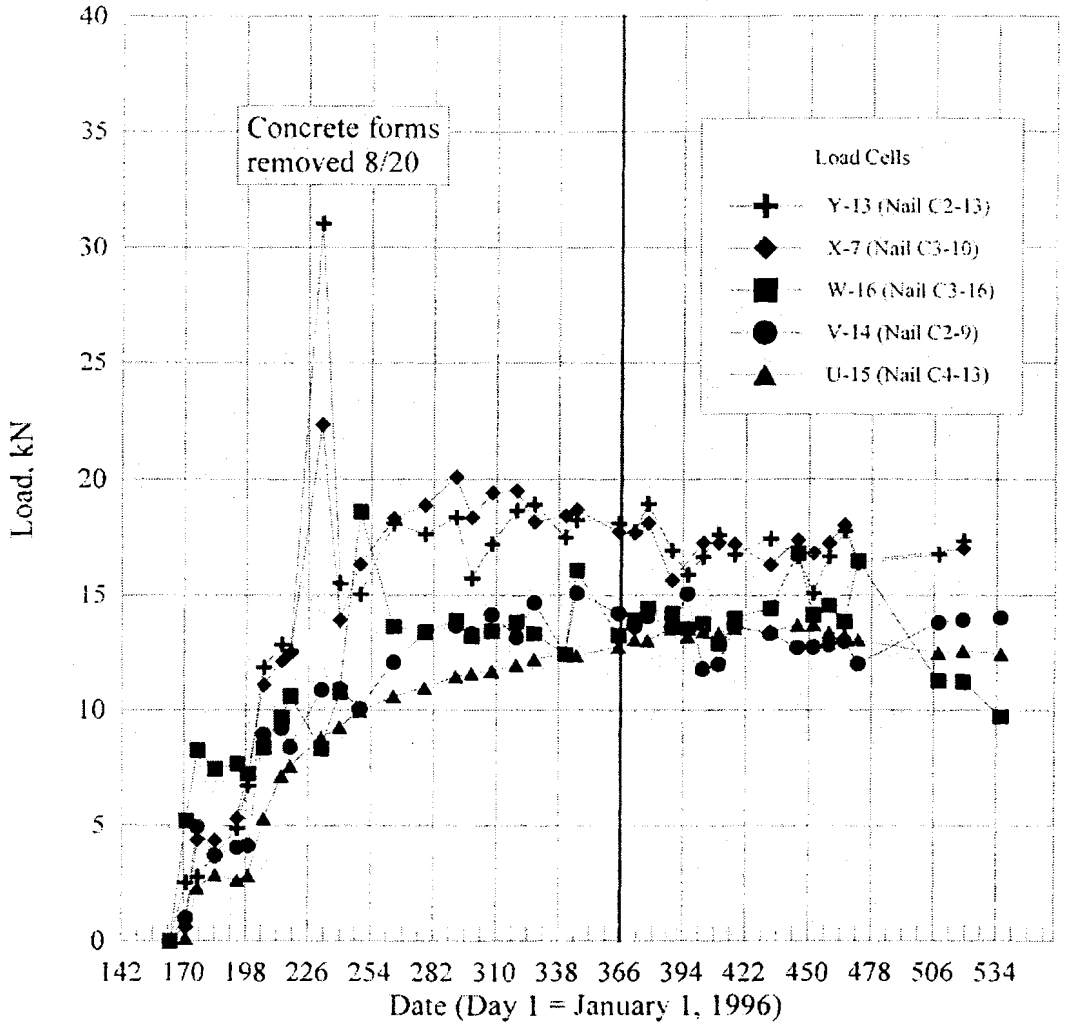


Figure 4-8: Load vs. time in load cells

### 4.4. Concrete strain gages

Figure 4-9 shows the results from two concrete strain gages, which were tied into the reinforcing steel of the concrete facing wall. The strain gages were mounted with their long axis perpendicular to the ground, in between soil nails as indicated in Figure 3-6. Temperatures from the sensors and the ambient air temperature at the wall (as logged manually at the time of each reading) have been included on Figure 4-9 to show how an increase in temperature corresponded with a decrease in stress and vice versa. It is also interesting to note the consistent lag between the sensor temperatures and the ambient air temperature. This is attributable to the latent heat capacity of the concrete.

Despite the apparent sensitivity to temperature change, the magnitudes of stresses in the concrete facing wall were quite small, ranging roughly from 0 to 1.38 MPa (0 to 200 psi) depending on the season. The steel-reinforced concrete expanded in hot weather and contracted in cold weather. The increase in tension in the concrete strain gages during cold weather indicates that the grouted soil nails pulled at the concrete as it tried to contract, and compressed the concrete as it tried to expand during the warm weather. However, the limited range of stress fluctuation indicates that the tied-in reinforced concrete facing was not adversely affected by frost pressures. This was an expected result; although some stress does get transferred to the concrete facing, its primary function in a soil nail wall is not to serve as a structural element, but rather to enhance the exterior appearance and promote good drainage for surface runoff.

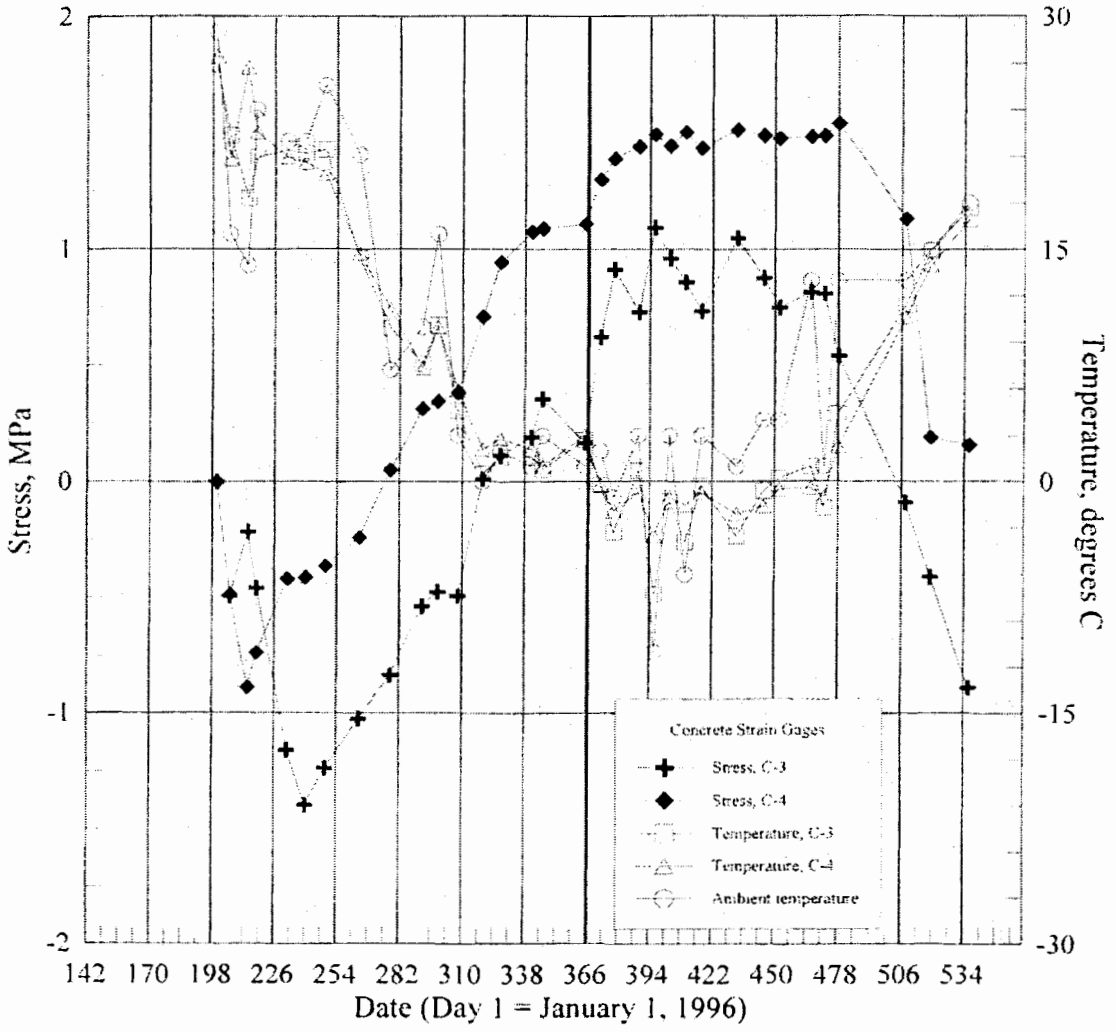


Figure 4-9: Stress vs. time in concrete strain gages

### 4.5. Total pressure cell (TPC)

Results from the total pressure cell (TPC) are shown in Figure 4-10. Although the TPC appeared to function well throughout the research period, the results (adjusted for temperature and barometric pressure) indicate virtually no pressure variation from the time of installation. The most likely explanation is that the load plate was not firmly set in contact with the soil. However, installers made a special effort to ensure good contact between the plate surface and the exposed face of the wall, including manual packing and tamping of all visible surface irregularities behind the plate. Another possible explanation for the lack of wall pressure is that the nails are spaced so closely that their areas of influence overlap and passively retain all the soil between them, resulting in negligible active earth pressures in the soil between nails (even in freezing conditions).

The largest observed fluctuations in the TPC occurred during days 198 to 215, corresponding to the calendar dates of July 16 to August 3, 1996. This corresponded with the concrete pour and curing, form removal, drilling through the new concrete to replace bolts on the bearing plates, and grouting up the drill holes. Apparently the pressure differentials experienced by the TPC from these activities outside the wall were greater than any forces originating in the soil nails themselves. This is also confirmed by the fact that all pressures were negative, i.e., the TPC was in compression. Again, the most likely explanation is that there was poor contact between the load plate and the soil so that the true effects of soil pressures were not accurately measured.

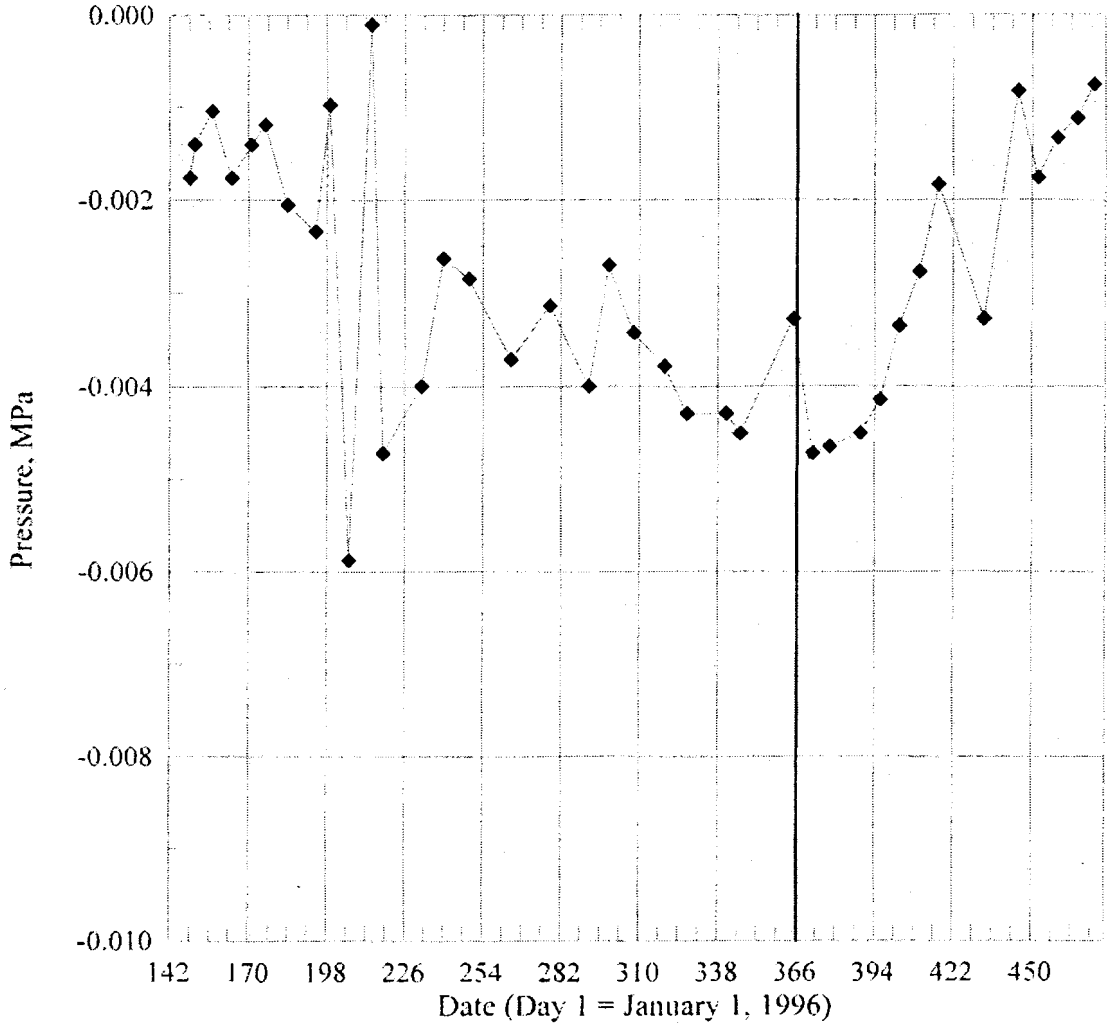


Figure 4-10: Stress vs. time in total pressure cell (TPC)

### 4.6. Thermocouples

Thermocouple temperatures along the the soil nails are shown in Figures 4-11 through 4-15. Temperatures in the soil between nails are shown in Figures 4-16 through 4-20. Average daily air temperatures and the historical daily average temperatures as measured by NOAA (1996-97) are shown in Figure 4-21 for reference. Some readings were lost or obviously misread due to datalogger problems, but the available data still provide a good picture of the thermal regime behind the wall over time. The soil nails exhibited slightly more temperature volatility and slightly deeper frost penetration than the wooden rods between the nails, as was expected due to the higher thermal conductivity of the steel nails. Sunlight appeared to play a role in frost penetration, as did the positions of the nails and their relative proximity to freezing air temperatures, both horizontally from the facing wall and vertically from the top of slope. For example, the readings on Nail C4-13 clearly reflect its more sheltered position below the finished pavement level and behind the concrete traffic barrier (refer to Figure 3-7). This nail appears to have lost all thermocouple readings beyond 2.1 m (7 ft) from the nail head, probably due to installation problems and lack of protective sheathing as described in Chapter Three. Thermocouple data is examined more thoroughly in Chapter Five.

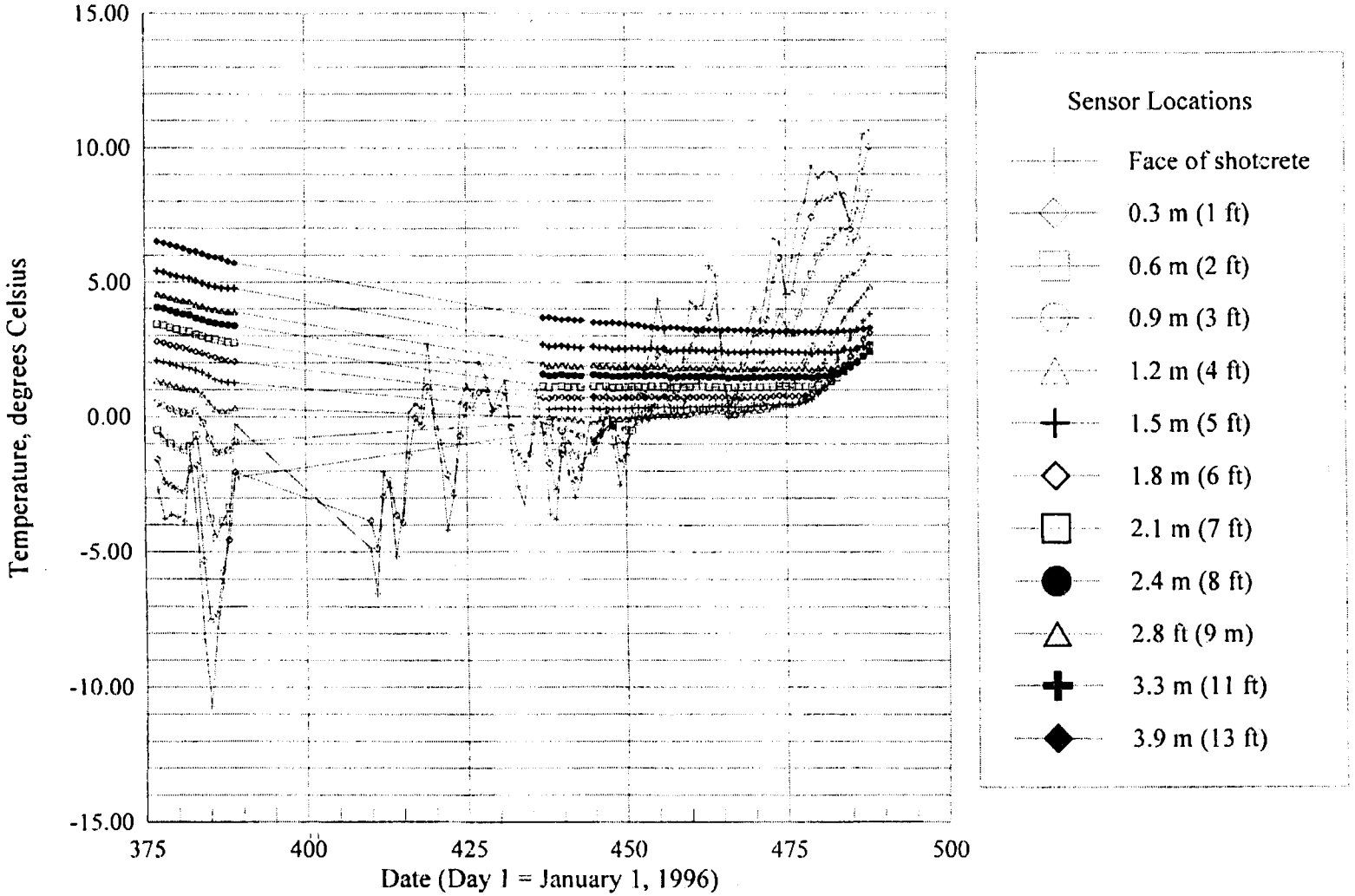


Figure 4-11: Thermocouple temperatures vs. time, Nail C2-9

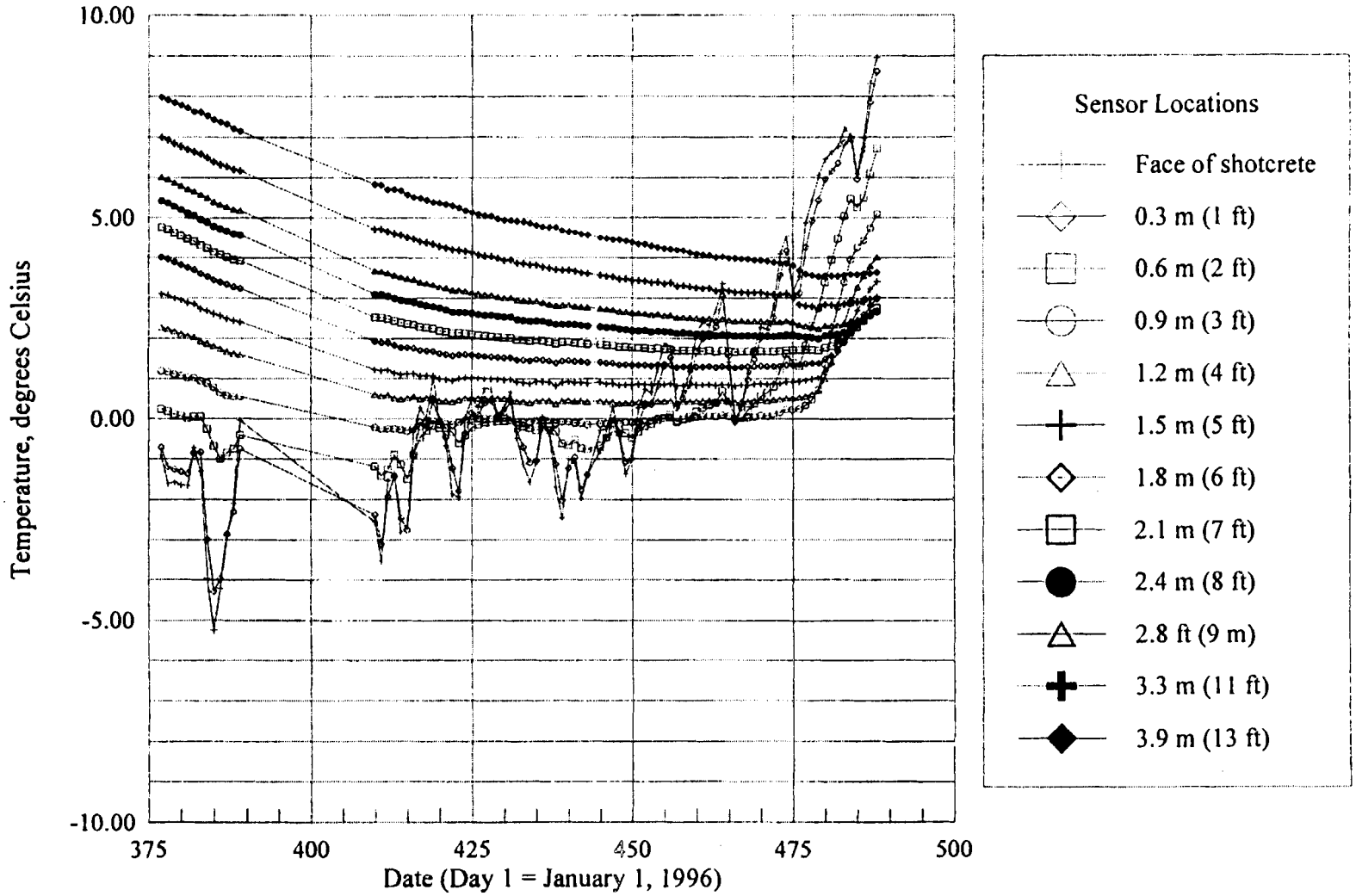


Figure 4-12: Thermocouple temperatures vs. time, Nail C2-13

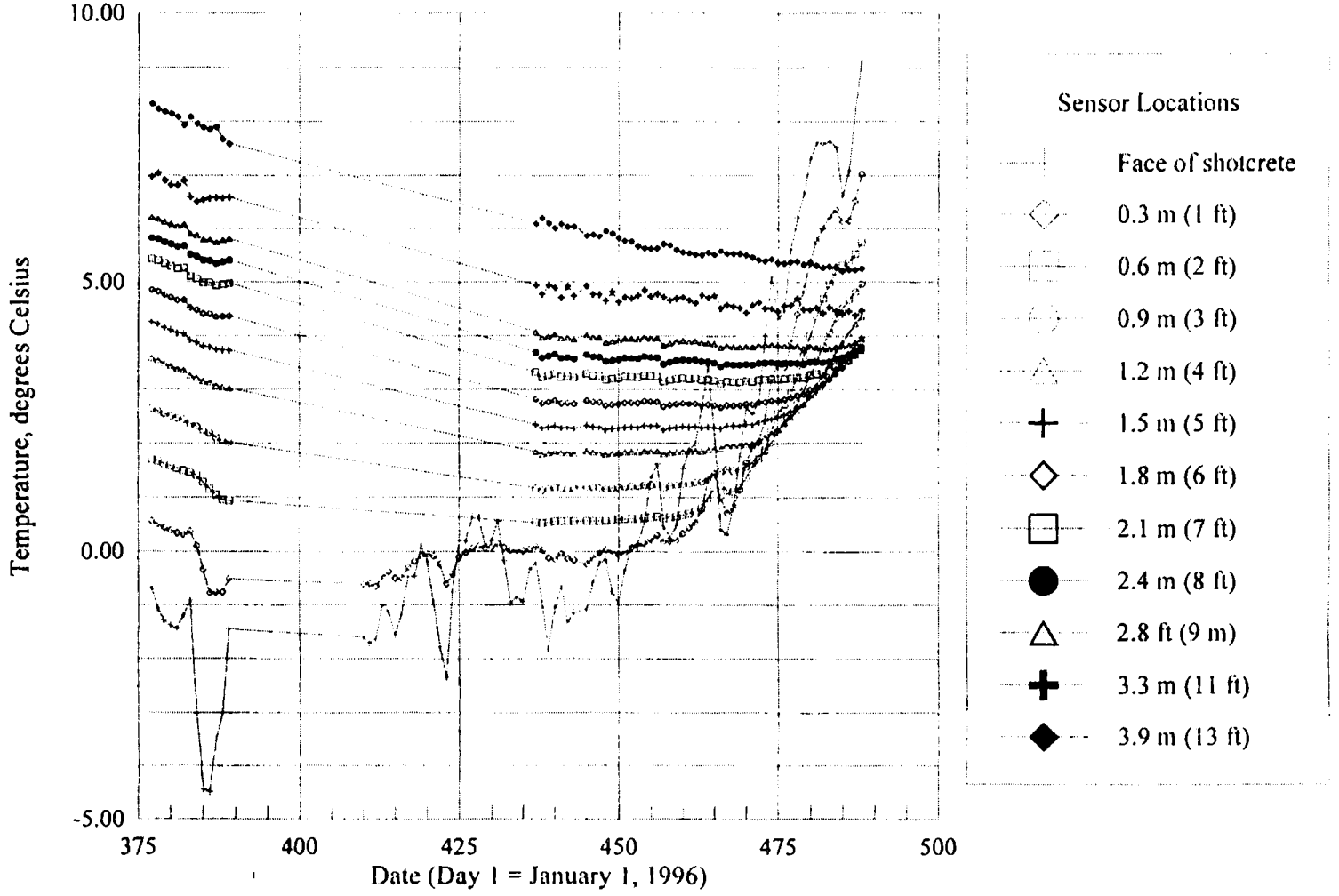


Figure 4-13: Thermocouple temperatures vs. time, Nail C3-10

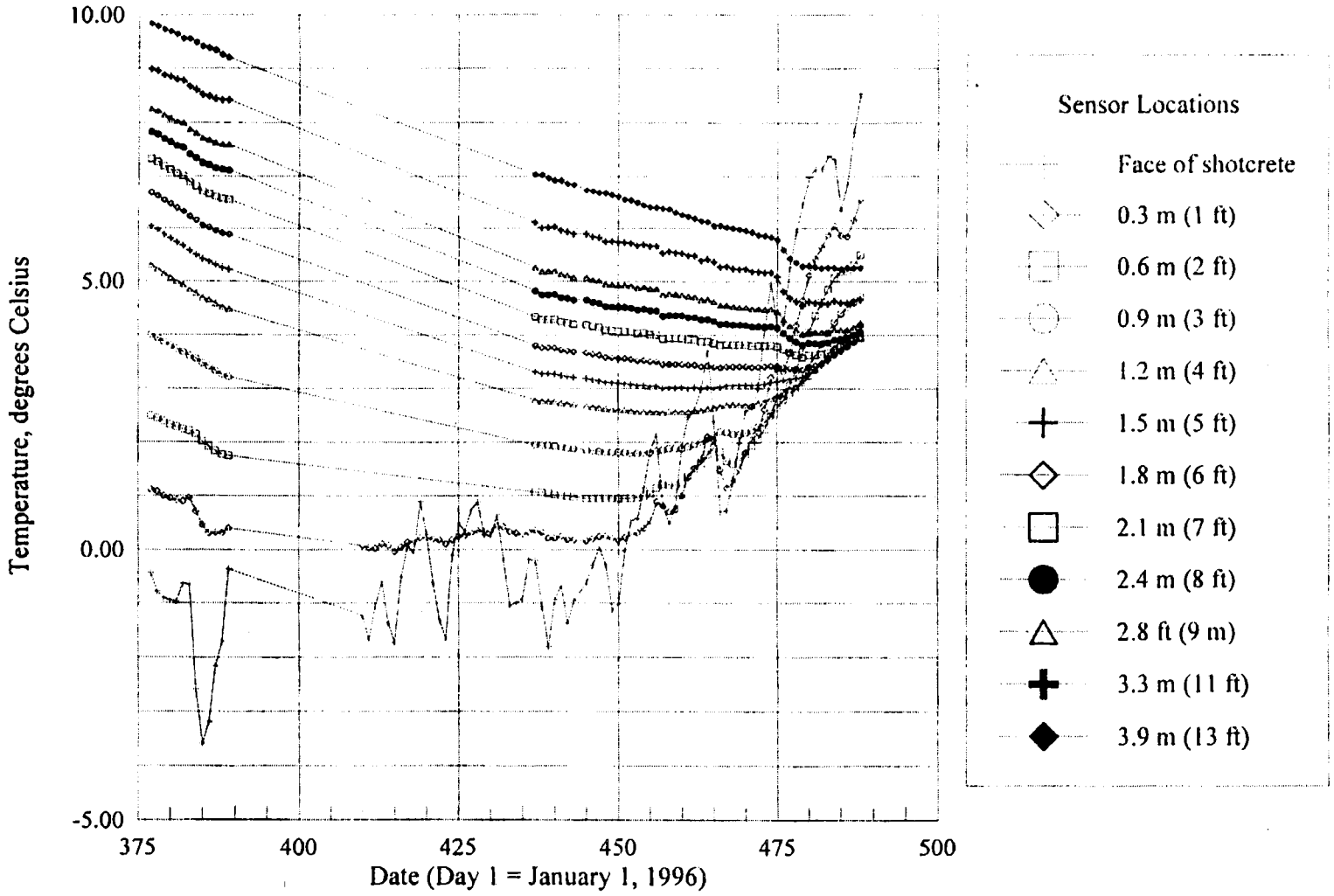


Figure 4-14: Thermocouple temperatures vs. time, Nail C3-16

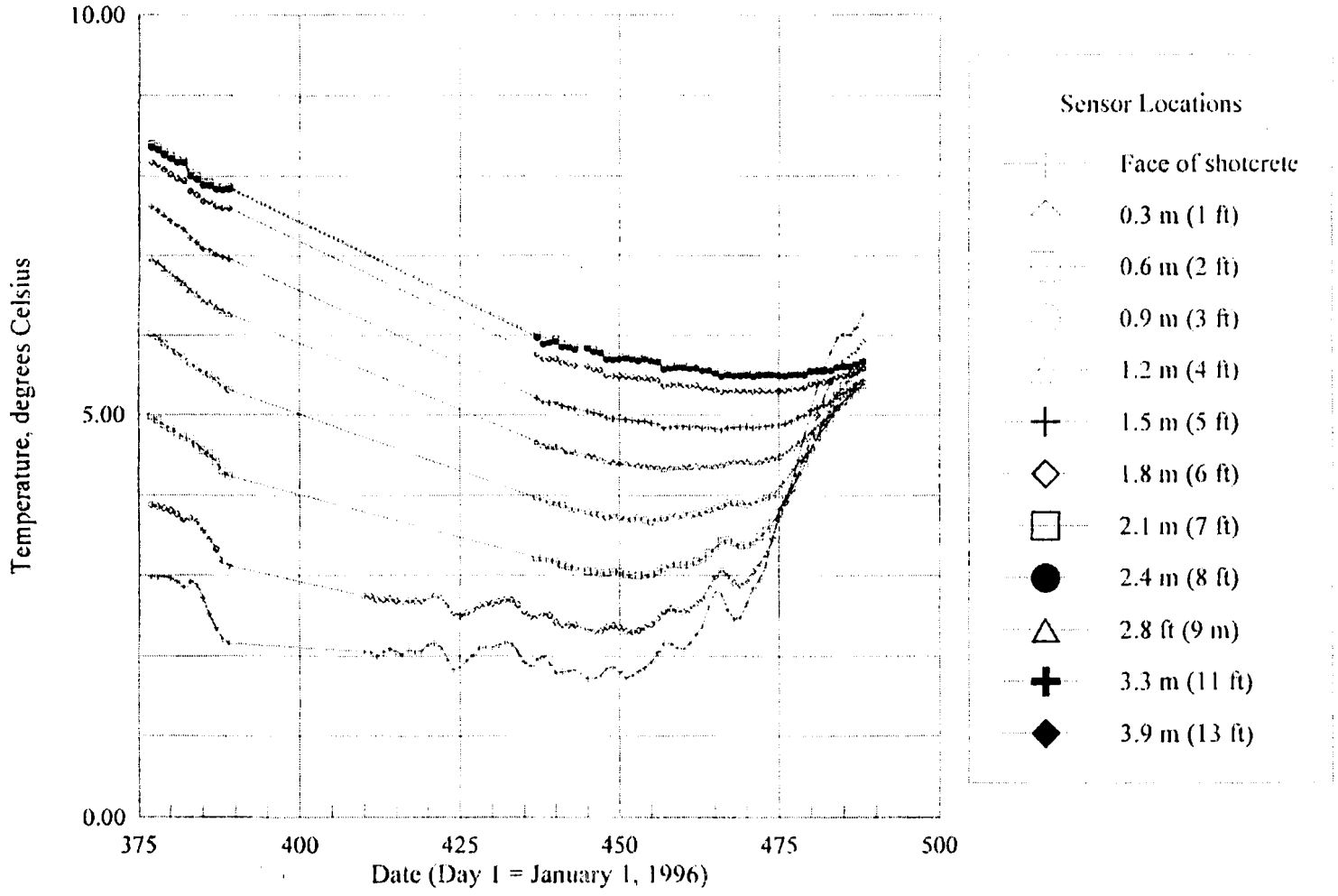


Figure 4-15: Thermocouple temperatures vs. time, Nail C4-13

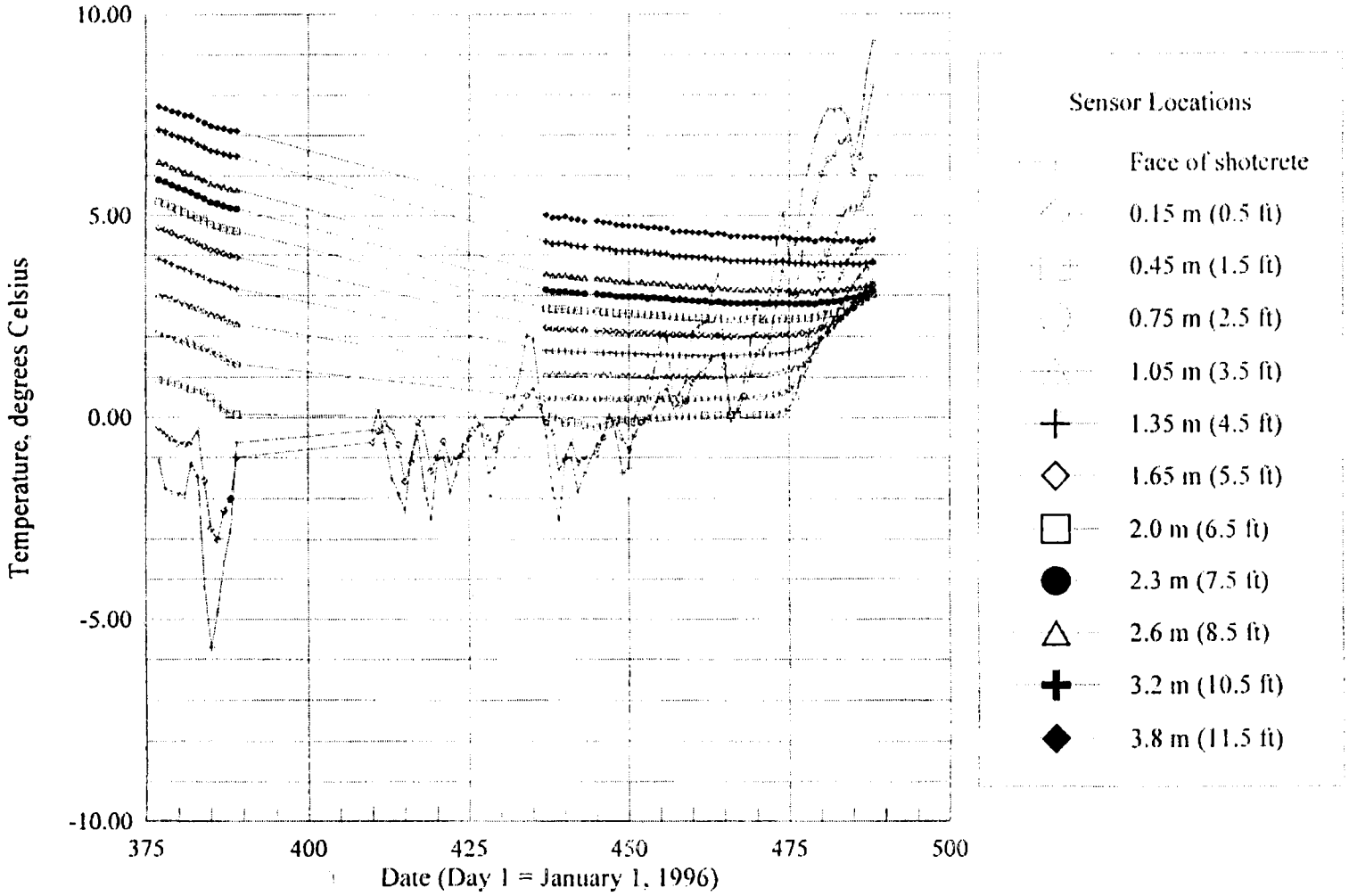


Figure 4-16: Thermocouple temperatures vs. time between nails C2-9 and C3-10

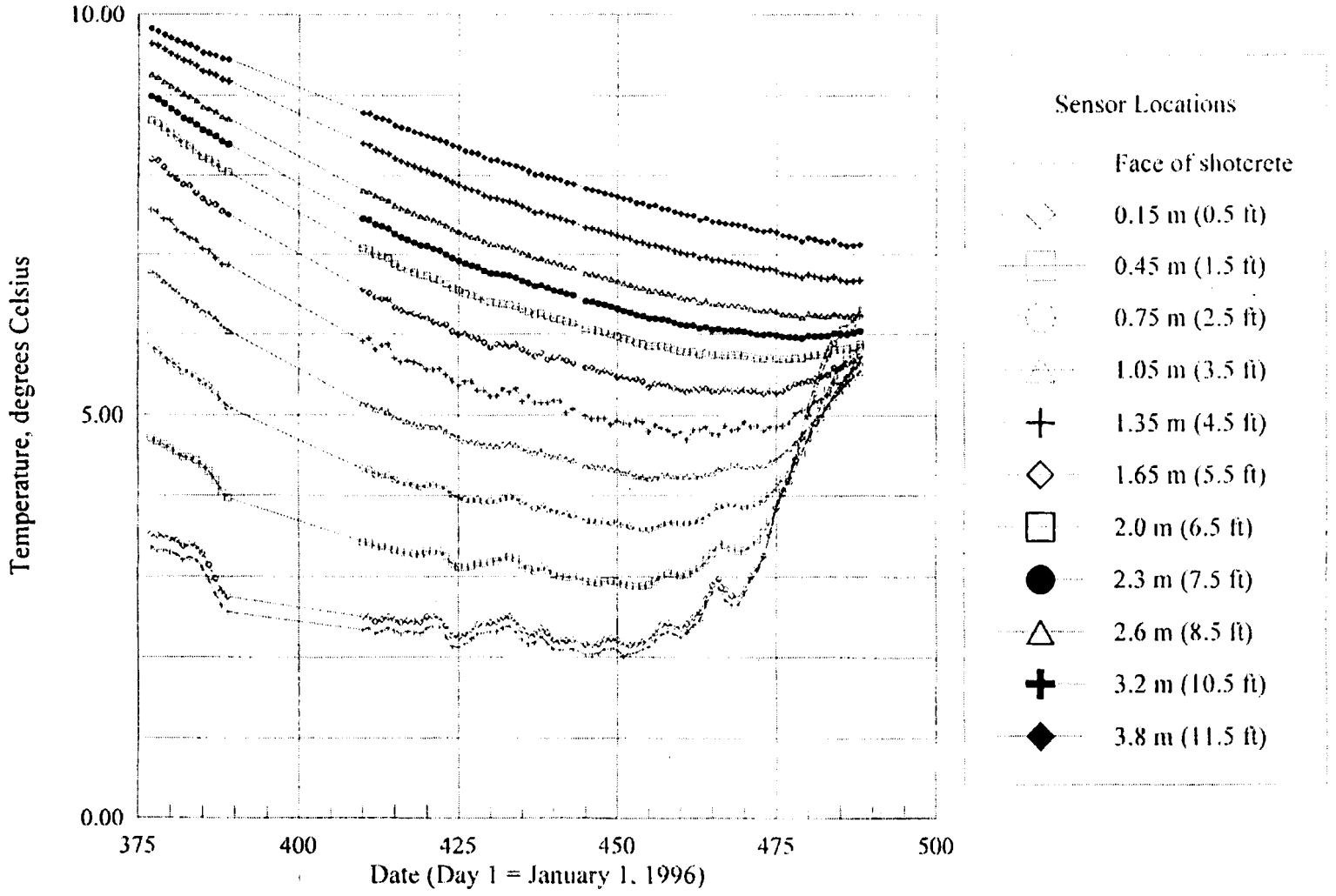


Figure 4-17: Thermocouple temperatures vs. time between nails C2-13 and C3-14

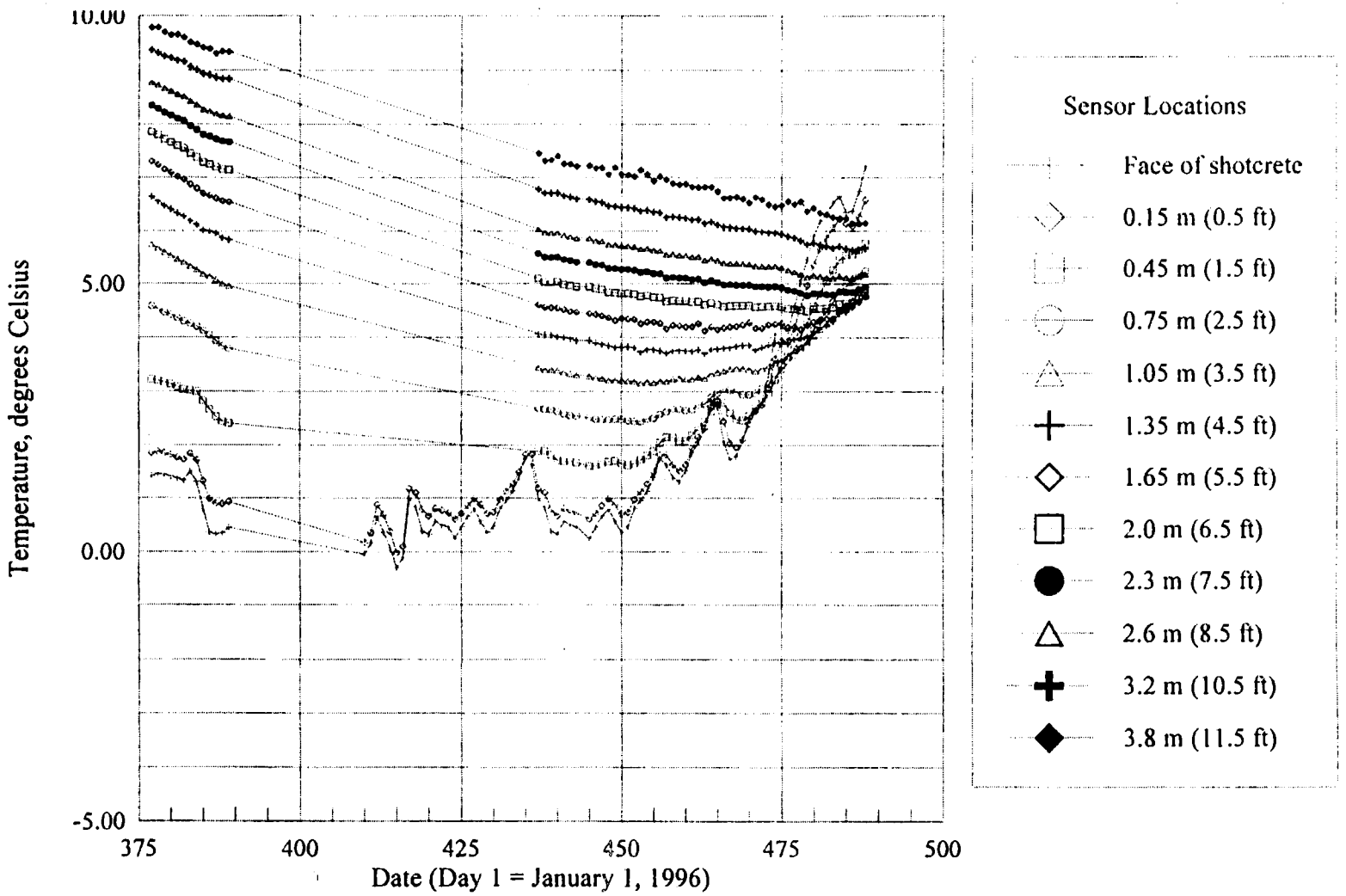


Figure 4-18: Thermocouple temperatures vs. time between nails C3-10 and C4-12

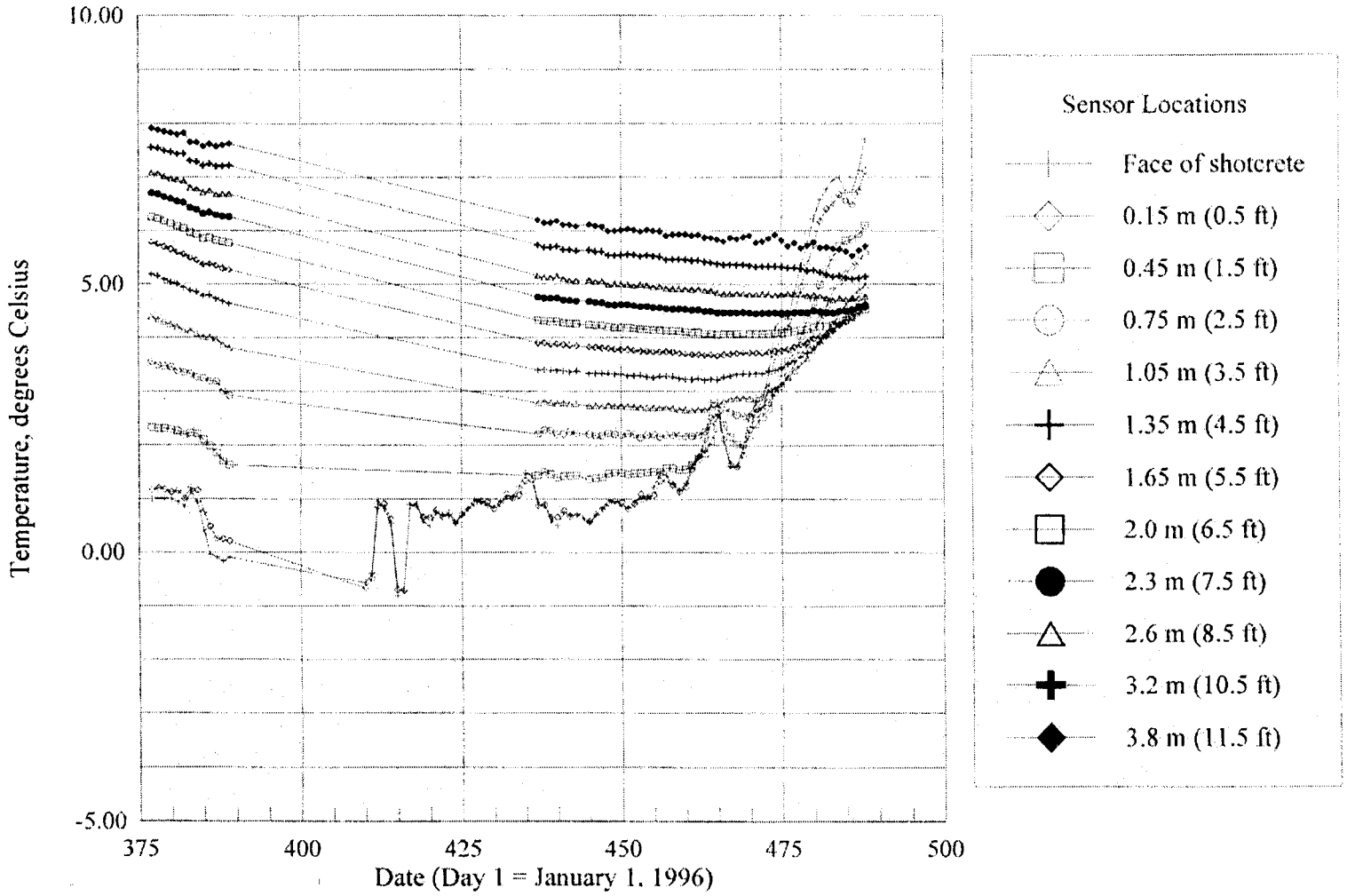


Figure 4-19: Thermocouple temperatures vs. time between nails C3-16 and C4-18

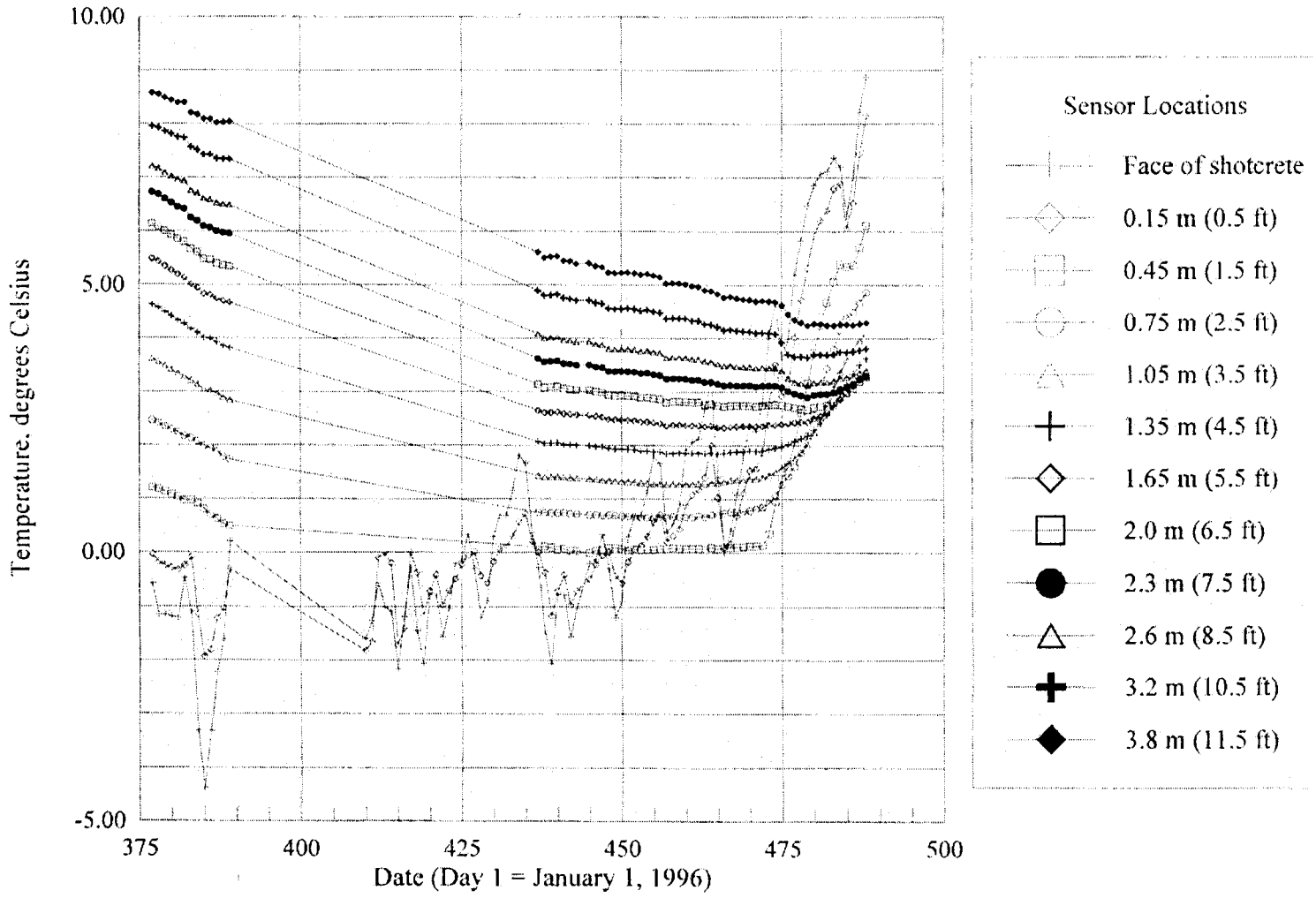


Figure 4-20: Thermocouple temperatures vs. time between nails C4-13 and C4-14

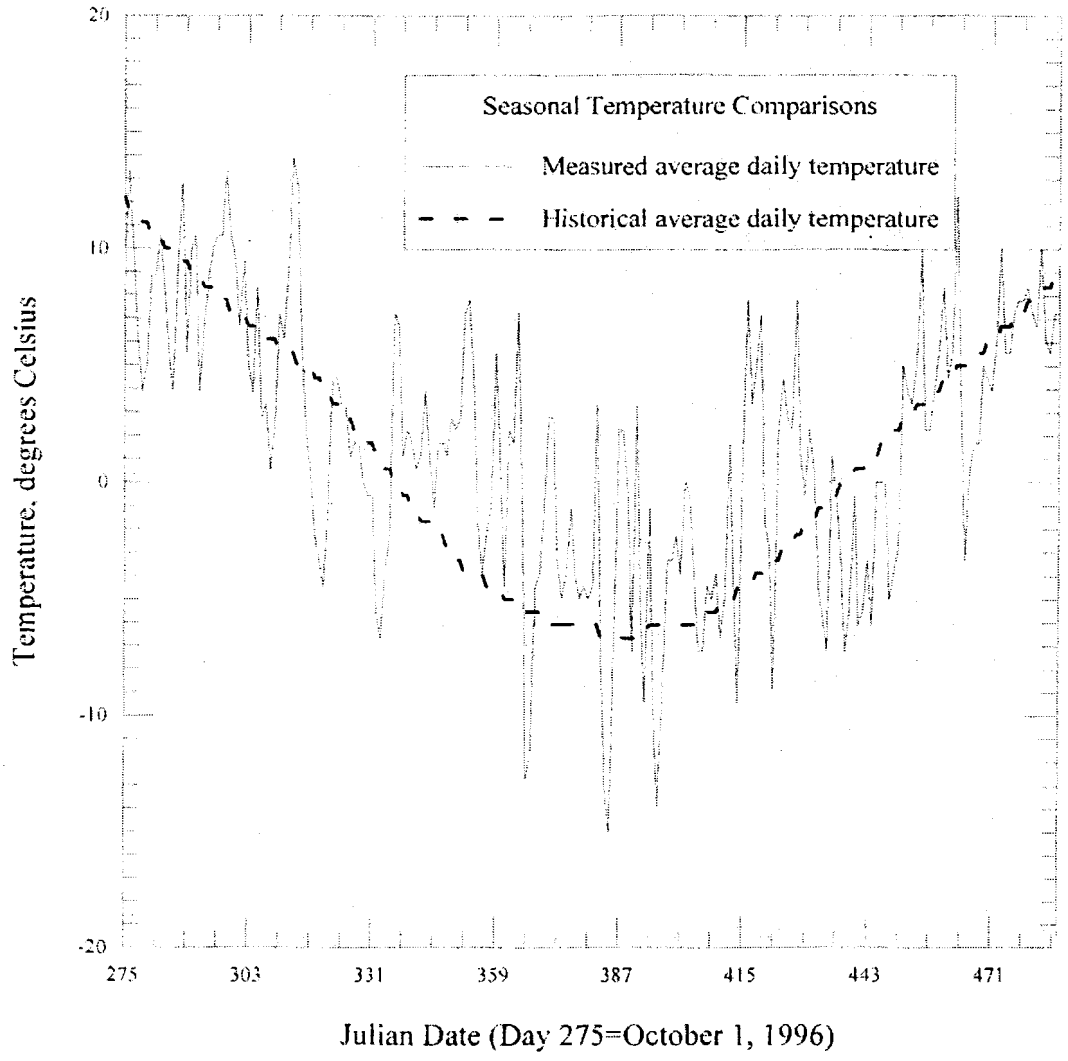


Figure 4-21: Ambient air temperatures vs. time

## 4.7 Survey data

Figure 4-22 shows a plan view of the X-Y positions of 10 survey points along the wall with corresponding pre- and post-construction elevations (Z) listed beside each point. The survey point labels used by the survey crew for points placed along the soil nail wall were 1,2,3,4,5,11,12,13,14, and 15, reading from west to east. The points were placed along the embankment crest prior to construction. Figure 4-22 shows that there was very little movement of any of the points along the X-Y plane view during construction, but most of the points subsided around 0.1-0.2 m (4-8 in) in the vertical dimension. Soil nail walls typically lose approximately 0.1 to 0.3 percent of the original height of slope during construction (Byrne et al., 1993), so this amount of subsidence was much higher than average for a 6 m (20 ft) wall. Some of the displacement occurred during initial excavation and drilling operations and thus may reflect the lack of cohesion in the fill. To the west of the railroad bridge (Figure 4-22), Points 1 and 3 fell approximately 0.5 m (1.7 ft) and 0.7 m (2.3 ft) respectively, as a result of the sloughing failure which occurred on this part of the shotcreted wall during construction (refer to construction sequence in Chapter Three). Once the sloughing problem was corrected and all the nails had been installed, there was virtually no additional movement in any of the survey points.

Although survey data was supposed to be collected weekly throughout the research period, no data was provided from the contracted survey company after July 31, 1996. Although the reasons for the cutoff were never clearly stated, the survey contract may have been terminated when it became apparent that the walls were stable and were not affecting the performance of the railroad bridge on the reconstructed abutment. (The

Maine Department of Transportation, as sponsor of this research effort, had requested the survey contract as additional early warning against catastrophic failure of the soil nail walls; survey points were not envisioned in the original research proposal from the University of Maine.) In any case, previous research (Juran and Elias, 1987) indicates that most of the movement in a soil nail wall occurs during the first few days following installation, as the soil pushes forward and the tension in the nails is fully mobilized. Thus the most interesting period for survey data, from an engineering research perspective, is covered by the available data.

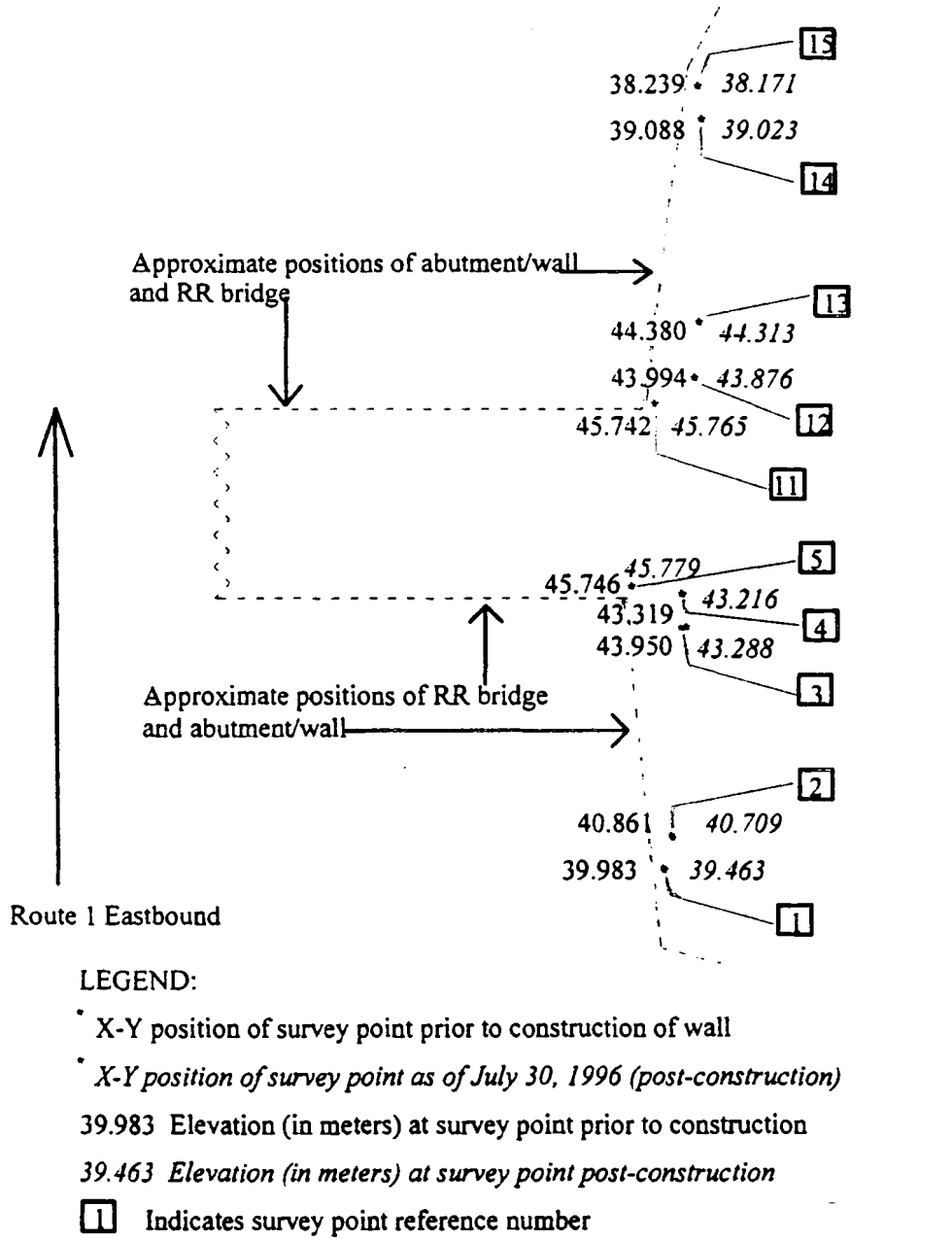


Figure 4-22: Changes in X-Y-Z space and locations of survey points

# CHAPTER 5

# ANALYSIS

## 5.1 Introduction

The results of the instrumentation project were examined in relation to the five objectives of the research study:

*Determine the magnitude and rate of freezing penetration behind the wall;

*Determine the effect of the soil nails on freezing penetration;

*Determine the magnitude of stresses on the nails and wall over the course of the seasonal freeze-thaw cycle;

*Determine the effects of freezing and frost heave on wall performance; and

*Develop recommendations for incorporating frost effects into soil nail design.

Each of these objectives will be examined separately in this chapter, although there was some overlap between objectives in the results and research findings. Throughout this chapter, depths of soil penetration are calculated based on an estimated 0.28 m (11 in) of exposed nail head encased in shotcrete and the exterior concrete wall, although in fact the thickness varied slightly due to variations in the application of the shotcrete.

## 5.2 Magnitude and rate of freezing penetration

The winter of 1996-1997 was warmer than average, as shown in Table 5-1 on the next page. Although the weather was slightly colder than average in the late fall and early

spring, it was warmer than average during December, January, and February -- typically the coldest months of the Maine winter -- and therefore warmer over the season as a whole. To further quantify the departure from normal temperature regimes, the freezing index was calculated by taking the average daily temperature (based on three-hour readings from NOAA, 1996-1997) and subtracting each average sub-freezing temperature value from 0° C (32° F), then adding the cumulative values together to obtain a seasonal value. This yielded a 1996-97 freezing index for Brunswick of 356 C degree-days (672 F degree-days), compared to the 30-year mean freezing index for the Brunswick area (Bigelow, 1969) of 427 C degree-days (800 F degree-days).

| MONTH | AVERAGE TEMP (° C / ° F) | DEPARTURE FROM NORMAL (° C / ° F) |
|---|---|---|
| October | 8.2 / 46.8 | -0.94 / -1.7 |
| November | 1.7 / 35.1 | -2.0 / -3.6 |
| December | 1.4 / 34.5 | +4.4 / +8.0 |
| January | -4.8 / 23.4 | +1.4 / +2.6 |
| February | -1.8 / 28.7 | +3.0 / +5.4 |
| March | -0.9 / 30.4 | -1.4 / -2.6 |
| April | 5.4 / 41.8 | -0.83 / -1.5 |

Table 5-1: Average monthly temperatures and departures from historical averages, October 1996-April 1997 (NOAA, 1996-1997)

The measured wall temperatures behaved generally as expected. The temperatures taken from the concrete strain gage thermistors, embedded in the concrete facing wall, dropped below freezing in early January 1997 and remained frozen through the end of March (Figure 4-9). The thermistor temperatures in the concrete wall generally followed fluctuations in air temperature (Figure 4-9 and Figure 4-21).

Temperatures within the soil showed less fluctuation as the depth from the surface increased. Referring to Figures 4-15 to 4-20, temperatures in the thermocouples located in the first 0.08 m (0.27 ft) of soil (0.3 m from the end of the rods) rose and fell in accordance with air temperature fluctuations (Figure 4-21), with a lag time of approximately 5-7 days; i.e., the soil temperature rose or fell approximately 5-7 days after a corresponding rise or fall in air temperature, although the amplitude of the temperature fluctuations was much smaller in the soil as compared to the air.

Temperatures in thermocouples located deeper in the soil, from 0.33 m to 0.63 m (1.1 to 2.1 ft), or 0.45 m to 0.9 m from the end of the rod or nail, fluctuated to a much lesser extent, as shown in Figures 4-11 through 4-20. Thermocouples located from 0.94 m to 3.7 m (3.1 to 12.1 ft) within the soil, or 1.2 m to 3.6 m from the end of the rod or nail, seemed to show a nearly linear decrease in temperature between January 11 (Day 377) and approximately February 15 (Day 426), when the slope of the temperature gradient decreased and in some cases leveled off. (Unfortunately, data was lost from all but the first two sensors on each thermocouple string during the period from February 2 (Day 413) and February 15 (Day 426), and no data at all was collected during the second half of January through February 2. Therefore this analysis is a best estimate based on the trends of available data before and after the period of missing data. The sensors furthest from the wall do appear to be decreasing linearly during this period, however.)

Temperatures deeper in the soil did not begin to increase again until after April 20 (Day 476), nearly a month after average daily air temperatures rose above the freezing

point. Figures 4-11 through 4-20 also demonstrate that the temperatures deeper in the soil tended to converge toward the end of the freezing season. This is consistent with Berggren's theory (also used in later frost penetration models) of a quasi-linear progressive frost front, created as warmer soils at depth continually lose heat to colder soil regions close to the surface, until a state of equilibrium is achieved (Jumikis, 1977).

Thermocouple data for parts of January and February was largely lost due to datalogger errors, as stated above. Since this was also the coldest part of the Maine winter, it is possible that the actual frost penetrations were greater than it was possilble to estimate with the usable results. Those results indicate that the depth of the frost front varied across the instrumented portion of the soil nail wall. Table 5-2 shows the estimated deepest frost penetrations into the soil with approximate dates, organized schematically according to nail "rows" and internail positions for comparison. Please refer to Figure 3-6 for the actual positions of thermocouples along the wall.

| | | | | |
|---|---|---|---|---|
| | | Nail C2-9<br>0.72 m, 2/18 | | Nail C2-13<br>0.92 m, 2/28 |
| | Therm. T1<br>-Never froze- | | Therm. T2<br>0.17 m, 2/18 | |
| Nail C3-10<br>0.08 m, 2/15 | | | | Nail C3-16<br>0.12 m, 2/26 |
| | Therm. T3<br>-Never froze- | | | Therm. T4<br>Wall only* |
| | | Nail C4-13<br>-Never froze- | Therm. T5<br>0.17 m, 2/25 | |

*Lack of sufficient data to determine precise date(s) of deepest frost penetration, which only reached to 0.15 m from the nail head, i.e., within the concrete facing wall rather than within the soil. Probably fluctuated above/below freezing within the concrete facing wall throughout February.

Table 5.2: Schematic representation of frost penetration behind wall

Several observations can be made from the data in Table 5-2. The first is that the deepest frost penetration occurred in the top row of nails, Nail C2-9 and C2-13. The top row of nails was in shadow most of the day from the railroad bridge span; this row was also subjected to a bidirectional frost front, inward from the face and downward from the top. A second observation is that there appear to be three distinct "zones" of frost penetration along the wall: deepest along the top row, slight to moderate to the west (i.e., to the right side of Table 5-2 since the wall faces north), and minimal to the east and along the bottom row. The frost depths on the east and west ends of the wall were probably influenced by sunlight conditions on the concrete facing wall. Nail C3-10, located on the east side which received sunlight all morning and early afternoon, experienced a frost depth of only 0.08 m (0.27 ft) into the soil; adjacent internail thermocouples T1 and T3 never froze at all. The west side of the wall received full sunlight in the afternoon only, and experienced slight to moderate frost penetration as shown in Table 5-2; internail thermocouple T4 indicated frost penetration within the concrete facing wall that never reached the soil behind it. (Unfortunately, the localized effects of sunlight cannot be confirmed from the concrete strain gage thermistor data, since both concrete strain gages were placed toward the shaded center of the wall.)

The bottommost row of nails was placed below the finished surface of the highway and behind the concrete traffic barrier as shown in Figure 3-6, so they were more protected from frost than nails in the other rows. These nails were also submerged below the groundwater table for at least half their length and this may have provided an additional source of conductive heat along the nails. A comparison in Table 5-2 between

Nail C4-13 and the adjacent thermocouple string T5 (mounted on wood, a much less conductive material than steel) shows that the freezing front along the thermocouple rod reached a soil depth of 0.17 m (0.55 ft), or 0.45 m as measured from the nail head, while Nail C4-13 never froze. (Internal strain gage thermistor readings at the shallowest strain gage depth of 0.63 m (2.1 ft) confirm that the temperature never dropped below 2.2° C (36° F) at Nail C4-13. These readings have not been presented as results because of their variability and unreliability in cold weather, particularly the Slope Indicator sensors; however, the Geokon strain gage thermistors at this location provided a useful comparison check against the thermocouple data.)

It is possible that localized freezing zones within the wall were influenced by thermal conduction through the steel H-piles and batter piles and the concrete abutment, as discussed in Chapter 2. However, this was impossible to quantify since the bridge elements were not instrumented and only approximate positions could be interpolated for the batter piles. Given the small cross-sectional area occupied by the piles and abutment relative to the overall volume of soil in the embankment, the influence (if any) of the bridge elements is presumed to have been slight and confined to the area immediately surrounding the piles and close to the frost front.

### 5.3 Effect of soil nails on freezing penetration

The high thermal conductivity of steel appears to increase frost penetration depths at some locations, and reduce penetration depths at others. From Table 5-2, it is evident that freezing temperatures generally penetrated more deeply along the soil nails than

along the wooden rods holding the thermocouple strings at nearby internail locations. In the topmost row of nails, Nail C2-9 and C2-13 achieved freezing temperatures at soil depths of 0.72 m (2.4 ft) and 0.92 m (3.1 ft) respectively. For comparison, thermocouple string T2 located approximately 0.6 m (2 ft) from Nail C2-13 froze only to a soil depth of 0.17 m (0.56 ft), and string T1 located the same distance from Nail C2-9 never froze at all. Nail C3-10 froze to a soil depth of only 0.08 m (0.27 ft), while thermocouple strings T1 and T3 within a 0.9-m (3-ft) radius of Nail C3-10 never froze at all. Nail C3-16 froze to a soil depth of 0.12 m (1.0 ft), while thermocouple string T4 located 0.6 m (2 ft) from Nail C3-16 experienced frost only in the concrete facing wall, and not in the soil at all.

The exception was Nail C4-13, which never froze despite being located only 0.6 m (2 ft) from thermocouple string T5, where the frost front penetrated to a depth of 0.17 m (0.56 ft). The bottom row of nails was below the finished grade of the roadway and was also covered by the deepest amount of fill within the wall, approaching 6 m (20 ft) at the center of the wall. Hence it was more insulated from the effects of cold weather penetration from the front of the wall, as well as from conduction heat loss along the steel beams and batter piles of the bridge abutment. This row of nails also extended below the fill into the native soil, a marine outwash with pockets of peat, and the nails were submerged for at least half their length in groundwater. It is possible that these conditions provided a heat sink effect, which helped to delay frost penetration along the nails in the bottom row.

For all other locations, the frost front penetrated more deeply along the instrumented nails than in the adjacent soil. These nails were placed above the groundwater table and thus lacked the additional heat source available to Nail C4-13. However, it appears that any heat transfer from the soil nails to the surrounding soil must have been minimal, as the internail locations within a 0.6 to 0.9-m (2 to 3-ft) radius of the nails did not reflect the same temperature regimes.

### 5.4 Magnitude of stresses on nails and wall over the course of the freeze-thaw season

Figures 5-1 through 5-6 show the stress vs. depth of gage relationships for all nails as a single-day "snapshot," taken approximately one month apart during each of the colder months of November through April. At soil depths of 0.63 m (2.1 ft) and 1.2 m (4.1 ft), or 0.9 and 1.5 m from the end of the nail, the figures show the averaged stress of both strain gages. The snapshots show that all nails experienced their highest stress regimes during February. In all but one of the nails, the highest stresses occurred in the gages within 1.5 m (5 ft) of the nail head, which confirms previous research as discussed in Chapter 2. The only exception to this rule was Nail C2-9, where the highest stresses along the nail consistently occurred at a soil depth of 2.1 m (7.1 ft). According to the available literature on soil nail walls (e.g., Guilloux et al., 1983), it is highly unusual for the highest stresses on a nail to be carried this far back along its length. This is because most soil nail walls develop their highest seasonal stresses due to tension between the nails and the facing wall connections, whereas high stresses at 2.1 m behind the wall are more likely associated with mobilized shear resistance as described in Chapter Two.

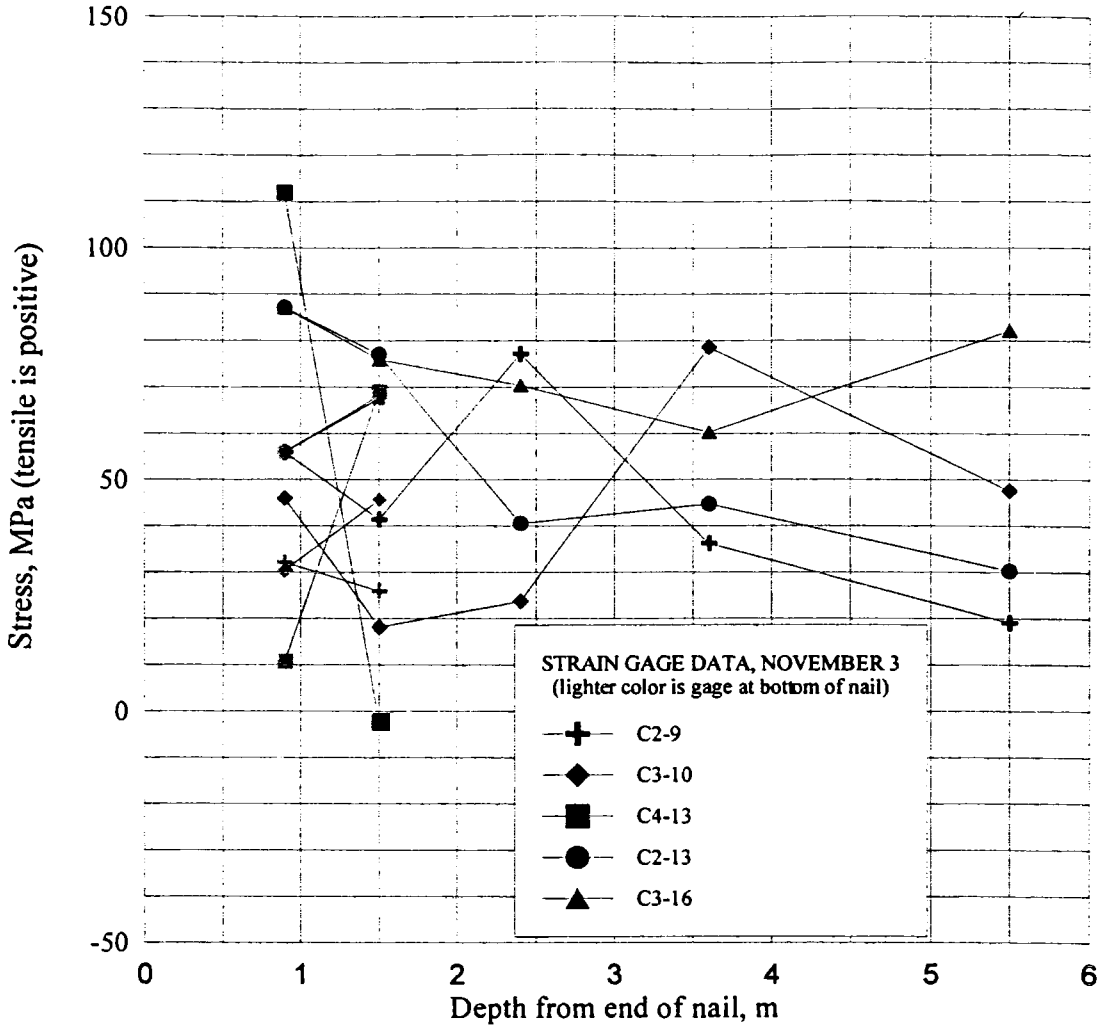


Figure 5-1: Stress in soil nails on November 3, 1996

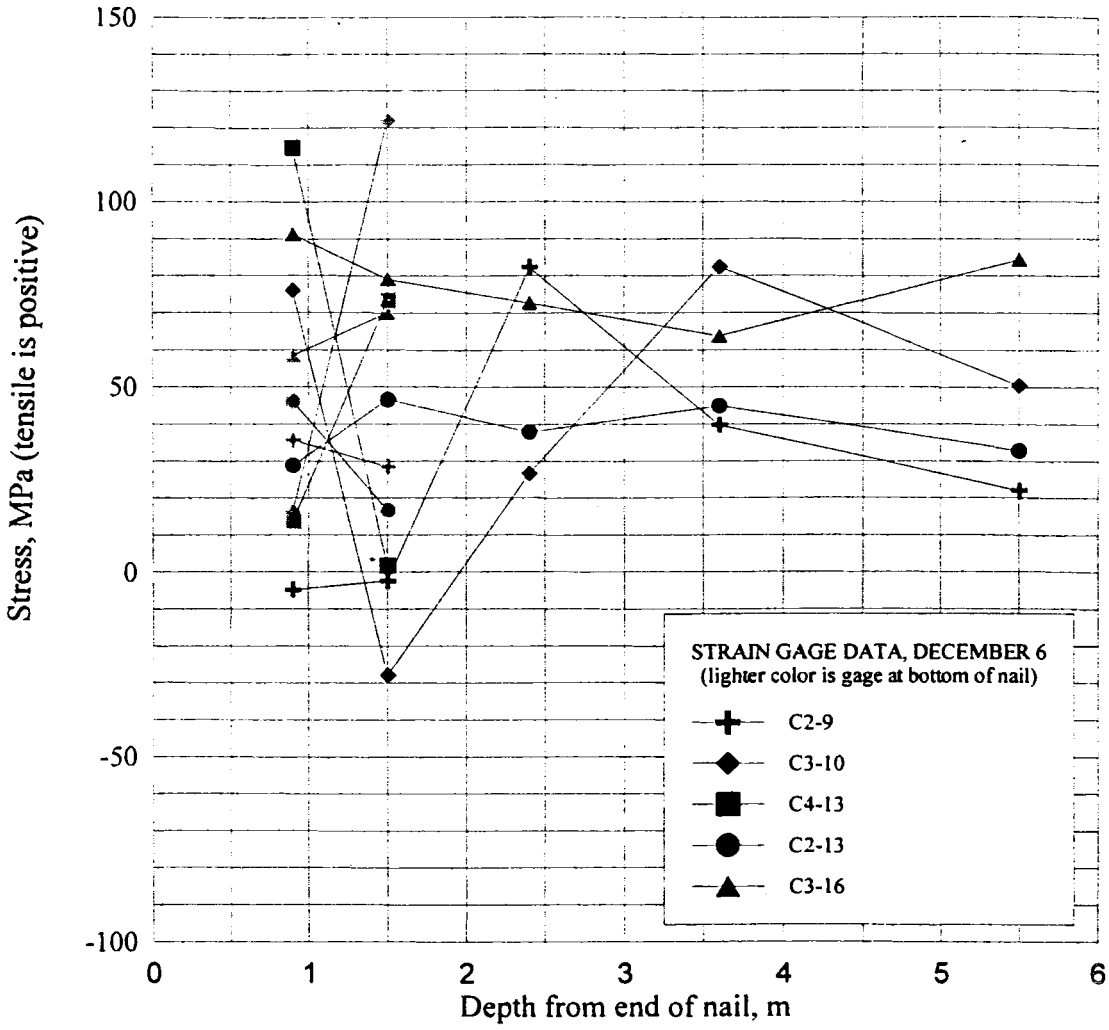


Figure 5-2: Stress in soil nails on December 6, 1996

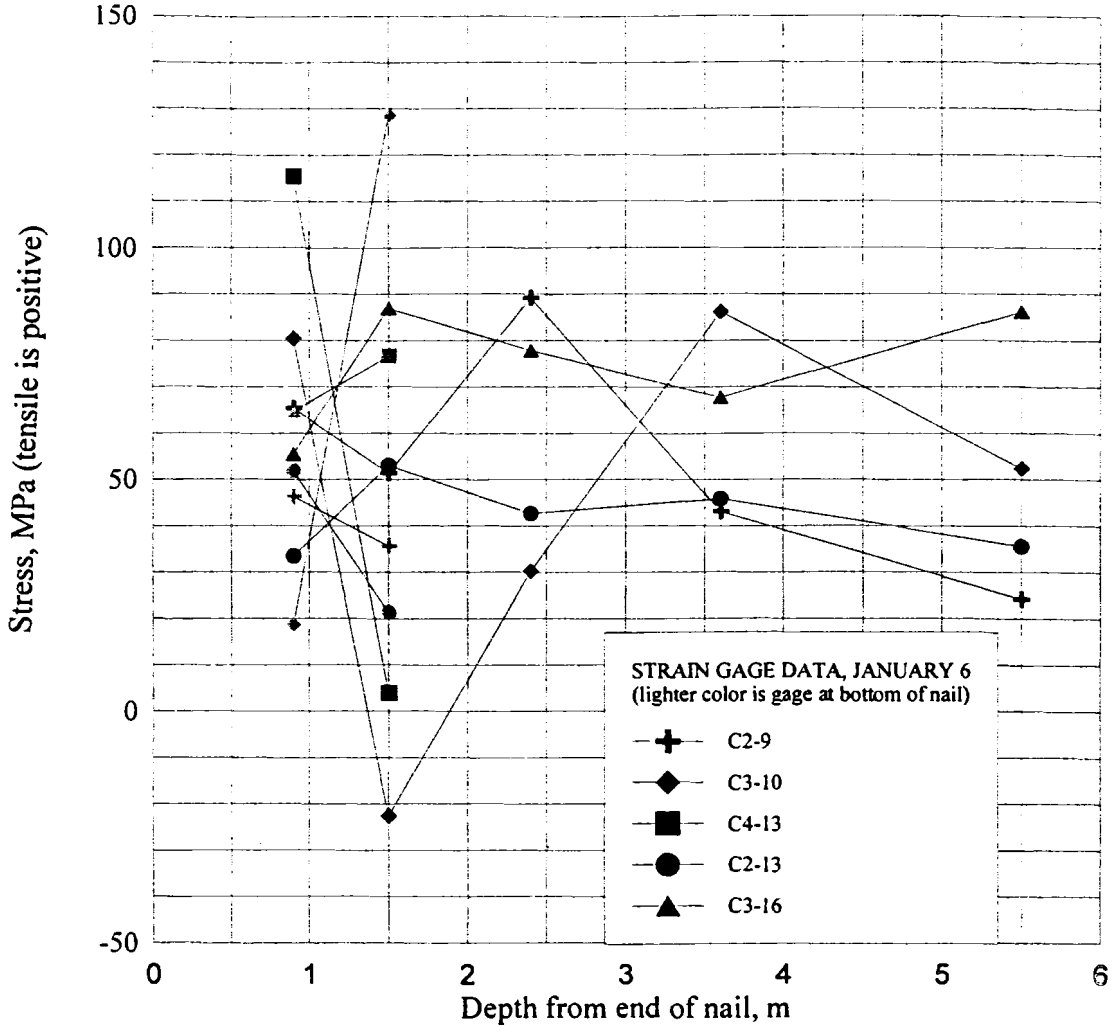


Figure 5-3: Stress in soil nails on January 6, 1997

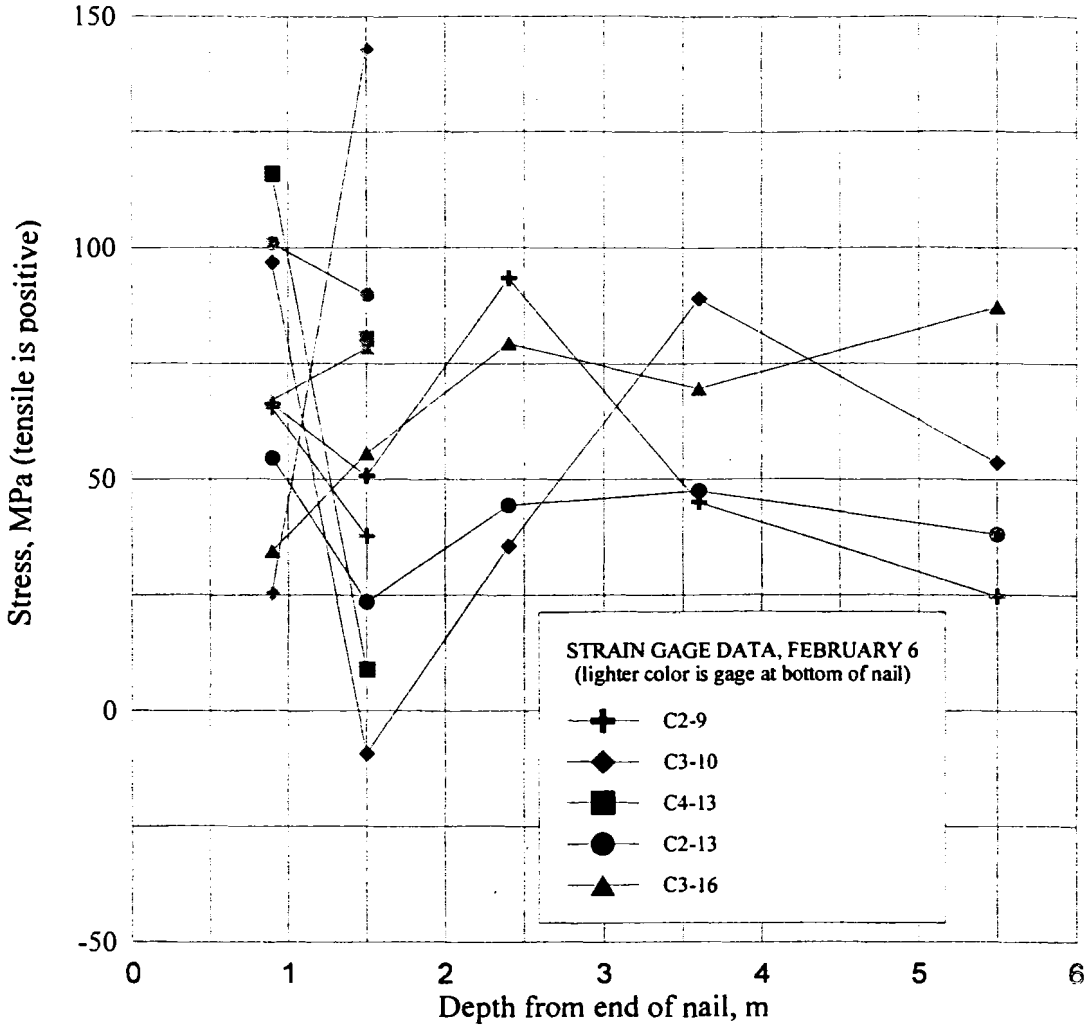


Figure 5-4: Stress in soil nails on February 6, 1997

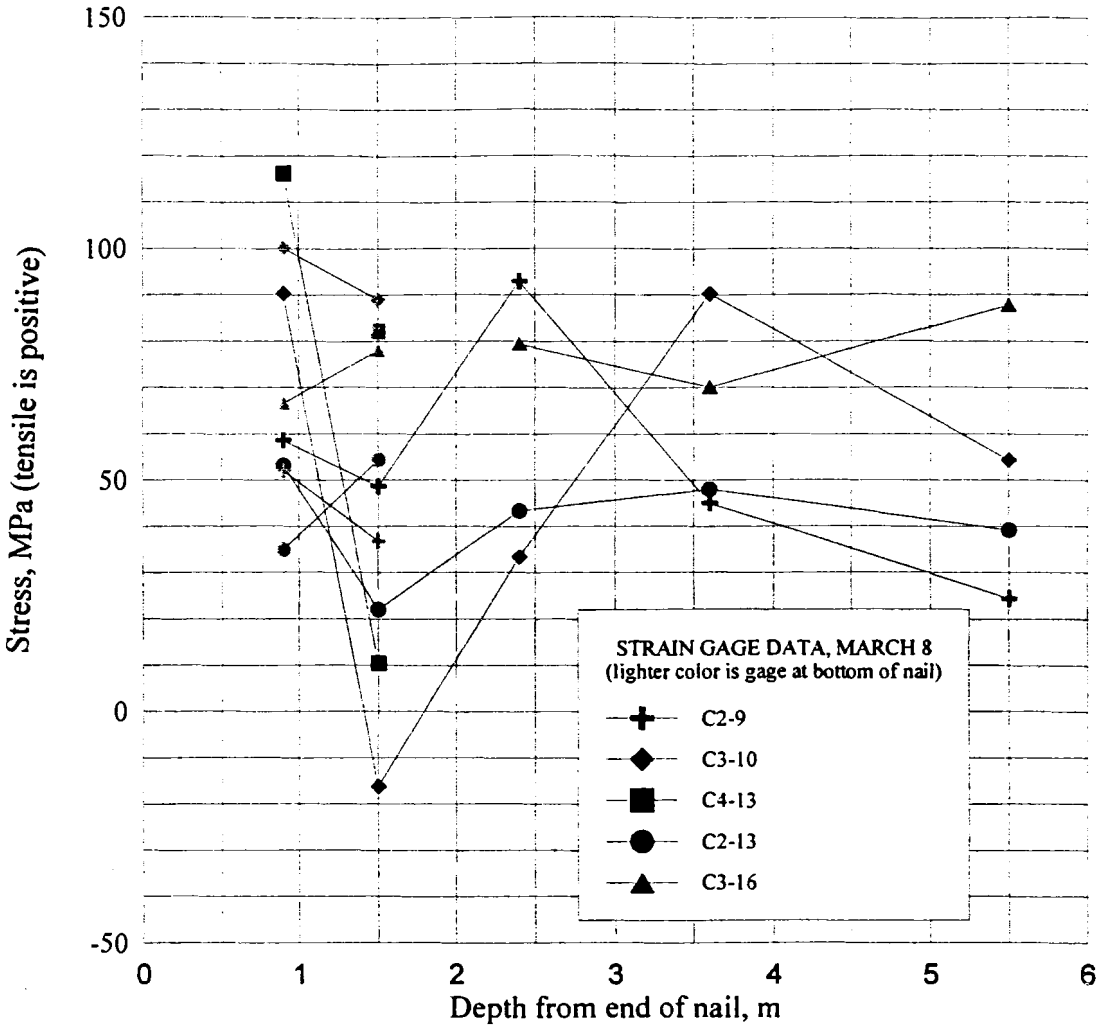


Figure 5-5: Stress in soil nails on March 8, 1997

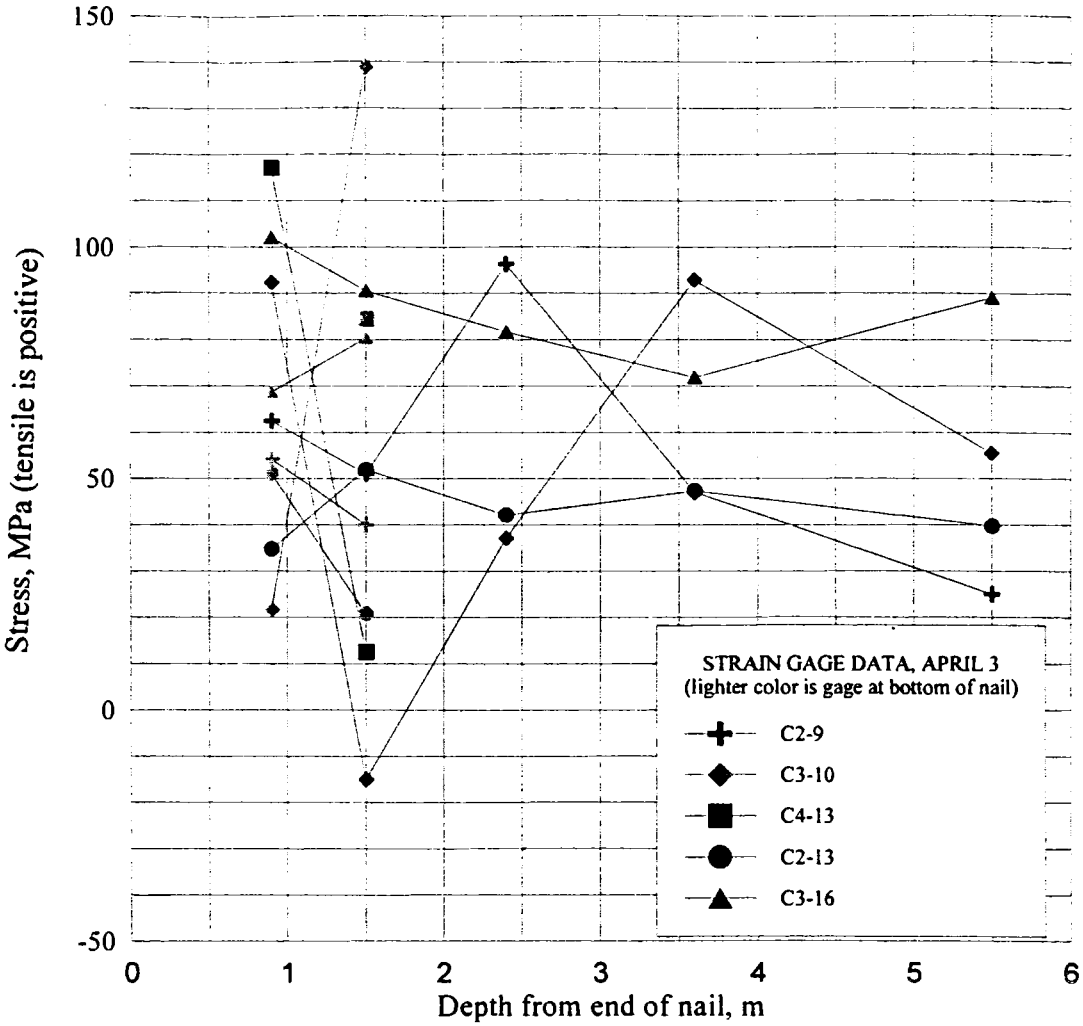


Figure 5-6: Stress in soil nails on April 3, 1997

The gages placed deepest within the soil, at 3.3 m (11.1 ft) and 5.2 m (17.1 ft), i.e., 3.6 and 5.5 m from the nail head, showed very little stress variation from month to month. This was expected, as the frost front never approached this region of the wall.

Figures 5-1 through 5-6 show that all nails stayed well within the rated yield stress for Dywidag #8 rebar, 400 MPa (60 Ksi). The highest single stress noted was in Nail 3-10 at a distance of 1.5 m (5 ft) from the end of the nail, a reading of 145 MPa (21.2 Ksi) on February 20, 1997. This is slightly higher than the design factor of safety of 3, but well within the expected tensile capacity of the rebar.

Since February 20 was also the date on which stress readings were highest on average for all the bars during the period of study, the extreme fiber bending stress was calculated for each nail on this date using the opposing stresses in the dual strain gages placed at 0.9 m (3 ft) and 1.5 m (5 ft) from the end of the nail. To obtain the bending stress in extreme fiber from the total stress in the nails, it was assumed that the stresses were symmetrical around the central axis of each bar, and that maximum deflection in the bars was along the line formed by the oppositely placed strain gages. (In fact, deformation in line with the gages may not have occurred, as several of the nails rotated during installation so that their strain gages were no longer at the "top" and "bottom" of the nail as intended. Thus the two strain gage positions on each nail may not have been aligned perfectly with the maximum deflection plane along the nail. However, it would have been impossible to estimate the bending stresses without assuming maximum deformation in line with the strain gages. The only nail for which adjustment has been

made is Nail C3-10, where the rotation of the nail during installation was approximately 180°. This changed the direction of bending, but not the magnitude.) The stress values in the two gages were averaged, and the average number was subtracted from the higher gage stress value to obtain the amount of stress on either side of the plane of rotation (through the center of the nail). Then the calculated bending stress at the gages was linearly interpolated back from the known height of each strain gage to obtain the extreme bending stress at the flattened portion of the nail. The results of this analysis are shown in Table 5-3. Note that the stress shown for nail C4-13 at the 0.9 m (3 ft) position was taken on December 11, 1996, which was the last date that strain gage #2 on this nail functioned. The stress for the 1.5 m (5 ft) position is taken from February 20, 1997, as are all values on all other nails.

| Nail | Stress, MPa (psi) 0.9 m (3 ft) | Stress, MPa (psi) 1.5 m (5 ft) |
|---|---|---|
| C2-9 | 0.279 (40.5) | 2.98 (432) |
| C2-13 | 4.61 (669) | 7.42 (1080) |
| C3-10 | 16.8 (2610) | 34.0 (4930) |
| C3-16 | 8.02 (1160) | 0.280 (40.6) |
| C4-13 | 23.0 (3340) | 15.9 (2310) |

Table 5-3: Extreme bending stress in nails at 0.9 m and 1.5 m, February 20, 1997

Table 5-3 shows that the bending stress in all nails was negligible, and infers that bending is unlikely to be the dominant failure mode in a soil nail wall placed in freezing temperatures. The highest two stresses noted was in Nail C3-10 at a distance of 1.5 m (5 ft) and 0.9 m (3 ft) from the end of the nail. Not surprisingly, the highest tensile stress in

any of the nails also occurred on Nail C3-10 at the 1.5 m (5-ft) position, as noted earlier in this chapter. However, even the highest bending stress at 1.5 m (5 ft) was only 34 MPa, as compared to 146 MPa for the corresponding tensile stress at that point.

At a distance of 0.9 m (3 ft) and to a lesser extent at 1.5 m (5 ft) from the end of the nails, bending stresses were generally higher in the nails toward the bottom of the wall. This is probably not surprising given that these nails carry the weight of the additional soil, grout, and nails above them. However, the existing literature indicates only that soil nail walls typically carry higher *tensile* stresses in the upper rows of nails; bending stress is not discussed. Indeeed, the observed extreme fiber bending stresses in the Brunswick wall indicate that bending stress is probably not significant for design purposes, since tensile strength is the overwhelmingly dominant stress mode even at the bottom of the wall.

Figure 4-8 shows load vs. time in the load cells. These values were converted to stress on the nail heads by taking the averaged load readout from the load cell (Figure 4-8) and distributing it across the cross-sectional area of the nail. The load cells indicated a gradual increase in stress on the nail ends as the temperatures cooled, although never to the high values seen during the gutter construction (day 229). However, the maximum seasonal peaks in the load cells were reflected during November and December (days 308 through 366), well in advance of the coldest soil temperatures which occurred in late

February (days 410 through 425). After December, the stresses on the nail ends leveled off or declined slightly. There was also no further correlation between the load cell stresses and external temperatures, even as the soil warmed in April and May.

The tensions in the load cells -- and, by implication, the nail end stresses -- were also very low compared with the stresses along the nails, ranging from 22.7 to 37.8 MPa (3.29 to 5.48 Ksi) during the coldest months, when maximum stresses at 0.9 m (3 ft) and 1.5 m (5 ft) from the end of the nail ranged from 54.9 to 146 MPa (7.96 to 21.2 Ksi). At the end of the research period in June 1997, the load cells held a residual loading of 18.4 to 35.1 MPa (2.67 to 5.09 Ksi) over the installation values in June 1996. This agrees with the results of previous research on frost effects in soil nail walls, such as Juran and Elias (1987) and Kingsbury et al. (2002), indicating cumulative increases in tension in the area immediately behing the facing wall with each successive winter. However, the lack of correlation between colder temperatures and higher load cell tension is puzzling. It is possible that the load cells (and by inference the nail ends) were influenced by the material qualities of the concrete facing wall in which they were embedded, and this in turn limited the expected rise in tensile stresses on the nail ends during the coldest months.

As shown in Figure 4-9, the concrete strain gages displayed a strong inverse correlation between decreasing temperature and tensile stress. Tensile stress increased almost directly with decreasing temperatures and vice versa. However, this behavior is much more likely to be related to the thermal characteristics of the concrete itself than to

any behavior in the soil nails or retained soil behind the wall, as concrete expands with heat and contracts with cold. There was no evidence, either from the concrete strain gages or from the external appearance of the concrete facing wall itself, that increased stresses in the soil nails had any effect on the wall's structural integrity.

### 5.5 Effects of freezing and frost heave on wall performance

Analysis of the results from Chapter Four indicate that the effects of frost heave on the wall's performance in its first year were negligible, perhaps not surprising given the low silt content in the embankment fill, the lack of any permanent water source behind the wall except in the deepest sections of the bottommost row of nails, and the relatively mild winter conditions of 1996-1997. The highest stress value observed in any nail was 146 MPa (21.2 Ksi) in Nail C3-10, which occurred on February 20, 1997 (day 417) at a soil depth of 1.5 m (5 ft). While this value slightly exceeded the desirable safety factor of 1/3 the rated yield strength of the steel, 400 MPa (60 Ksi), there was no correlated increase in stress on the load cell (Figure 4-8) attached to the head of Nail C3-10, which one would expect if there were excessive deformation in the nail behind the wall. Nor was there any correlated increase noted in the the concrete strain gages (Figure 4-9). In fact, none of the other instruments exhibited any identifiable reaction to this highest stress value, and the wall continues (as of May 2003) to perform as designed with no major cracks in the reinforced concrete facing.

Due to a datalogger malfunction which disturbed most of the thermocouple readings throughout February, the thermocouple attached to Nail C3-10 did not produce an accurate reading for the temperature at this location during the period of maximum stress. The internal thermistors on the strain gages on Nail C3-10 were also unreadable during this period. Thus the temperature corresponding to the highest stress reading in February had to be interpolated, following the curve of valid data points in January and March. Using this method, the estimated approximate temperature at 1.5 m (5 ft) behind the wall during late February was about 3.5° C (38° F). This is assumed to have been the period when the frost in the soil behind the wall was at its approximate maximum; the ambient air temperature registered at the time of the highest stress reading on February 20 was 2.7° C (37° F), but there had been sustained subfreezing temperatures during the nights and most of the days during the previous month. Thus the peak seasonal nail stress occurred during the period of deepest frost penetration, but not within frozen soil. Because soil nails distribute stresses along their entire grouted length, it is not necessarily surprising that the point of highest recorded stress was located behind the localized frost front.

Interestingly, the peak stress occurred in the instrumented nail located closest to the horizontal and vertical center of the wall (refer to Nail C3-10 in Figure 3-6), located in a row of nails placed slightly higher than 1/3 the height of the wall. The highest values for extreme-fiber bending stress in the Brunswick wall also occurred in the center and bottom rows of nails. In contrast, the literature review in Chapter 2 indicated that soil nail walls typically carry the highest stresses in nails located higher in the wall (and

much lower stresses in nails close to the bottom of the wall). It is possible that differential heaving among the nails -- for example, the effects of a two-dimensional frost heave induced from both the top and front of the wall -- most strongly affected the central elements in this particular soil nail wall system, because they were the most constrained. However, more research of this type will be required before any firmer conclusions can be drawn.

# CHAPTER 6

# SUMMARY AND CONCLUSIONS

The first soil nail wall in Maine was constructed as part of the Brunswick-Topsham Bypass Project in 1996. The University of Maine, in a collaborative effort with the Maine Department of Transportation, attached instrumentation to selected components of the soil nail wall in order to analyze its behavior over the winter of 1996-97. In particular, the research focused on how seasonal frost heaving might affect the wall's performance. The five objectives of the study were as follows:

- Determine the magnitude and rate of freezing behind the wall;
- Determine the effect of the soil nails on freezing penetration;
- Determine the magnitude of stresses on the nails and wall over the course of the seasonal freeze thaw cycle;
- Determine the effects of freezing and frost heave on wall performance; and
- Develop recommendations for incorporating frost effects into soil nail design.

The major findings under each of these objectives are summarized below.

In the first winter season following construction, the frost penetration within the wall ranged in depth from 0 to 1.2 m (4 ft) behind the reinforced concrete facing wall. Freezing temperatures were registered within the facing wall by early January, but frost penetration into the nails and soil behind the wall did not reach maximum depths until late February.

Thermocouple data indicated that the frost front penetrated deeper along the steel nails than in the surrounding soil. However, this effect was sufficiently localized that thermocouple strings within a 0.6 to 0.9 m (2 to 3 ft) radius did not show any influence from the colder temperatures in the nails. The sole exception to this rule was C4-13, the only instrumented nail in the bottom row of nails. C4-13 never froze, yet the adjacent soil showed slight frost penetration. This nail was placed at a level below the finished grade of the roadway and behind the cast-in-place concrete trafiic barrier, so it was considerably buffered from the cold outside air temperatures. It was also submerged for approximately half its length in groundwater, and extended beyond the fill layer into the native soil which consisted of marine outwash with peat deposits. It is possible that these conditions helped to conserve loss of heat through conduction along the nails in the bottom row, as compared to the adjacent fill soil where 0.17 m (7 in) of frost penetration was measured.

Nail stresses in the first 1.5 m (5 ft) behind the facing wall increased steadily as freezing temperatures began to penetrate the wall, although the areas of greatest frost penetration did not directly correlate to the highest nail stresses. Deeper within the wall, the increases in stress were still observable but less pronounced. The nail with the highest observed stress reading, registered during the period of assumed maximum frost penetration in late February, was located close to the horizontal and vertical center of the wall at a point 1.5 m (5 ft) within the soil, in the unfrozen zone behind the frost front. Its stress in tension was slightly over 1/3 the rated yield strength of the steel nail. It is possible that differential heaving among the nails -- for example, the effects of a two-

dimensional frost heave induced from both the top and front of the wall -- most strongly affected the central elements in the soil nail wall system, since they were the most constrained. This in turn suggests that failure due to frost action does not have to occur within the frost front or even in the areas of deepest frost penetration; the stresses observed in the areas of deepest frost penetration were all well below 1/3 the rated capacity of the steel nails. Other possible contributing factors to this high peak stress were the pockets of peat noted near the bottom of the wall (which could have put additional stressses on the row of nails directly above those placed in the soft peat), and additional conduction along the H-beam support piles in the abutment, which were not instrumented. In any case, there were no correlated observations of adverse wall performance characteristics associated with the occurrence or aftermath of the peak stress reading.

Nail C2-9 in the second highest row of the Brunswick soil nail wall recorded its peak seasonal stress a full 2.4 m (8 ft) behind the wall. This behavior can be considered unusual both within the limits of this study, and throughout the published literature on soil nail walls as cited in Chapter 2. Both theory and empirical evidence suggest that the highest stresses due to frost effects are typically observed in the first 1.5 m (5 ft) of each nail. In this particular case, however, the stress at 2.4 m (presumably shear resistance along the failure surface for the overall soil nail wall system) continued to rise as frost penetration penetrated behind the wall, then fell off again slightly as the soil temperatures increased above freezing. This in turn may indicate other factors at work in the wall in Brunswick besides cyclic soil mobilization resisted by the grouted nails in response to

frost heave. However, no adverse effects on other sensors or on visual aspects of the wall's performance were noted in conjunction with this observation.

### 6.1 Recommendations for incorporating frost effects into soil nail wall design

Based on the results of this research effort (with the caveat that it covers only a single year's timespan through a relatively mild winter season), the midcoast Maine climate does not appear to present a major barrier to constructing uninsulated soil nail walls in soils of low-to-moderate silt content, particularly when there is little or no groundwater behind the wall. Placement of nails on 1.2-m (4-ft) centers, while perhaps conservative, appears to provide sufficient redundancy to maintain structural strength for a 6 m (20 ft) wall.

Designers should anticipate that freezing temperatures will penetrate more deeply along the nails than within the surrounding soil. The soil zone between the nails freezes more slowly than the steel nails, because of the difference in conductivity between the two materials. Thus the measured temperatures along the nails can be assumed to indicate the maximum depth of frost penetration behind the wall. For the given winter conditions and nominal 1.2 m (4 ft) nail spacing in Brunswick, the frozen annulus surrounding each nail probably did not extend far beyond the diameter of the grouted HDPE sheath, since the internail locations within a 0.6 to 0.9-m (2 to 3-ft) radius of the nails did not reflect the same temperature regimes as the adjacent nails. However, this would require further research to confirm.

In a relatively mild winter characterized by a freezing index of 356 degree-days (in an area where the average freezing index is 427 degree-days), the deepest frost penetration along a nail was approximately 1.8 m (4 ft) behind a 0.25-m (0.83-ft) thick concrete facing wall. By comparison, the deepest frost penetration in the soil between the nails was 0.45 m (1.5 ft) behind the facing wall. The highest stress was observed on the instrumented nail closest to the horizontal and vertical center of the wall, 1.5 m (5 ft) deep in the soil -- a point well behind the freezing front. This nail experienced tensile stress of over 1/3 the rated structural strength of the steel, with an extreme fiber bending stress that was approximately 25% of the measured tensile stress.

The research produced design recommendations for incorporating protection from frost effects in future soil nail projects, as follows:

- Continue to place nails conservatively, at 1.4-m (4-ft) centers, to help protect the wall's structural integrity even if individual nails experience peak stresses in excess of their design factor of safety.
- Assume that frost will penetrate more deeply along the steel nails than it does within the native soil. It is possible that the small diameter of the nails (and to a lesser extent the insulating value of the HDPE sheath and the surrounding grout) may somewhat limit the outward conduction of freezing temperatures to the surrounding soil. Nonetheless, in a highly frost susceptible soil with a source of water present (such as nearby groundwater or a leaking water pipe), conductive heat transfer along the nails might present the potential for the formation of damaging ice lenses within the wall. For more well-drained soils

(such as that in the Brunswick wall), deeper frost penetration in the surrounding soil due to conduction along the nails does not appear to present a problem.

- The structural strength of the facing wall appears to play a role in the overall resistance of the nail heads to tensile forces. This confirms the assumptions of less conservative limit equilibrium design models which calculate the strength of the facing wall as a functional component in the soil nail wall system.
- Two-dimensional frost stress, caused by frost fronts penetrating the soil from both the front and top of the wall, may introduce differential heaving and variable stress levels on individual nails.
- In northern Maine and in highly frost susceptible soils, or in any case where additional protection against frost heave is warranted, French research (Unterreiner, 1994) suggests two design techniques that have been proven to work effectively. The first is to install shorter nails between the design nails for additional support at the face. The second is to increase the design length by an amount equal to the anticipated depth of frost for the expected winter climate, and leave this additional length ungrouted at the head of each nail. The choice of alternatives should be based on economic considerations, as they are equally effective. More recent research in Maine by Kingsbury (1999) suggests that insulation of both the face and the top of the wall can help to alleviate stresses in the top rows of nails due to bi-directional frost fronts.

The construction of a functional soil nail wall in Brunswick represented a geotechnical achievement milestone for the Maine Department of Transportation. This technique, widely used in Europe for nearly thirty years, has the potential to reduce costs and greatly facilitate road widening activities, particularly in areas of limited accessibility for heavy equipment. Major concerns about soil nail wall performance in cold weather climates were addressed and somewhat allayed in this study, although there are still many unanswered questions. These may form the basis for future research.

# CHAPTER 7

# AREAS FOR FUTURE INVESTIGATION

Monitoring the performance of the Brunswick soil nail wall fulfilled its stated objectives. However, a few questions were left unanswered due to a lack of instrumentation, data, or complete understanding of the mechanisms at work. The answers to some of these questions could prove to be important for future design reliability of soil nail walls constructed in cold climates.

This research effort determined that maximum frost penetration can occur at some distance from the most highly stressed point(s) within the overall soil nail wall system. The highest observed cold-weather stresses in the wall occurred on Nail C3-10 -- near the center of the wall -- rather than in the top row of instrumented nails where the highest frost penetration depths were recorded. One can theorize that a two-dimensional frost front, moving inward from the front of the wall and downward from the top of the wall, resulted in differential frost heave which in turn created "pressure points" in areas where the soil and nails were most constrained from movement. An exploration and detailed mapping of these conflicting frost fronts within a soil nail wall could identify likely pressure points and identify potential countermeasures, such as sizing up the nails within these differential heave zones. However, this is still all highly speculative at this point, and it remains to be confirmed in future instrumented research projects on soil nail walls.

Another interesting question is why the highest recorded stress on Nail C2-13 -- which *was* located in the deepest frost penetration area at the top of of the wall -- occurred at a distance of 2.4 m (8 ft) behind the concrete facing wall. Previous soil nail research, and indeed the results from the other four instrumented nails in this study, have indicated that frost effects have the greatest influence in the first 1.5 m (5 ft) of nail length, where the nails are in held tension by the connections to the facing wall. For unknown reasons, shear stress appears to have predominated over tensile stress in this one nail.

The steel H-piles in the bridge abutment may have accelerated conductive heat transfer and served as additional constraints in the soil-nail system, but the piles were not instrumented so their effect could not be quantified. Despite a fairly small cross-section relative to the volume of soil retained behind the wall, it is possible that the steel H-piles could have a significant impact on frost behavior, and could be the source of trouble on future soil nail walls constructed under bridges in cold-weather climates.

Instrumentation that did not contribute much to this study should be tried again in future research efforts. The total pressure cell, slope inclinometers, vertical thermocouple, and continuous survey points all could have provided additional insights regarding soil nail wall movements in cold weather. And certainly it would have been preferable to have automated readable daily stress and thermocouple readouts from the soil mass during February -- when the peak frost effects in the wall were observed --

rather than having to interpolate from January to March for temperatures and rely on weekly manual readings for stress from a readout device not designed for subfreezing temperatures. Future researchers are advised to standardize their sensors to the maximum degree practicable (i.e., buy from a single vendor), and to program, install, troubleshoot, and field test automated data system elements well in advance of the cold weather.

Another area for future exploration is the range of conditions that be accommodated by a soil nail wall. This study indicated that at least one nail experienced a maximum stress that slightly exceeded its design stress (1/3 of rated yield strength) in a relatively mild winter season, without creating any negative effects on the wall's overall structural integrity. On the other hand, there have been several noted soil nail wall failures in similar or even milder climates, both in Europe and in North America, which can be directly attributed to frost action on the soil nails or facing connections. One of the key differences is that the Brunswick wall lacked a flowing water source behind the wall (discounting the groundwater table at the bottom, since the soil did not contain enough silt particles to cause capillary wicking). Kingsbury (1999) monitored a soil nail wall constructed in a dense, frost-susceptible glacial till in a much colder climate than Brunswick's (mean freezing index of 843° C-days) with several flowing water sources behind the wall, and observed far higher seasonal stress readings in the single uninsulated section than in a comparable section with insulation at the wall face. However, it is possible that a designer might be able to forgo insulation for a similarly constructed wall under similar conditions provided that there was no flowing water behind the wall, since

frost heaving only occurs if a water source is available to create ice lenses within the frozen soil zone. The behavior of such a wall system merits further study, since insulation can be a significant cost in the overall construction material budget for a soil nail wall.

The instrumentation within the Brunswick soil nail wall remains largely operational, and remote monitoring could be resumed on either a continuous or a periodic basis. Long-term monitoring of wall performance data may lead to additional discoveries related to settlement, creep, and residual stress in the soil nails.

It is hoped that this first research effort in the State of Maine will pave the way for future soil nail utilization, and will encourage geotechnical engineers in cold weather regions to consider soil nailing alternatives to traditional retaining walls.

## REFERENCES


AASHTO (1992), Standard Specifications for Highway Bridges, 15th edition, American Association of State Highway and Transportation Officials, Washington, D.C.

AASHTO (1994), LRFD Bridge Design Specifications, 1st edition, American Association of State Highway and Transportation Officials, Washington, D.C.

Aldrich, H.P. and H.M. Paynter (1953), Analytical Studies of Freezing and Thawing in Soils, U.S. Army Corps of Engineers, Arctic Construction and Frost Effects Laboratory, New England Division, Boston, First Interim Report.

Aldrich, H.P. (1956), "Frost Penetration Below Highway and Airfield Pavements," in Highway Research Board Bulletin #135: Factors Influencing Ground Freezing, National Academy of Sciences -- National Research Council Publication 425, Washington, D.C., pp. 124-149.

Alston, C. (1991), "Construction of a Geogrid- and Geocomposite-Faced Soil-Nailed Slope in Eastern Canada," in Transportation Research Record No. 1330, Transportation Research Board, Washington, D.C., pp. 87-95.

Bang, S. (1979), Analysis and Design of Lateral Earth Support System, Ph.D. dissertation, University of California, Davis.

Berggren, W.P. (1943), "Prediction of Temperature Distribution in Frozen Soils," in Transactions of the American Geophysical Union, Part 3, Washington, D.C., pp. 71-77.

Bigelow, N., Jr. (1969), "Freezing Index Maps of Maine," Technical Paper 69-5R, Materials and Research Division, Maine State Highway Commission, Augusta, ME, 11 pp.+ tables and figures.

Blanchard, D. and M. Fremond (1985), "Soils Frost Heaving and Thaw Settlement," Proceedings, 4th International Symposium on Ground Freezing, S. Kinosita and M. Fukida, eds., Sapporo, Japan.

Broms, B.B. and I. Ingelson (1971), "Earth Pressure Against the Abutments of a Rigid Frame Bridge," in Geotechnique, Vol. 21, No. 1, pp. 15-18.

Byrne, R.J., J.L. Walkinshaw, R.G. Chassie, A. DiMillio, J.W. Keeley, K.A. Jackura, D.A. Bruce, R. Chapman, P. Nicholson, and C. Ludwig (1993), FHWA Tour for Geotechnology – Soil Nailing, FHWA-PL-93-020, June, pp. 21, 31.

Byrne, R.J., D. Cotton, J. Porterfield, C. Wolschlag, and G. Ueblacker (1996), Manual for Design and Construction Monitoring of Soil Nail Walls, FHWA-SA-96-069, November, 468 pp.

Carew, A.J. and A.J. Feldman (1965), "Erddruck Sandiger Hinterfullungen auf die Kammerwande von Schiffahrtsschleusen" (tr: Earth Pressure of Sandy Fills on the Walls of Ship Hoists), in Gidrotekhnicheskoye Stroitel'stvo (tr: Hydrotechnical Construction), No. 9, pp. 22-26.

Chamberlain, E.J., P.N. Gaskin, D. Esch, and R.L. Berg (1984), "Classifying Frost Susceptibility," in Frost Action and its Control, R.L. Berg and E.A. Wright, eds., ASCE Technical Council on Cold Regions Engineering Monograph, New York, pp. 104-141.

Chassie, R.G. (1992), "Soil Nailing Overview," ASCE Spring Seminar Handout, ASCE Geotechnical Group, University of Washington, Seattle, 64 pp.

Dixon, Leif A. (1998), "Effects of Bitumen Coating on the Axial and Lateral Loadings of Abutment Piles Subject to Downdrag," M.S. thesis, University of Maine, 197 pp.

Elias, V. and I. Juran (1991), Soil Nailing for Stabilization of Highway Slopes and Excavations, Earth Engineering and Sciences, Inc., Baltimore, for FHWA, McLean, VA, pp. 88-89.

Farouki, O. T. (1981), Thermal Properties of Soils, U.S. Army Cold Regions Research and Engineering Laboratory, Hanover, NH, Department of the Army Publication IT665803M651, 136 pp.

Fremond, M., and P.J. Williams in collaboration with J. Aguirre-Puente et al. (1977), Soil Freezing and Highway Construction, monograph prepared following a seminar-course held at Ottawa, Canada, October 17-21, 1977, organized by the Paterson Centre, Carleton University, and l'Ecole Nationale des Ponts et Chaussees, Paris; French edition published by l'Ecole Nationale des Ponts et Chaussees, Paris, under title Gel des Sols et des Chaussees (1979); Carleton University, Ottawa, 105 pp.

FNRP (1991), French National Research Project CLOUTERRE: Recommendations CLOUTERRE 1991, English translation by B. Myles (1993), FHWA-SA-93-026, Washington, pp. 61, 75.

Gassler, G. and G. Gudehus (1981), "Soil Nailing – Some Soil Mechanical Aspects of Reinforced Earth," in Proceedings, 10th International Conference on Soil Mechanics and Foundation Engineering, Vol. 3, Session 12, Stockholm, pp. 665-670.

Guilloux, A., G. Notte, and H. Gonin (1983), "Experiences on a Retaining Structure by Nailing in Moraine Soils," in Proceedings, 8th European Conference on Soil Mechanics and Foundation Engineering, Helsinki, pp. 499-502.

Ingersoll, L.R., O.J. Zobel, and A.C. Ingersoll (1954), Heat Conduction with Engineering, Geological and Other Applications, University of Wisconsin, Madison, pp. 286-288.

Jumikis, A.R. (1977), Thermal Geotechnics, Rutgers University Press, New Brunswick, NJ, 375 pp.

Juran, I. (1997), private communication, e-mail, May 27.

Juran, I., J. Beech, and E. DeLaure (1984), "Experimental Study of the Behavior of Nailed Soil Retaining Structures on Reduced Scale Models," in International Symposium on In Situ Soil and Rock Reinforcement, Paris.

Juran, I. and V. Elias (1987), "Soil Nailed Retaining Structures: Analysis of Case Histories," in Soil Improvement – A Ten-Year Update, J.P. Welch, ed., ASCE Geotechnical Special Publication No. 12, New York, pp. 232-244.

Kingsbury, D.W. (1999), "Performance of a Soil Nail Wall in a Frost-Susceptible Environment," M.S. thesis, University of Maine, 298 pp.

Kingsbury, D., T. Sandford, and D. Humphrey (2002), "Soil Nail Forces Caused by Frost," in Transportation Research Record 1808: Journal of the Transportation Research Board, Washington, D.C., pp. 38-48.

Kuzevanov, V.V. and O.A. Shulyatyev, "Experimental Study on Interaction Between Piles or Pile Foundations and Frost-Heaved Soils," in Proceedings, 14th International Conference on Soil Mechanics and Foundation Engineering, Hamburg, Vol. 3, pp. 1517-1520.

Lefur, B., J. Bataille, and J. Aguirre-Puente (1964), "Etude de la Congelation d'une Lame Mince dont une Face est Maintenue a Temperature Constante, l'Autre Face Etant Soumise a une Temperature Variable en Fonction du Temps (Probleme de Stefan Unidimensionnel)" (tr: Study of the Freezing of a Thin Plate in which One Face is Kept at Constant Temperature, while the Other Face is Subjected to Temperature Varying as a Function of Time (One-Dimensional Problem using Stefan's Method)), in Comptes Rendus des Seances de l'Academie des Sciences (tr: Proceedings of the Sessions of the Academy of Sciences), Section 259, pp. 1483-1485.

Li, Y., R.L. Michalowski, B. Dasgupta, and R.L.Sterling (1989), "Preliminary Results from Simulation of Retaining Wall Displacement by Frost Action," in Cold Regions Engineering: Proceedings of the Fifth International Conference, ASCE Technical Council on Cold Regions Engineering, New York, February, pp. 389-396.

Long, Livet, Boutonnet, Marchal, Olivier, Nabonne, and Plaut (1984), "Repair of a Reinforced Earth Wall," in International Conference on Case Histories in Geotechnical Engineering, Vol. 1, University of Missouri-Rolla, pp. 335-340.

Lunardini, V.J. (1980), Phase Change Around a Circular Pipe, U.S. Army Cold Regions Research and Engineering Laboratory (CRREL) Report No. 80-27, December, 26 pp.

Lunardini, V.J. (1981), Heat Transfer in Cold Climates, Van Nostrand Reinhold Company, New York, pp. 40-45.

Mitchell, J.K. and W.C.B. Villet (1987), Reinforcement of Earth Slopes and Embankments, Appendix C: Soil Nailing, National Cooperative Highway Research Report No. 290, Transportation Research Board, Washington, pp. 258-296.

Mitchell, J.K. (1993), Fundamentals of Soil Behavior, John Wiley & Sons, Inc., New York, pp. 289-290.

Morgenstern, N.R. and D.C. Sego (1981), "Performance of Temporary Tiebacks Under Winter Conditions," in Canadian Geotechnical Journal, V. 18, pp. 566-572.

Neumann, F. (ca. 1860), Lectures given in 1860s; later collated and published, originally by C.F. Riemann and later by H. Weber. See Weber, H. (1912), Die Partiellen Differential-Gleichungen der Mathematischen Physik nach Riemann's Vorlesungen in 5. Aufl. (tr: Partial Differential Equations for Mathematical Physics After Riemann's Lectures, 5th Edition), F. Vieweg und Sohn, Braunschweig, Germany, 2:121.

Nicholson, P. (1986a), "In Situ Ground Reinforcement Techniques," in International Conference on Deep Foundations, Beijing, China, September, pp. 1-9.

Nicholson, P. (1986b), "Soil Nailing a Wall," in Civil Engineering, ASCE, New York, December, pp. 37-39.

Porterfield, J.A., D.M. Cotton, and R.J. Byrne (1994), Soil Nailing Field Inspectors Manual – Soil Nail Walls, FHWA-SA-93-068, April, 86 pp.

Portnov, I.G. (1962), "Exact Solution of Freezing Problem with Arbitrary Temperature Variations on Fixed Boundary," in Soviet Physics Doklady, American Institute of Physics, New York, Vol. 7 (an English translation of the 'physics' section of the Proceedings of the Academy of Sciences of the USSR).

Sandegren, E., P.O. Sahlstrom, and H. Stille (1972), "Behavior of Anchored Sheet Pile Exposed to Frost Action," in Proceedings, 5th European Conference on Soil Mechanics and Foundation Engineering, Madrid, Vol. 1, pp. 285-293.

Sandford, T. C. (1997), "Freezing Pressures in 'Frost-Free' Materials Caused by Cyclic Water Levels," in Proceedings, 14th International Conference on Soil Mechanics and Foundation Engineering, Hamburg, Vol. 2, pp. 887-890.

Schlosser, F. (1983), "Analogies et Differences dan le Comportement et le Calcul des Ouvrages de Soutenement en Terre Armee et par Clouage de Sol" (tr: Analogies and Differences in Behavior and Design Methods for Reinforced Earth and Soil Nail Retaining Structures), in Annales de l'Institut Technique du Batiment et des Travaux Publics (tr: Annals of the Technical Institute of Construction and Public Works), Paris, No. 418.

Schwing, E. and G. Gudehus (1988), "Soil-Nailing – Design and Application to Modern and Ancient Retaining Walls," in Proceedings, International Geotechnical Symposium on Theory and Practice of Earth Reinforcement, Fukuoka, Japan, October, pp. 605-616.

Shen, C.K., L.R. Herrman, K.M. Romstad, S. Bang, Y.S. Kim, and J.S. Denatale (1981), In Situ Earth Reinforcement Lateral System, Department of Civil Engineering, University of California, Davis, Report No. 81-03.

Sieczkowski, W.F., Jr. (1989), Soil Nailing – In Situ Reinforcement, M.S. thesis, Advanced Construction Technology Center, University of Illinois at Urbana-Champaign, Urbana, Document No. 89-52-01, 82 pp.

Sinyavskaya, V.M. and A.E. Pavlova (1971), "Effect of Periodic Displacements of a Lock Wall on Earth Pressure and Reinforcement Stresses," in Hydrotechnical Construction, No. 3, pp. 247-254.

Smoltczyk, U., K. Hilmer, E. Franke, and B. Schuppener (1977), "Earth Pressure Variations due to Temperature Change," in Proceedings, 9th International Conference on Soil Mechanics and Foundation Engineering, Tokyo, Vol. 1, pp. 725-733.

Small, J. (1959), First Steps in Heat Transfer, Blackie & Son Ltd., Glasgow, pp. 1-30.

Stille, H. (1976), Behavior of Anchored Sheet Pile Walls, Ph.D. dissertation, Royal Institute of Technology, Stockholm, Sweden, 192 pp.

Stocker, M.F., G.W. Kerber, G. Gassler, and G. Gudehus (1979), "Soil Nailing," in Proceedings, International Conference on Soil Reinforcement, Paris, Vol. 2, March, pp. 469-474.

Tsytovich, N. A. (1960), Bases and Foundations on Frozen Soil, English translation by L. Drashevska, Highway Reserach Board Special Report No. 58, National Academy of Sciences – National Research Council Publication 804, Washington, D.C., p. 51.

Unterreiner, P. (1994), Contribution a l'Etude et a la Modelisation Numerique des Sols Cloues: Application a Calcul en Deformation des Ouvrages de Soutenement (tr: Contribution to the Study and Numeric Modeling of Soil Nails: Design Estimates for Deformation of Retaining Structures), Ph.D. dissertation, Centre d'Enseignement et de Recherche en Mecanique des Sols/ Ecole Nationale des Ponts et Chaussees-Laboratoire Central des Ponts et Chaussees (CERMES-ENPC-LCPC), Paris, 989 pp.

Vengeon, J.M. (1989), Murs Cloues. Methodes de Calcul et Susceptibilite au Gel (tr: Soil Nail Walls. Design Methods and Frost Susceptibility), final academic report under instruction of M. Khizardjian, Ecole Central de Lyon, France; cited in Unterreiner (1994).

Whetten, N.L. and J.W. Weaver (1995), A Phase II Subsurface Investigation for U.S. Route 1 Underpass Widening Beneath the MDOT Railroad Bridge, Topsham-Brunswick Bypass Project, in the Town of Brunswick, Cumberland County, Maine, Report prepared for T.Y. Lin International, Alexandria, Virginia, by Haley and Aldrich, Inc., Scarborough, Maine, July 14, 77 pp. exclusive of appendices.

Yanigasawa, E. and C.H. Park (1997), "Heat Transfer Analysis in the Ground Considering Porewater Movement," in Proceedings, 14th International Conference on Soil Mechanics and Foundation Engineering, Hamburg, Vol. 1, pp. 233-236.

## BIOGRAPHY OF THE AUTHOR

Sandra McRae Duchesne was born in El Paso, Texas on January 20, 1956. She graduated from high school in 1974 and received a Bachelor of Arts degree from Smith College in 1978, with a double major in Russian Civilization and Government. Ms. Duchesne worked for over a decade in the federal government and the private sector in Maryland and in Maine, and was commissioned as an officer in the United States Navy Reserve in 1987. In 1990 Ms. Duchesne enrolled at the University of Maine to study Civil Engineering, receiving her Bachelor of Science degree in 1993 with concentrations in Environmental and Geotechnical Engineering. In 1995 she enrolled in the graduate program of the Civil and Environmental Engineering Department at the University of Maine, with a concentration in Geotechnical Engineering.

Ms. Duchesne worked for two private consulting engineering firms and for the Maine Department of Transportation prior to taking her current position as a transportation planning engineer for the Bangor Area Comprehensive Transportation System (BACTS). She is registered as a Professional Engineer in Maine, and is an active member of the American Society of Civil Engineers, the Institute of Transportation Engineers, and the Society of Women Engineers. She is a candidate for the Master of Science degree in Civil Engineering from The University of Maine in May, 2003.